CONFIDENTIAL

Copy 290
RM L54B03

NACA RM L54B03

NACA

RESEARCH MEMORANDUM

A LOW-SPEED INVESTIGATION OF THE AERODYNAMIC, CONTROL, AND HINGE-MOMENT CHARACTERISTICS OF TWO TYPES OF CONTROLS AND BALANCING TABS ON A LARGE-SCALE THIN DELTA-WING—FUSELAGE MODEL

By Marvin P. Fink and Bennie W. Cocke

Langley Aeronautical Laboratory
Langley Field, Va.

CLASSIFIED DOCUMENT

This material contains information affecting the National Defense of the United States within the meaning of the espionage laws, Title 18, U.S.C., Secs. 793 and 794, the transmission or revelation of which in any manner to an unauthorized person is prohibited by law.

CLASSIFICATION CHANGED TO UNCLASSIFIED
AUTHORITY: NACA RESEARCH ABSTRACT NO. 112
EFFECTIVE DATE: FEBRUARY 15, 1957 WHL

NATIONAL ADVISORY COMMITTEE
FOR AERONAUTICS

WASHINGTON
March 24, 1954

CONFIDENTIAL

NATIONAL ADVISORY COMMITTEE FOR AERONAUTICS

RESEARCH MEMORANDUM

A LOW-SPEED INVESTIGATION OF THE AERODYNAMIC, CONTROL, AND HINGE-MOMENT CHARACTERISTICS OF TWO TYPES OF CONTROLS AND BALANCING TABS ON A LARGE-SCALE THIN DELTA-WING—FUSELAGE MODEL

By Marvin P. Fink and Bennie W. Cocke

SUMMARY

A low-speed investigation of the aerodynamic and control characteristics of a 3-percent-thick, 60° delta-wing—fuselage configuration was made in the Langley full-scale tunnel to obtain data at large scale on control configurations of general interest and to determine whether significant Reynolds number effects existed for a very thin wing subject to leading-edge vortex-type flow.

Aerodynamic forces, moments, and hinge moments were obtained at a Reynolds number of 10×10^6 for the model with half-delta and horn-balance-type tip controls, including the effects of inboard-trailing-edge flap deflection and control-tip-radius modification. A limited study of balancing tabs on the horn-balance-type control was also included.

The results of this investigation compared with previous tests at low Reynolds numbers do not indicate any major Reynolds number effects on aerodynamic, control, or hinge-moment characteristics within the Reynolds number range from 2.3×10^6 to 10.0×10^6. Of the tip-type controls investigated the horn-balance type was the most effective as a lateral control throughout the angle-of-attack range. The effectiveness of the half-delta controls was approximately proportional to area in the low angle-of-attack range; however, at high angles of attack a control of 5 percent wing area was more effective than one of 10 percent wing area. Positive deflection of inboard plain trailing-edge flaps resulted in marked reduction of tip-control effectiveness at high angles of attack with the most serious reduction noted for the half-delta controls. Negative flap deflections generally improved tip-control effectiveness.

The half-delta controls of 5 and 10 percent wing area, respectively, had similar hinge-moment characteristics about hinge lines located at 58 percent of their respective root chords. Low hinge moments were

obtained for this hinge point although data are characterized by sharp nonlinearities above 10° deflections throughout the angle-of-attack range.

Balancing tabs proved effective in reducing the hinge moments while retaining good rolling characteristics with the horn-balance-type control in the low angle-of-attack range. A full-span attached tab was the most effective of the tabs investigated throughout the angle-of-attack range and a detached tab had least effectiveness at high angles of attack.

INTRODUCTION

The current interest in thin low-aspect-ratio wings for use in high-speed flight has resulted in investigations of delta wings having various thickness ratios and leading-edge sweep angles through a wide Mach number range. These studies have included effectiveness tests for a wide range of control configurations, but only a limited amount of hinge-moment data is available. Most of these investigations have been limited to tests of small models at low Reynolds numbers. In view of the known effect of Reynolds number on the flow in the region of the wing tips for wings of moderate thickness which are subject to the complexities of a leading-edge-separation vortex-type flow, it appeared advisable to investigate some of the more promising types of delta-wing tip controls on a large-scale thin delta wing to determine whether any significant Reynolds number effects on hinge moments or control effectiveness existed at low Mach numbers. A 30-foot-span delta-wing—fuselage model configuration was therefore constructed and tested in the Langley full-scale tunnel without control deflections at Reynolds numbers up to 14.0×10^6. The wing had an aspect ratio of 2.31, an NACA 65A003 airfoil section, and was provided with half-delta and horn-balance-type tip controls. The wing and control configurations were chosen to permit direct comparison with data from previous tests of a 6-foot-span model (ref. 1) at a Reynolds number of 2.3×10^6.

This paper presents the results of control-effectiveness and hinge-moment investigations for the various tip-control arrangements at a Mach number of 0.09 and a Reynolds number of 10.0×10^6 and includes the effects of inboard flap deflection and control-surface tip-radius modification. Also included are data from a limited investigation of the effects of spanwise and chordwise location on the effectiveness of a balancing tab installed on the horn-balance-type control. Results cover the control deflection range of ±30° through the angle-of-attack range from 0° to 24.3°.

SYMBOLS

The wing moments are referred to the model axes originating at the projection of the quarter-chord point of the mean aerodynamic chord on the plane of symmetry. The positive directions of coefficients, moments, and control deflections are shown in figure 1.

C_L	lift coefficient, L/qS
C_Y	lateral-force coefficient, Y/qS
C_D	drag coefficient, D/qS
C_m	pitching-moment coefficient, $M/qS\bar{c}$
C_n	yawing-moment coefficient, N/qSb
C_l	rolling-moment coefficient, L'/qSb
C_{l_p}	damping-in-roll parameter
C_h	hinge-moment coefficient (for half-delta tip control, $H/qS_a\bar{c}_a$; for horn-balanced tip or flap control, $H/2qQ$)
C_{l_δ}	rate of change of rolling-moment coefficient with control deflection, between $\pm 10^\circ$ deflection, $\Delta C_l/\Delta\delta$
C_{h_α}	rate of change of hinge-moment coefficient with angle of attack, between $\pm 10^\circ$ deflection, $\Delta C_h/\Delta\alpha$
C_{h_δ}	rate of change of hinge-moment coefficient with control deflection, between $\pm 10^\circ$ deflection, $\Delta C_h/\Delta\delta$
$C_h'\delta_a$	hinge-moment parameter
C_h'	total hinge moment, asymetrically deflected ailerons
L	lift, lb
Y	lateral force, lb
D	drag, lb

M	pitching moment, ft-lb
N	yawing moment, ft-lb
L'	rolling moment, ft-lb
H	hinge moment, ft-lb
ρ	mass density of air, slugs/cu ft
q	free-stream dynamic pressure, $\frac{1}{2}\rho V^2$, lb/sq ft
V	free-stream velocity, ft/sec
S	total wing area, sq ft
S_a	area of one control surface, sq ft
S_t	area of control-surface tab
Q	moment of area of control surface rearward of hinge line about hinge line, cu ft
c	wing chord measured parallel to plane of symmetry, ft
$\bar{c}$	wing mean aerodynamic chord measured parallel to plane of symmetry, $\frac{2}{S}\int_0^{b/2} c^2 dy$, ft
$\bar{c}_a$	control mean aerodynamic chord
b	wing span, ft
y	distance along lateral axis, ft
α	angle of attack of wing chord line, deg
δ	control deflection, positive trailing edge down, deg
δ_a	aileron deflection, positive trailing edge down, deg
δ_f	flap deflection, positive trailing edge down, deg
δ_t	tab deflection with reference to chord of control surface, deg

$pb/2V/\delta = C_{l_\delta}/C_{l_p}$ rolling effectiveness parameter

pb/2V wing-tip helix angle, radians

p rolling angular velocity, radians/sec

R Reynolds number, based on wing $\bar{c}$

MODEL AND TESTS

Model

The model of this investigation consisted of a 60° delta wing having a span of 30 feet and an area of 390 square feet mounted on the longitudinal center line of a 45-foot fuselage of parabolic profile and circular cross section. The wing had an NACA 65A003 airfoil section, an aspect ratio of 2.31, and no twist or dihedral. The wing was mounted on the fuselage with the $\bar{c}/4$ point of the wing 21 feet behind the fuselage nose station. The ratio of maximum fuselage diameter to wing span was 0.15. Ordinates for the airfoil sections and fuselage are presented in tables I and II and the general arrangement and principal dimensions of the model are shown in figure 2.

The model was equipped for testing three control arrangements: namely, (1) a half-delta tip having an area of 5 percent of the wing semispan area, (2) a half-delta tip having an area of 10 percent of the wing semispan area, and (3) a horn-balance-type control of 10 percent of the wing semispan area. The delta tip controls were designed as balanced controls; however, the horn-balance-type control with only 13 percent balance area was not expected to be a balanced control. For the 10-percent half-delta tip and 10-percent horn-balance configurations, plain trailing-edge flaps extending from the inboard end of the control to the fuselage were included to permit studies of effects of inboard flap deflection on the outboard control effectiveness. Layouts and principal dimensions of the three basic control configurations are given in figures 2 and 3. As indicated by the sketches, the controls were originally constructed with pointed tips; however, provisions were made to allow for tests to determine the effects of rounding the tips to obtain a radius more practical for thin-wing construction. Details of this tip modification are indicated in figure 4.

Provision was made for testing both attached and detached balancing tabs (fig. 5) on the horn-balance control. The attached tabs investigated were constructed from 1/16-inch duralumin which was preformed for attachment to the control trailing edge and which allowed testing at a tab

gearing of $\delta_t/\delta_a = -1.0$ for a control deflection range of $\pm 30^\circ$. The detached tab used had an approximate airfoil section of 3-percent thickness and could be tested in either inboard or outboard positions. General arrangements and principal dimensions for the tab configurations are given in figure 5.

Tests

The model was mounted for tests on the scale-balance system in the Langley full-scale tunnel (fig. 6). Lift, drag, and pitching-moment data were measured over the angle-of-attack range from -4° to 24.3° for the model with controls neutral through a Reynolds number range from 4.0×10^6 to 14.0×10^6. Model angle of attack was limited to 24.3° for these tests by the proximity of the rear end of the fuselage to the boundary of the tunnel air stream.

Control-effectiveness and hinge-moment investigations were conducted for each of the three basic control configurations A, B, and C, (see fig. 3) through the 0° to 24.3° angle-of-attack range with controls deflected through a 30° to -40° range with the trailing-edge flap neutral. Subsequent tests were then made for controls B and C over the same deflection range with the respective inboard trailing-edge flaps (indicated in fig. 3) deflected to angles of -10°, 20°, and 30°.

In order to determine the effects of tip configuration, the tip sections of controls B and C were then rounded to a radius as indicated in figure 4. Effectiveness and hinge-moment data were again obtained with the trailing-edge flaps neutral. Rounding the tips in the manner indicated reduced the control area by approximately 5 percent.

In view of the general interest in the use of detached tabs for balancing flap-type controls at high Mach numbers, some additional tests were included to obtain data on the relative balancing effectiveness for attached and detached balancing tabs of equal area on the horn-balance-type control (control C) through the angle-of-attack range of 0° to 24.3°. Because of time limitation, each tab arrangement was tested for only one simulated gearing $\left(\delta_t/\delta_a = -1.0\right)$. Rolling effectiveness and hinge-moment data were obtained over the 30° to -40° control deflection range for each of the tab configurations illustrated in figure 5.

For all tests, aerodynamic forces and moments on the model were obtained from the tunnel scale-balance system and hinge moments on all controls were obtained from electrical strain-gage installations incorporated in the control-attachment design. All control-effectiveness and hinge-moment data were obtained at a Mach number of approximately 0.09 and a Reynolds number of 10.0×10^6 based on a wing mean aerodynamic chord of 17.41 feet.

All data have been corrected for tunnel-stream-angle misalignment and jet-boundary effects. Jet-boundary corrections were determined by the methods of references 6 and 7. Control deflection angles have not been corrected for deflection under load; however, calibrations indicated deflection under maximum load did not exceed 1°.

PRESENTATION OF DATA

The longitudinal characteristics of the basic model over a range of Reynolds number are presented in figure 7 and longitudinal data at $R = 10 \times 10^6$ for the model with various controls deflected are shown in figures 8 to 10.

Basic lateral characteristics (C_l, C_n, and C_Y against δ) for each of the control configurations investigated are shown in figures 11 to 14 and rolling-moment data are compared in figures 15 to 17 to show the effects of Reynolds number, control configuration, and inboard flap deflection. Control parameters (C_{l_δ}, C_{n_δ}, and $pb/2V/\delta$ against α) are presented in figures 18 to 20 for several of the control configurations. Hinge-moment data for each of the control configurations are presented in figures 21 to 23 and the hinge-moment parameters (C_{h_δ} against α) are compared in figure 24.

Lateral characteristics and hinge-moment data for the horn-balance-type control with various balancing-tab arrangements are presented in figures 25 and 26 and hinge-moment parameters ($C_h{}'_{\delta_a}$ against C_l) for the various tabs are compared in figure 27.

DISCUSSION OF RESULTS

Longitudinal Characteristics

Reynolds number.- In order to determine whether any significant effects of Reynolds number were experienced by the model, a range of Reynolds number from 4×10^6 to 14×10^6 was investigated. The results of the tests with controls neutral (fig. 7) did not indicate any appreciable Reynolds number effects in that range and all subsequent tests were therefore made at $R = 10 \times 10^6$.

Longitudinal control.- Inasmuch as there is an appreciable amount of published data on the longitudinal characteristics of half-delta and plain trailing-edge flap-type controls on delta wings, it was not the purpose of this investigation to study these parameters on this model; however, since these data, although obtained by deflecting a control on one wing semispan only, may be of some general interest, they are presented (figs. 8 and 9) and are not discussed in detail.

Of the three tip controls tested, the horn-balanced control (control C) proved to be the most effective as a longitudinal trim device (fig. 10). This may be expected of a control of this type inasmuch as it is principally a trailing-edge flap and the results of these tests are similar to those of references 2 and 4 for trailing-edge flaps. Comparison between the trimming effectiveness of control C and that of the adjacent inboard flap (at approximately equal area) shows the flap to have better trimming characteristics than the tip control. The flap adjacent to control B shows more effectiveness than the one adjacent to control C, but since the flap adjacent to B was approximately 25 percent larger the increase in effectiveness follows approximately the ratio of area increase.

It may be interesting to note that for the half-delta controls (A and B) the pitching-moment coefficients of the 10-percent control (B) are slightly less than twice the values of those for the 5-percent control (A), and the relative longitudinal effectiveness of the two controls remains about the same throughout the angle-of-attack range.

Lateral Characteristics

Basic control.- Of the three controls tested, the rolling-moment coefficients (fig. 15) show control C, the 10-percent horn-balance control, to be the most effective throughout the angle-of-attack range. For this control the maximum control effectiveness $\left(C_{l_\delta} = 0.0011, \text{fig. } 18\right)$ is reached at $\alpha = 0^\circ$ and there is a gradual reduction over the α range to $C_{l_\delta} = 0.0004$ at 24.3°. Control A $\left(S_a/S = 0.05\right)$ was the least effective at the lower angles of attack, but was more effective than control B $\left(S_a/S = 0.10\right)$ in the high angle range. The effectiveness of control A decreased almost linearly through the angle-of-attack range, decreasing from 0.00050 to 0.00025 at angles of $\alpha = 0^\circ$ and $\alpha = 24.3^\circ$, respectively. As was the case with tip controls on delta wings of thicker section (6.6 percent c) in previous investigations (ref. 3), the present test also shows the rolling effectiveness of half-delta controls in the low angle-of-attack range to be about proportional to the control area. Control B maintained almost twice the effectiveness of control A over the angle-of-attack range from 0° to 17°. Values of C_{l_δ} for the two controls at 0° angle of attack were 0.0009 and 0.0005, respectively, with gradual reductions noted up to $\alpha = 17^\circ$. Above $\alpha = 17^\circ$, control B lost effectiveness very rapidly till C_{l_δ} was zero at $\alpha = 24^\circ$.

All three tip controls showed a marked reduction of rolling-moment coefficient (fig. 15) for the high positive control deflections in the moderate to high angle-of-attack range. This reduction is due to stall at the wing tip over this range. Rolling-effectiveness characteristics

(fig. 19) $pb/2V/\delta$ obtained using C_{l_p} values from reference 5 show trends similar to those indicated by control-effectiveness data.

Yawing-moment coefficients for the three controls were adverse at all angles of attack for positive control deflections and adverse above about 7° angle of attack for the negative control deflections.

In order to determine the effects of rounding the wing tip on the control effectiveness, the wing tips were rounded to a radius of 14.3 inches (fig. 4) which resulted in an area reduction of about 5 percent of the control area. Comparison of the control effectiveness of this rounded tip (fig. 18) with that of the original tip shows that the modified controls (B and C) were approximately as effective as the original controls over the entire angle-of-attack range.

Reynolds number.- For a Reynolds number comparison, the incremental rolling-moment coefficients of the 30-foot model and a 6-foot model (ref. 1) are presented at Reynolds numbers of 10.0×10^6 and 2.3×10^6, respectively (fig. 17). Comparison of the lift and drag data for the two models indicated good agreement although there was some model difference, namely, location of the fuselage with respect to the wing. It is felt, therefore, that the flow about the two wings, which are of the same plan form and airfoil section, is so closely related that the lateral control and hinge moments of the two models would be adequate for comparison.

Increments of rolling moment $\left(\Delta C_l = C_l - C_{l_{\delta=0}}\right)$ caused by control deflection are presented in order to remove from the data any effects on roll due to model differences. Inasmuch as the data from the small model (ref. 1) do not include a 10-percent half-delta control, the only data available for comparison are the 5-percent half-delta controls and the 10-percent horn-balance-type controls. It is interesting to note the generally good agreement of the two sets of data from two models of such difference in size and Reynolds number. These results therefore indicate that any effects of Reynolds number within the range indicated $\left(2.3 \text{ to } 10.0 \times 10^6\right)$ are not large and, for very thin highly swept wings, the use of small-scale models for low-speed testing could be profitably utilized for detailed studies.

Effect of inboard flap deflection.- The effects of inboard flap deflection (in conjunction with tip-control deflection) on the lateral characteristics are presented in figure 12 for the 10-percent half-delta control (B) and in figure 13 for the 10-percent horn-balance control (C). A comparison of controls B and C with flaps deflected is shown in figure 16 as the variation of C_l with δ and in figure 20 as the variation of C_{l_δ} with α.

Flap deflection shows no great effect on the control effectiveness of control B below an angle of attack of about 8° (fig. 20). At angles of attack from 8° to 16°, flap deflection aggravated the decrease in control effectiveness caused by increasing the angle of attack, and resulted in a decrease in effectiveness of about 40 percent for a flap deflection of 20°. The decrease in effectiveness was considerably greater for a flap deflection of 30°. The effectiveness became zero at about 20° angle of attack for 20° flap deflection and at about 16° angle of attack for the 30° flap deflection. Flap deflections of -10° had no appreciable effect on the control up to $\alpha = 17°$ but resulted in increased effectiveness at the higher angles of attack. It would appear that as a result of downward flap deflection the inboard sections experience an additional loading which might introduce an earlier and more intense leading-edge-separation vortex and which, in turn, would sweep across the tip sections and stall the tips at a lower angle of attack than for the flap neutral condition. The converse would be expected for negative inboard flap deflection which explains the increased tip-control effectiveness for that case.

The horn-balance control (C) has better rolling-moment characteristics with flaps deflected than does control B (fig. 20). Virtually, no effects due to flap deflection on control effectiveness are apparent below an angle of attack of 10°. In the higher angle-of-attack range, increased flap deflection caused an appreciable loss in control effectiveness. At angles of attack above approximately 16° the control effectiveness was reduced about 60 percent, but the control did not experience the reversal exhibited by control B.

Hinge-Moment Characteristics

Basic controls.- Both the 5-percent and the 10-percent half-delta controls show very similar hinge-moment characteristics (figs. 21(a) and 21(b)) throughout the angle-of-attack range for the entire control-deflection range. At a low value of α both controls are very nearly balanced but for values of α of 6.6° and above (fig. 21(a)) the controls become overbalanced and exhibit marked nonlinearities at both negative and positive control deflections exceeding 10°. The variation of C_h with α (fig. 21(b)) is also rather nonlinear in the α range from -4° to 8° becoming more linear at high angles of attack. Consideration of the C_{h_α} effects on the total hinge moments that would exist in a steady rolling condition indicate that the control will be slightly underbalanced at $\alpha = 0°$ but for values of α above 4° the effects of C_{h_α} will generally increase the control overbalance. The exact cause of the nonlinear characteristics cannot be ascertained since pressure-distribution data are not available and the flow characteristics over the deflected tip are therefore not defined. However, it should be noted

that hinge-moment coefficients for the controls are very low and the movement of the center of pressure required to produce the changes shown in aerodynamic balance would be small.

The hinge-moment characteristics of the horn-balance control (figs. 21(c) and 21(d)) are very much like those of a plain trailing-edge control on the 10-percent-thick 60° delta wing of reference 2 having the leading-edge-vortex type of flow separation. The plots of C_h against δ (fig. 21(c)) show the hinge-moment characteristics to be fairly linear with control deflection up to the higher angles of attack and for positive control deflection. The variation of C_h with α (fig. 21(d)) is also fairly linear and typical of an unbalanced trailing-edge-flap type of control. Consideration of the effects of C_{h_α} on total aileron hinge moments for the steady rolling case indicate that the effects of C_{h_α} would serve to reduce the hinge moments in a steady roll but it does not appear that an overbalanced condition would ever be reached.

The reduction of control area which results from enlarging the wing tip radius (see fig. 4) causes similar effects on the hinge moments of controls B and C (figs. 21(a) and 21(c)). The most apparent effects on C_{h_δ} occurred at the low angles of attack between control deflections of $\pm 10^\circ$ where the wing tip was under its greatest loading. In the higher angle-of-attack range, where the wing tip is stalled C_{h_δ} was virtually unchanged although a reduction in the absolute hinge-moment coefficient was apparent over the entire control-deflection range at all values of α. Examination of the plots of hinge-moment parameter C_{h_δ}, obtained between control deflections of $\pm 10^\circ$, indicates a rather sizeable effect of the tip modification at low angles of attack (fig. 24(a)); however, it should be noted that the effect diminished with increased control deflection (figs. 21(a) and 21(c)).

Reynolds number.- The hinge-moment data of the 6-foot-span model of reference 1 and the 30-foot-span model are presented in figure 22 to give a comparison of the control hinge moments at high and low Reynolds numbers. Inasmuch as 10-percent half-delta control data are not available for the small model, only the 5-percent half-delta and the 10-percent horn-balanced controls are presented. It is interesting to note the similarity of the trends of the hinge moment of the controls as these data represent Reynolds numbers of 10.0×10^6 and 2.3×10^6 for the large and small models, respectively. For two models having such widely separated Reynolds numbers, the significance lies not so much in the magnitude of the numbers which are in fair agreement but in the proximity of angle of attack at which the nonlinearities occur. This close similarity indicates that both models, even in the tip regions, are experiencing the same flow characteristics and it would appear that for a wing

of this thin section the characteristics of the leading-edge-vortex type of flow are not appreciably affected by Reynolds number.

Effect of inboard flap deflection.- The effects of inboard flap deflection on the hinge moments of controls B and C are presented in figure 23 and slopes C_{h_δ} taken through ±10° control deflection in figure 24(b).

The effects of positive inboard flap deflection on the hinge-moment characteristics of control B (fig. 23(a)) are most pronounced at high negative control deflections. Flap deflections of 20° and 30° caused large positive moments associated with high negative control deflections in the moderate angle-of-attack range. With positive control deflection, the effects of inboard flap deflection are not so severe and the hinge-moment characteristics remain similar to those of the basic configuration throughout the angle-of-attack range. The effect of flap deflection on C_{h_δ} (fig. 24(b)) is not very pronounced and only at low angles of attack is there any apparent change in the C_{h_δ} on control B with positive flap deflection. A flap deflection of -10°, however, caused a reduction in the value of the hinge-moment parameter C_{h_δ} over the entire angle-of-attack range (fig. 24(b)) and generally made the control characteristics more linear (fig. 23(a)). The horn-balanced control, not being so nearly balanced as control B, was not so critical to the effects of loading changes due to flap deflection as was the half-delta control. Positive flap deflection caused somewhat higher hinge moments at the higher negative control deflections at angles of attack below about 10° (fig. 23(b)). At the higher angles of attack and negative control deflections, the effects of inboard flaps caused the hinge moments of the control to be more negative for the positive flap deflections and less negative for the negative deflections. The slopes of the hinge-moment curves (fig. 24(b)) over the ±10° deflection range show an increase in C_{h_δ} over the entire angle-of-attack range except for the 30° flap deflection which becomes slightly less than the basic configuration above 14°.

Effects of Balancing Tabs

In order to add to the limited low-speed data on balancing tabs on high-speed-type controls, a short investigation was made of several tab arrangements (fig. 5) on the horn-balance control.

Deflection of the tab, by an amount equal and opposite to the control deflection, had only small effects on the lateral characteristics of the control. The rolling-moment coefficients (fig. 25) were slightly reduced in the higher control-deflection range over the entire angle-of-attack range. Yawing moments were essentailly unaffected by the addition of tabs.

It appears that the balancing tabs of this investigation have about the same balancing properties that have been noted on previous tests of controls with tabs (ref. 8). The most effective deflection range for tabs seems to be about ±20°. Control hinge-moment coefficients (fig. 26(b)) show that the full-span attached tab was the most effective; for the gear ratio tested $\left(\delta_t/\delta_a = -1.0\right)$ the tab caused appreciable overbalance of the control over the effective range of the tab (±20°). The half-span attached tab (figs. 26(c) and (d)) proved to be effective enough to reduce the hinge moments due to control deflection to low values over the ±20° control deflection range at all angles of attack. There was no appreciable difference between the effects on the hinge moment of the inboard and the outboard location. The half-span detached tab (figs. 26(e) and (f)) produced a nearly balanced control at the low angles of attack, but at high angles the tab was not effective enough at either the inboard or outboard position to cause any apparent hinge-moment reduction over the basic control.

In order to put the results of the control with the various tab arrangements on a comparable basis, a plot of $C_h'\delta_a$ against C_l representing simultaneous left and right control operation as ailerons is presented as figure 27 for a low, moderate, and high angle of attack. (See ref. 8.) At rolling-moment coefficients below 0.04 and at -0.5° angle of attack (fig. 27) all the tab arrangements proved to be effective in reducing the value of the hinge-moment parameter $C_h'\delta_a$. The full-span attached tab causes the greatest change in $C_h'\delta_a$, producing overbalance up to $C_l = 0.03$ where it becomes less effective than the other tabs. These results indicate that a gearing ratio of less than unity would provide sufficient balancing in the lower C_l range. All the half-span tab arrangements showed about equal balancing properties throughout their effectiveness range.

In the moderate angle-of-attack range ($\alpha = 13.6°$) location of the tab on the control appears to have some effects on the hinge moment. The inboard half-span and full-span attached tabs show about 40 percent higher C_l values for hinge moments near zero than any of the other tabs. At $\alpha = 24.3°$ the controls have lost virtually all their rolling effectiveness and, except for the full-span tab, the tabs generally have no beneficial effect.

CONCLUSIONS

The results of the low-speed investigation of the lateral control and hinge-moment characteristics of a 60° delta-wing—fuselage model with half-delta controls of 5 and 10 percent of the semispan area and a horn-balance-type control of 10 percent of the semispan area and of the effects

of balancing tabs on the rolling-moment and hinge-moment characteristics are concluded as follows:

1. Over the range of Reynolds number investigated (4×10^6 to 14×10^6), there was no indication of significant effects on the longitudinal aerodynamic characteristics of the model. A comparison of the rolling moments and hinge moments with data of a previous test obtained at low Reynolds numbers showed no large effects on these characteristics in the Reynolds number range from 2.3×10^6 to 10×10^6.

2. The horn-balance-type control was the most effective as a lateral control throughout the angle-of-attack range.

3. The effectiveness of the half-delta controls was about proportional to the control area in the lower angle-of-attack range, but at high angles of attack the 5-percent control was more effective than the 10-percent control.

4. The hinge moments of the 5-percent and 10-percent half-delta controls had very similar characteristics showing marked nonlinearities over the angle-of-attack range. Both controls with the hinge line at 58 percent of the control root chord were nearly balanced as was evidenced by the relatively low hinge moments throughout the angle-of-attack range.

5. Rounding the wing tip had little effect on the rolling characteristics of either the half-delta or the horn-balance control but, for the low angle-of-attack range, resulted in a slight overbalancing of the half-delta tip and reduced the hinge moments of the horn-balance-type control.

6. Positive inboard flap deflection caused a loss in control effectiveness with increased angle of attack for both the 10-percent half-delta and the 10-percent horn-balanced controls. The effects were more pronounced on the half-delta than on the horn-balance control.

7. Balancing tabs proved effective in reducing the hinge moments and retaining good rolling characteristics with the horn-balance-type control in the low angle-of-attack range. The full-span attached tab produced the greatest change in hinge-moment parameter throughout the angle-of-attack range with the detached tab being the least effective of the tabs at high angles of attack.

Langley Aeronautical Laboratory,
National Advisory Committee for Aeronautics,
Langley Field, Va., January 27, 1954.

REFERENCES

1. Scallion, William I.: Low-Speed Investigation of the Aerodynamic, Control, and Hinge-Moment Characteristics of Two Types of Controls on a Delta-Wing—Fuselage Model With and Without Nacelles. NACA RM L53C18, 1953.

2. Hawes, John G., and May, Ralph W., Jr.: Investigation at Low Speed of the Effectiveness and Hinge Moments of a Constant-Chord Ailavator on a Large-Scale Triangular Wing With Section Modification. NACA RM L51A26, 1951.

3. Jacquet, Byron M., and Queijo, M. J.: Low-Speed Wind-Tunnel Investigation of Lateral Control Characteristics of a 60° Triangular-Wing Model Having Half-Delta Tip Controls. NACA RM L51I10, 1951.

4. Wolhart, Walter D., and Michael, William H., Jr.: Wind-Tunnel Investigation of the Low-Speed Longitudinal and Lateral Control Characteristics of a Triangular-Wing Model of Aspect Ratio 2.31 Having Constant-Chord Control Surfaces. NACA RM L50G17, 1950.

5. Wolhart, Walter D.: Wind-Tunnel Investigation at Low Speed of the Effects of Symmetrical Deflection of Half-Delta Tip Controls on the Damping In Roll and Yawing Moment Due to Rolling of a Triangular-Wing Model. NACA RM L51B09, 1951.

6. Sivells, James C., and Salmi, Rachel M.: Jet-Boundary Corrections for Complete and Semispan Swept Wings in Closed Circular Wind Tunnels. NACA TN 2454, 1951.

7. Katzoff, S., and Hannah, Margery E.: Calculation of Tunnel-Induced Upwash Velocities for Swept and Yawed Wings. NACA TN 1748, 1948.

8. Harris, Thomas A.: Reduction of Hinge Moments of Airplane Controls Surfaces by Tabs. NACA Rep. 528, 1935.

TABLE I

FUSELAGE COORDINATES

Station	Distance from nose, in.	Body radius, in.
1	0	0
2	8.10	1.99
3	16.20	3.90
4	24.30	5.79
5	32.40	7.50
6	40.50	9.17
7	48.60	10.78
8	56.70	12.31
9	64.80	13.77
10	65.55	13.91
11	81.00	16.58
12	97.20	18.93
13	113.40	20.85
14	129.60	22.74
15	145.80	24.15
16	162.00	25.34
17	178.20	26.18
18	194.40	26.71
19	210.60	26.91
20	226.80	26.95
21	259.20	26.74
22	291.60	26.25
23	324.00	25.49
24	356.40	24.45
25	388.80	23.15
26	421.20	21.60
27	453.60	19.76
28	486.00	17.64
29	518.40	15.24
30	540.00	13.53

TABLE II

NACA 65A003 AIRFOIL ORDINATES

Station, percent c	Ordinate, percent c
0	0
.5	.234
.75	.284
1.25	.362
2.50	.493
5.00	.658
7.50	.796
10.00	.912
15.00	1.097
20.00	1.236
25.00	1.342
30.00	1.420
35.00	1.472
40.00	1.498
45.00	1.497
50.00	1.465
55.00	1.402
60.00	1.309
65.00	1.191
70.00	1.053
75.00	.897
80.00	.727
85.00	.549
90.00	.369
95.00	.188
100.00	.007
L.E. radius = 0.058 percent c	

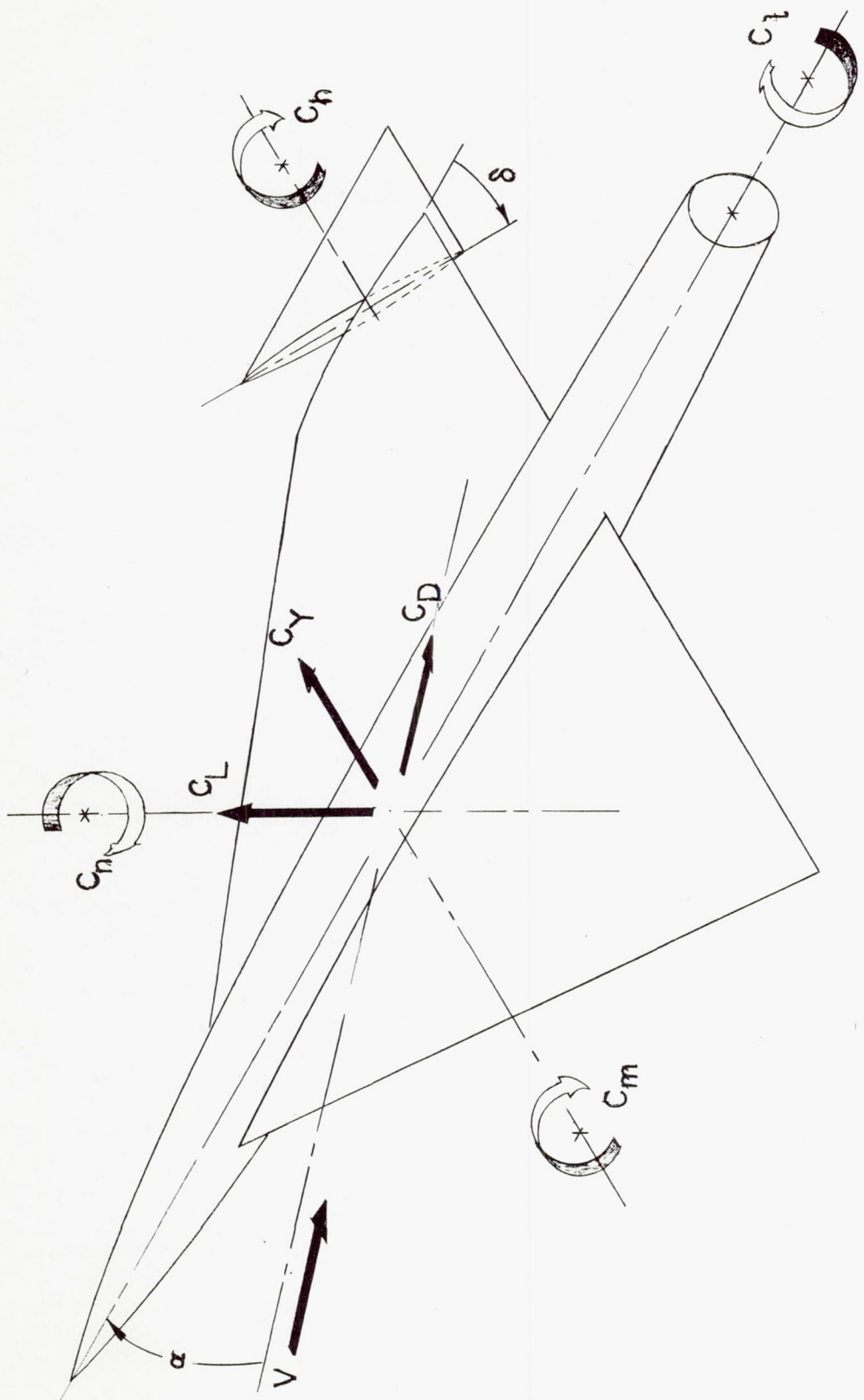


Figure 1.- System of axes used. Arrows indicate positive direction of forces, moments, and angular displacements.

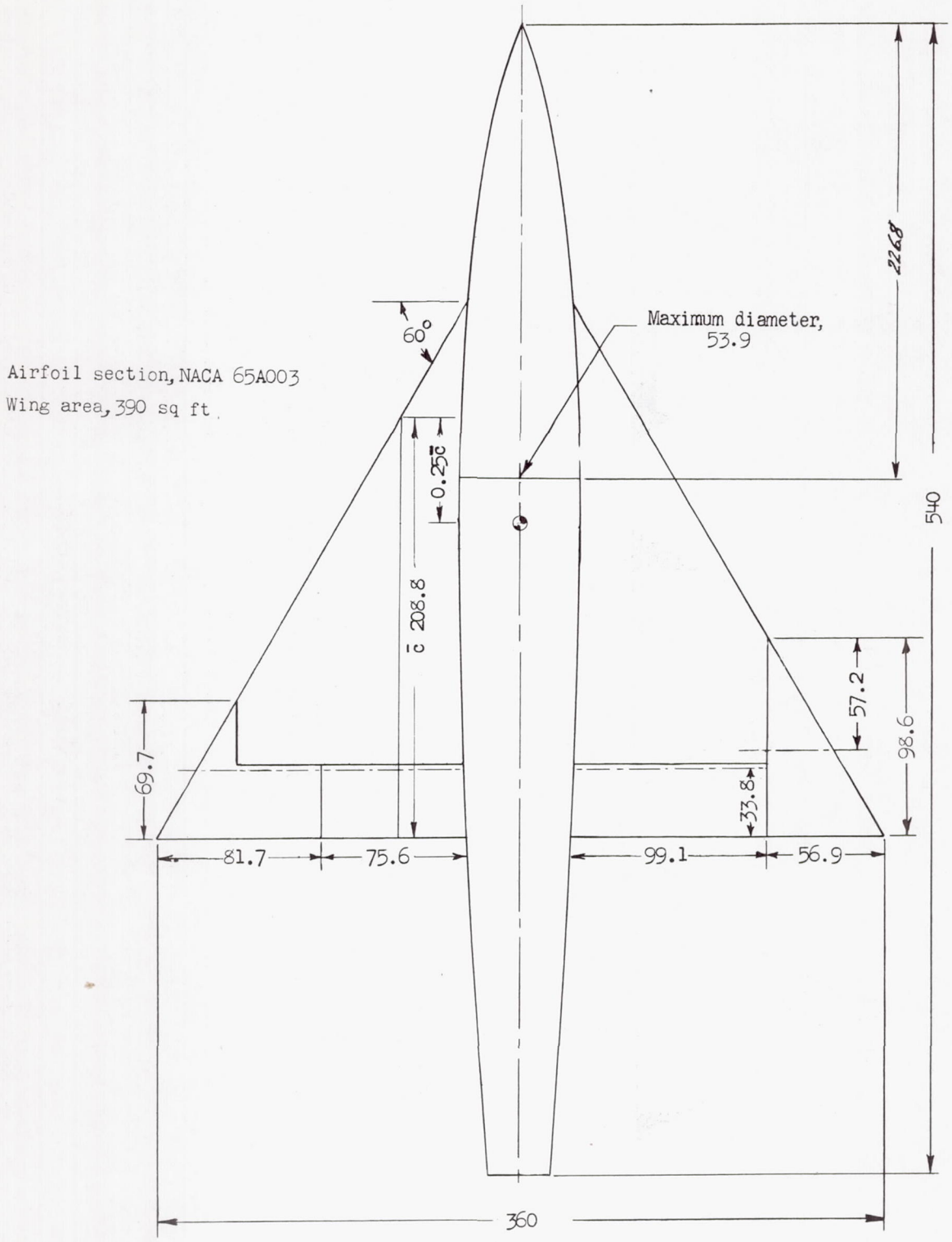
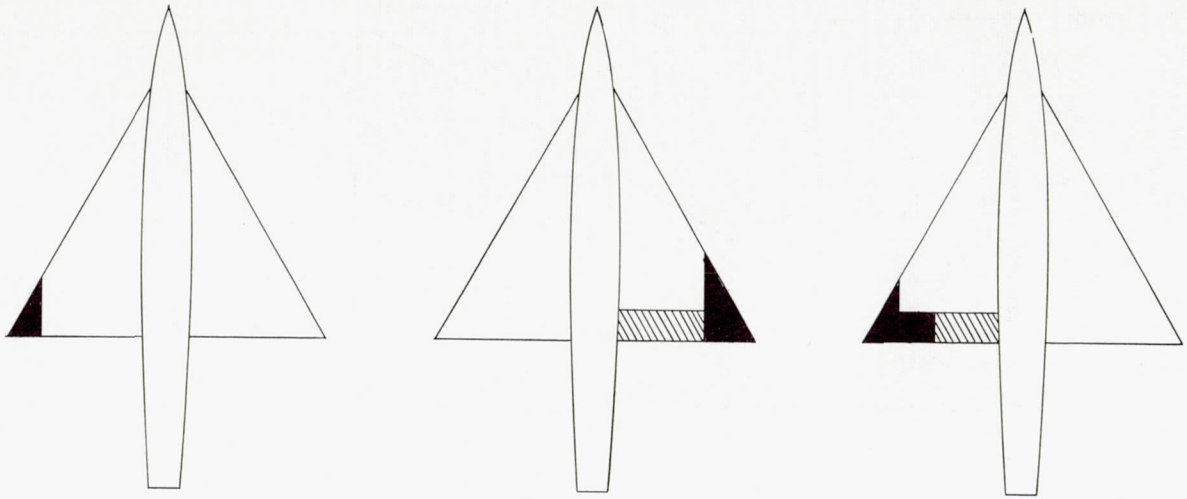


Figure 2.- Principal dimensions. All dimensions are in inches.



Control A	
Half-delta type	
Control area	0.05 S/2
Control MAC	3.92 ft
Hinge line location, % control root chord	.58
Inboard end of control	.78 b/2
Outboard end of control	1.00 b/2

Control B	
Half-delta type	
Control area	0.10 S/2
Control MAC	5.50 ft
Hinge line location, % control root chord	.58
Inboard end of control	..68 b/2
Outboard end of control	1.00 b/2

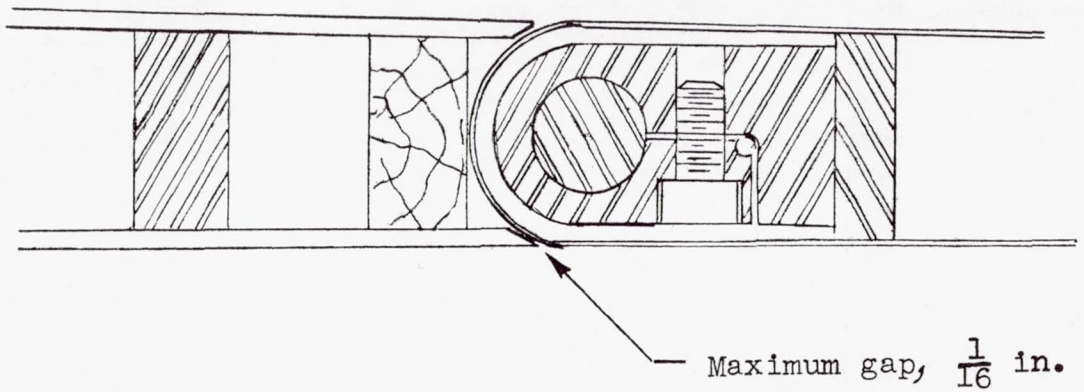
Inboard Flap	
Plain trailing-edge type	
Flap area rearward of hinge line	.119 S/2
Flap chord	2.8 ft
Inboard end at fuselage	
Outboard end	.68b/2

Control C	
Horn-balance type	
Control area	0.10 S/2
Area rearward of hinge line	.087 S/2
Moment area	.125 S/2
Hinge-line location ahead of trailing edge	33.8 in.
Inboard end of control	.54 b/2
Outboard end of control	1.00 b/2

Inboard Flap	
Plain trailing-edge type	
Flap area rearward of hinge line	.091 S/2
Flap chord	2.8 ft
Inboard end at fuselage	
Outboard end	.54 b/2

(a) Control arrangement.

Figure 3.- Location and description of control and flap configurations tested.



(b) Typical section showing the gap between the flap and the wing and the friction clamp.

Figure 3.- Concluded.

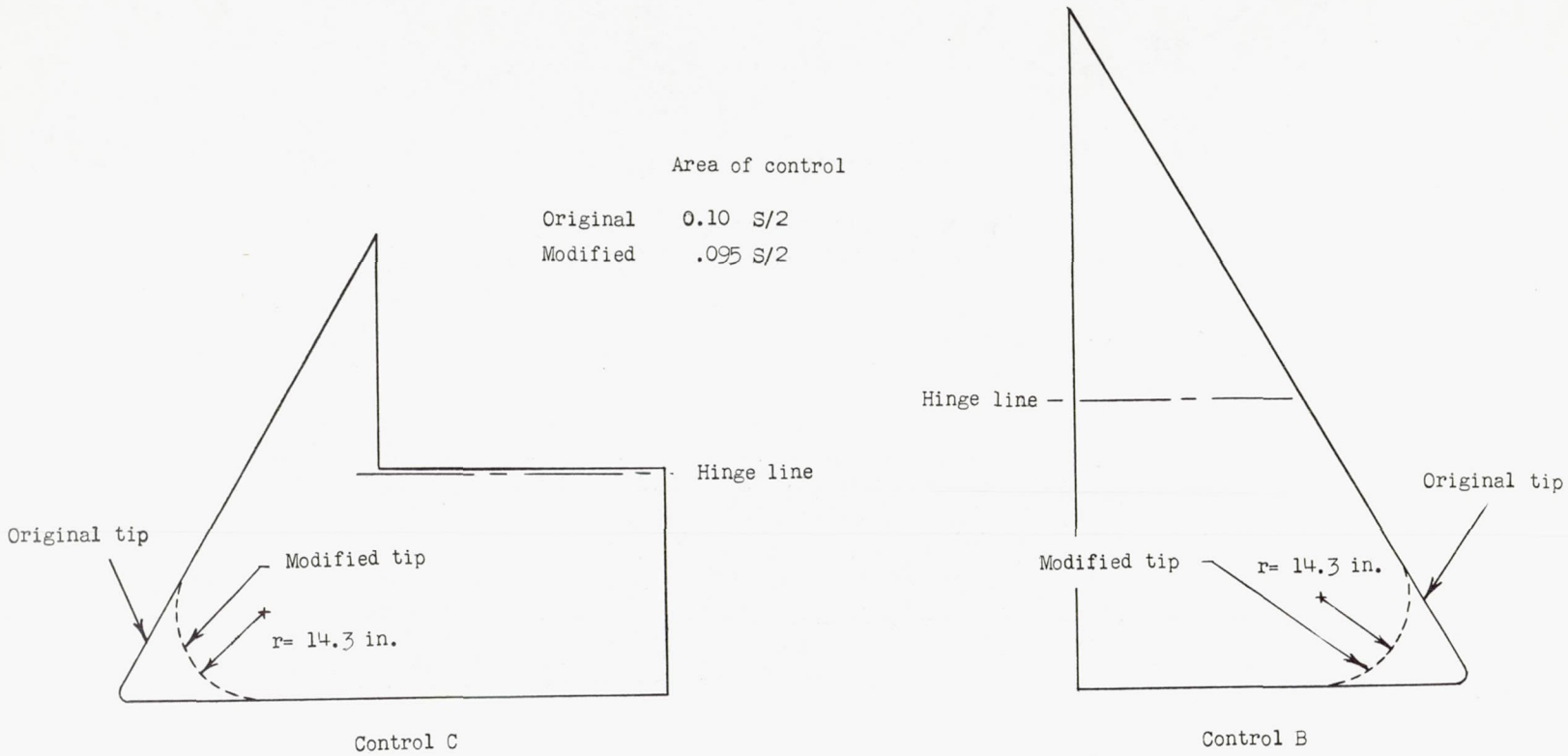


Figure 4.- Sketch of controls B and C indicating original and modified tip arrangements.

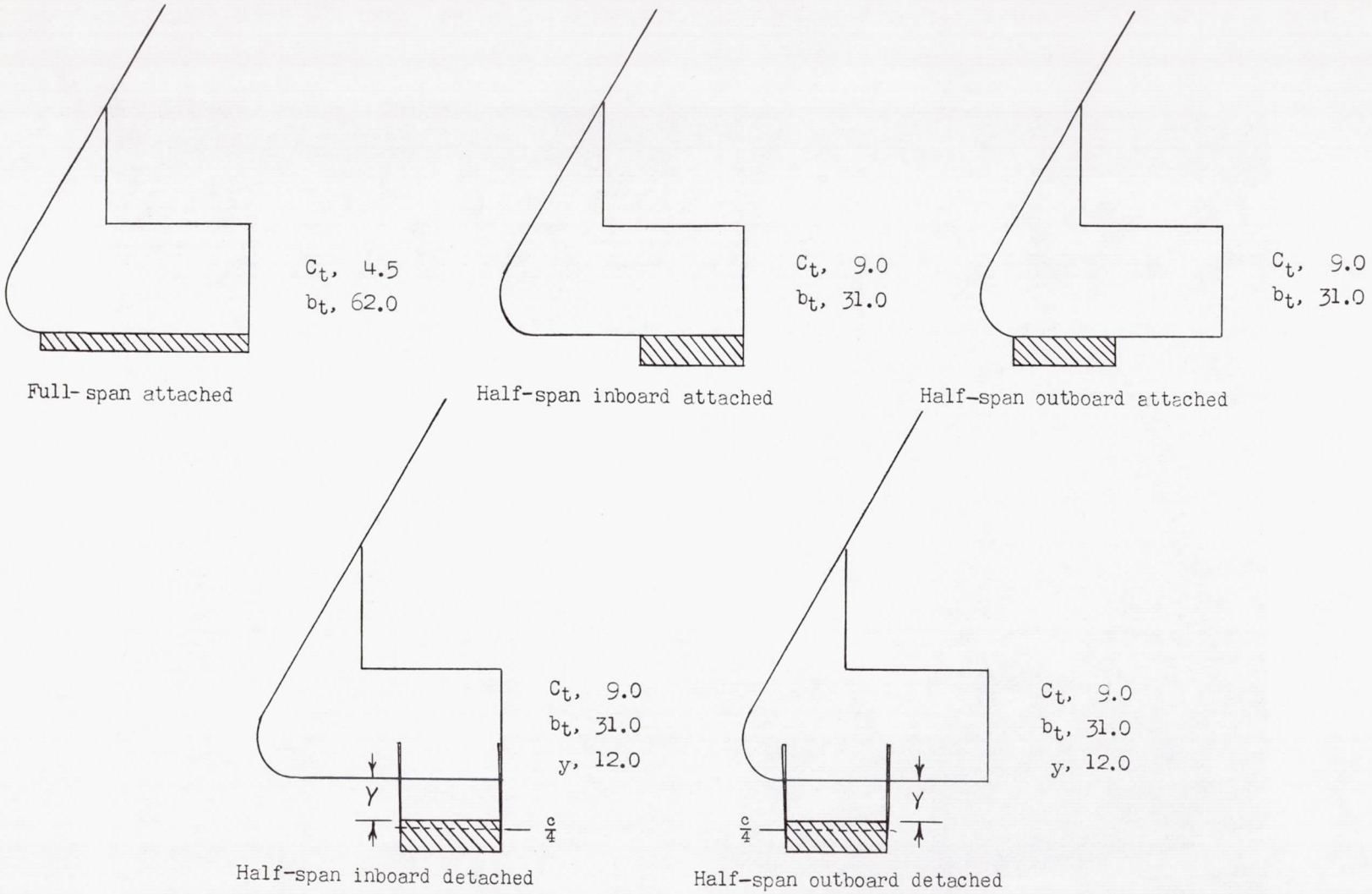
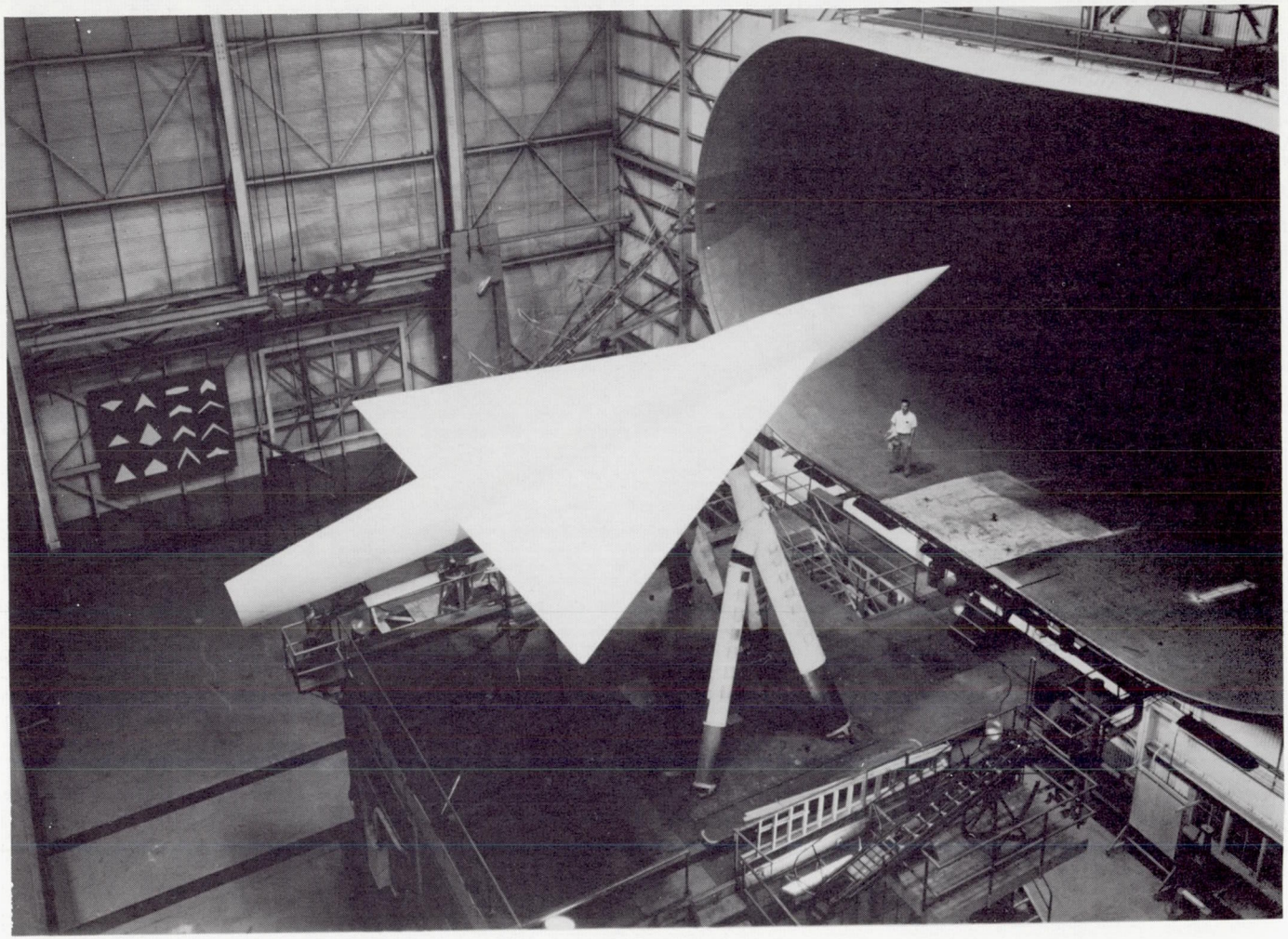


Figure 5.- Balancing-tab configurations tested on the horn-balance-type control. $S_a/S = 0.10$; $\delta_t/\delta_a = -1.0$. All dimensions are in inches.



L-77421

Figure 6.- Photograph of the model in the Langley full-scale tunnel test section.

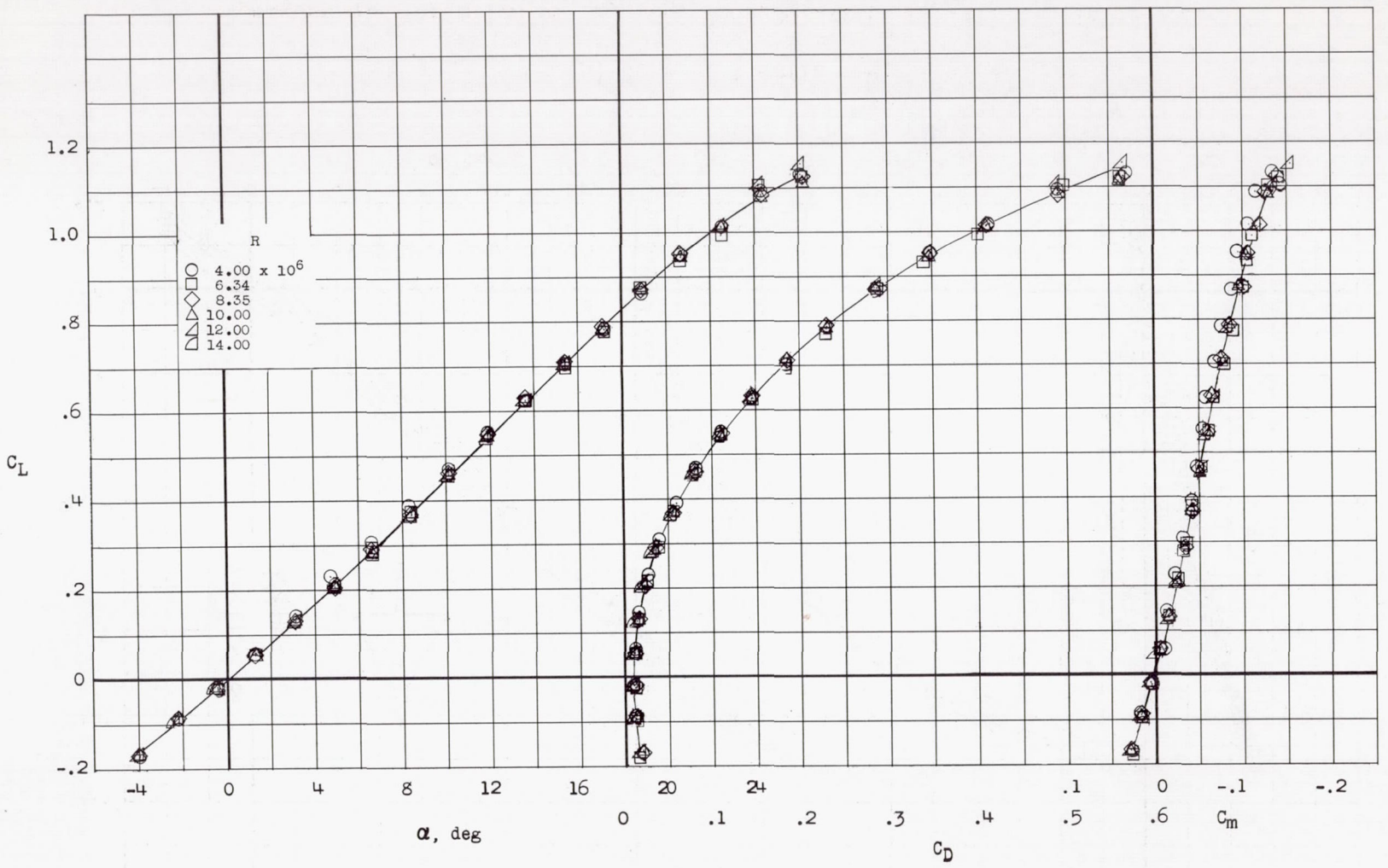


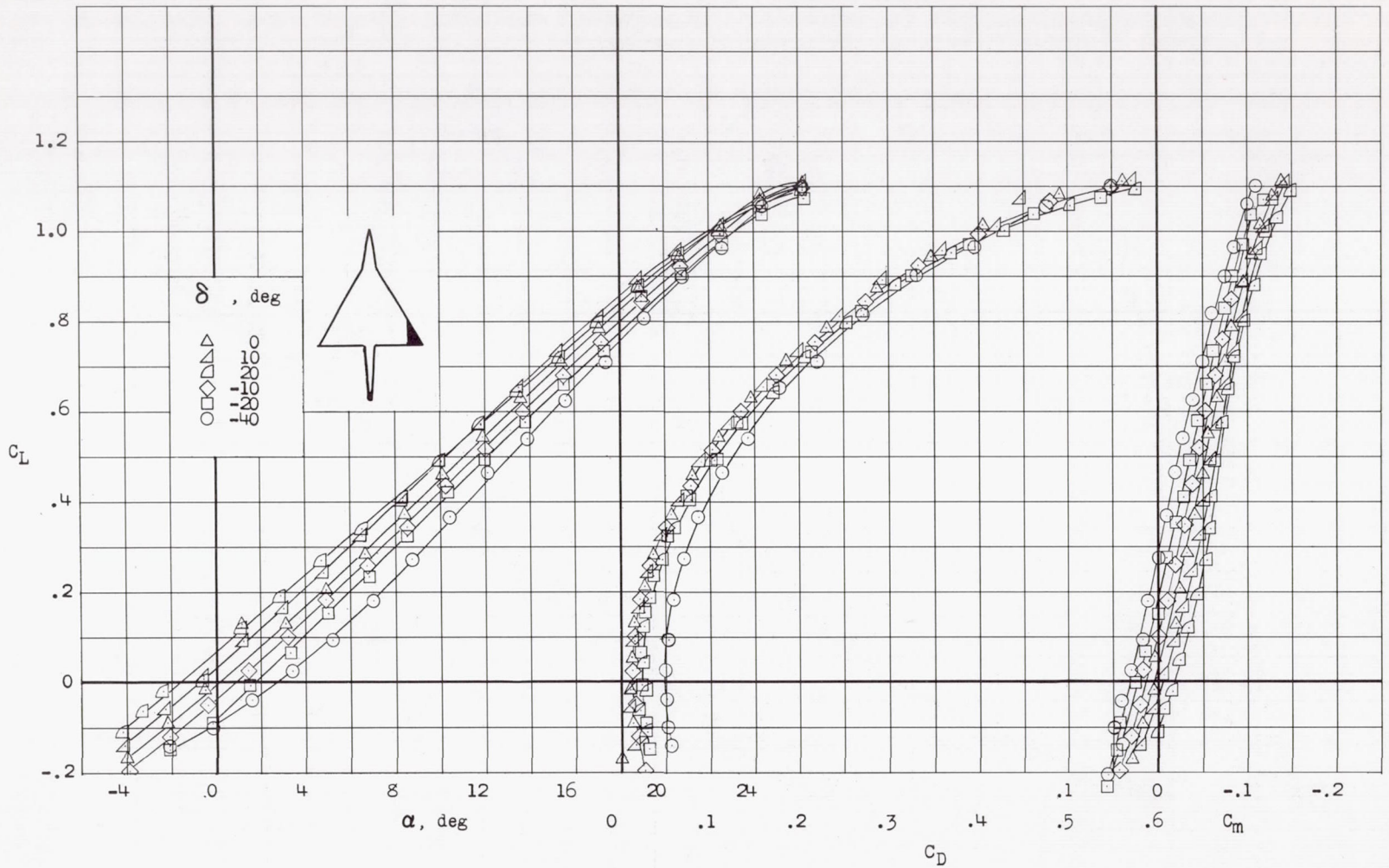
Figure 7.- Variation of α, C_D, and C_m with C_L for the large-scale delta-wing model with controls and flap neutral for several Reynolds numbers.



(a) Control A deflected.

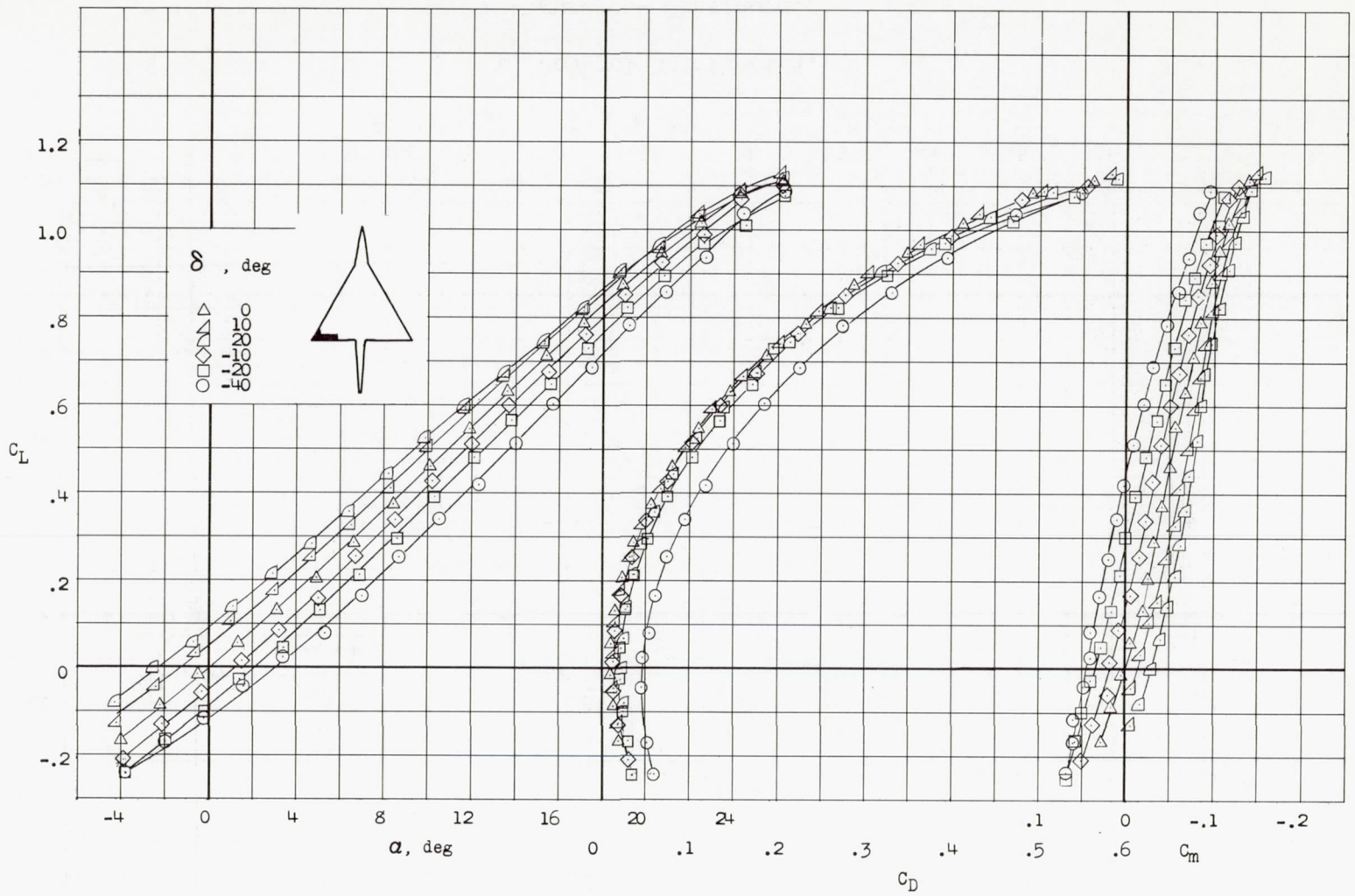
Figure 8.- Variation of α, C_D, and C_m with C_L for the large-scale delta-wing model with controls deflected.

CONFIDENTIAL



(b) Control B deflected.

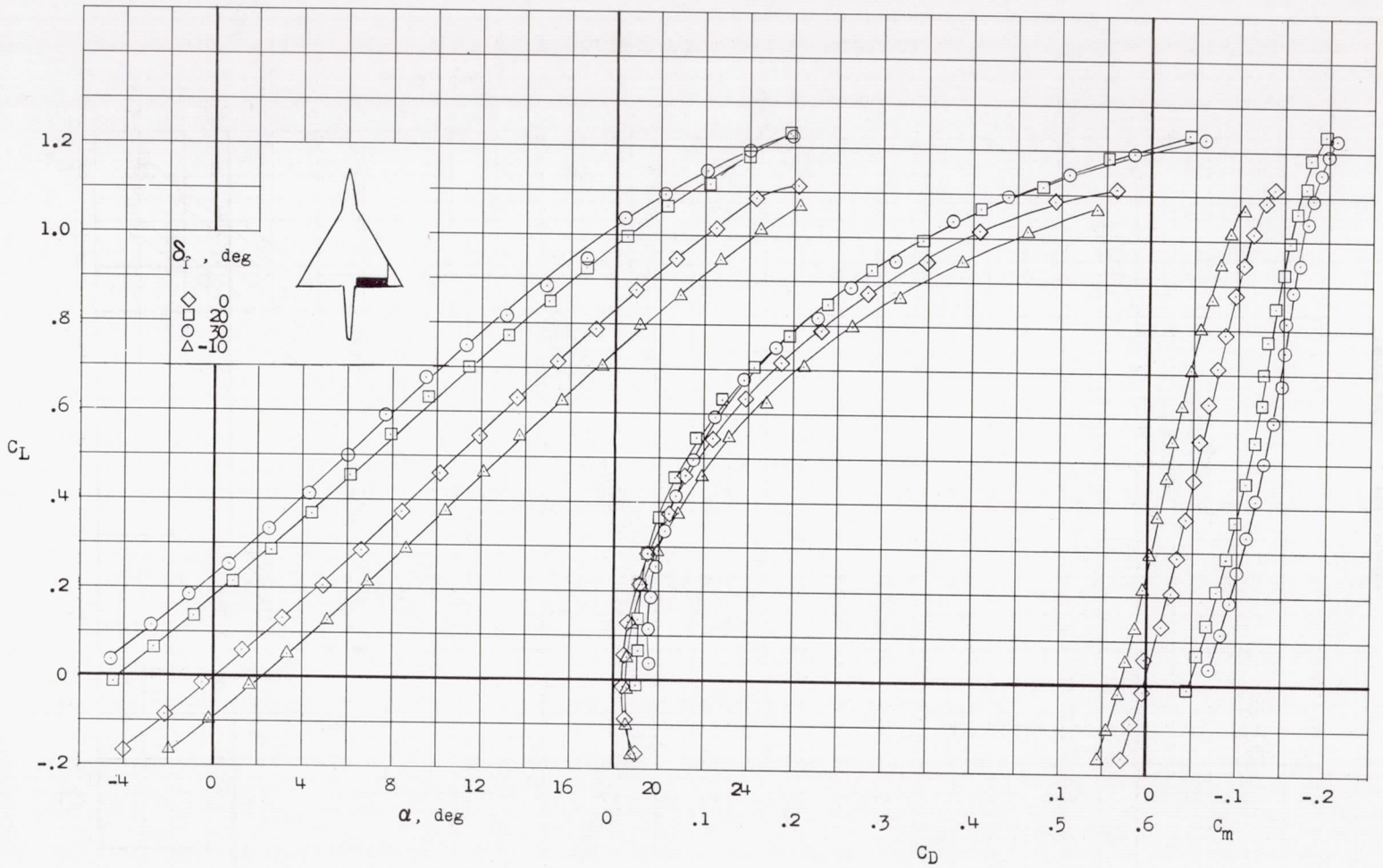
Figure 8.- Continued.



(c) Control C deflected.

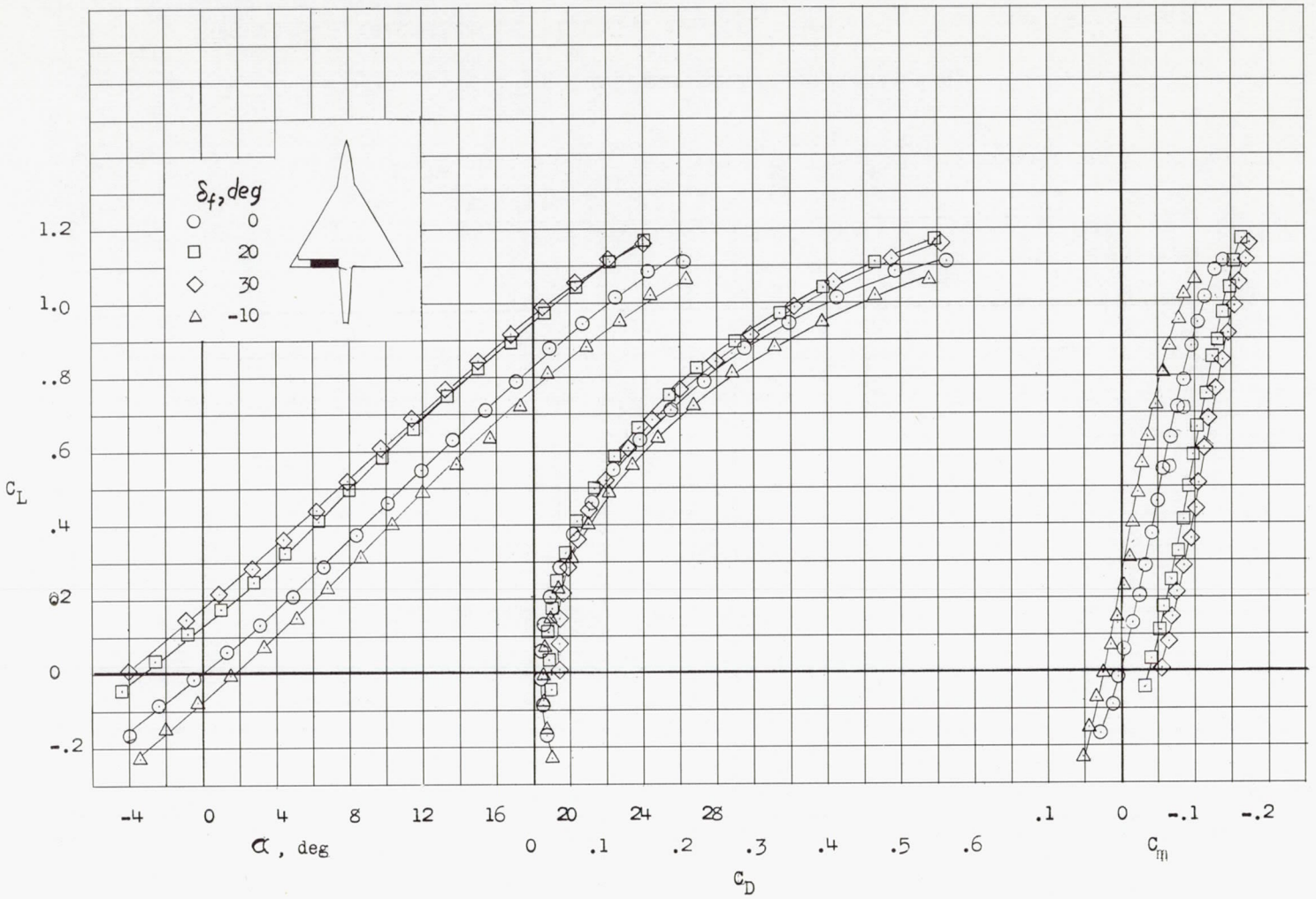
Figure 8.- Concluded.

CONFIDENTIAL



(a) Flap configuration for control B.

Figure 9.- Variation of α, C_D, and C_m with C_L for the large-scale delta-wing model with controls 0° and flap deflected.



(b) Flap configuration for control C.

Figure 9.- Concluded.

CONFIDENTIAL

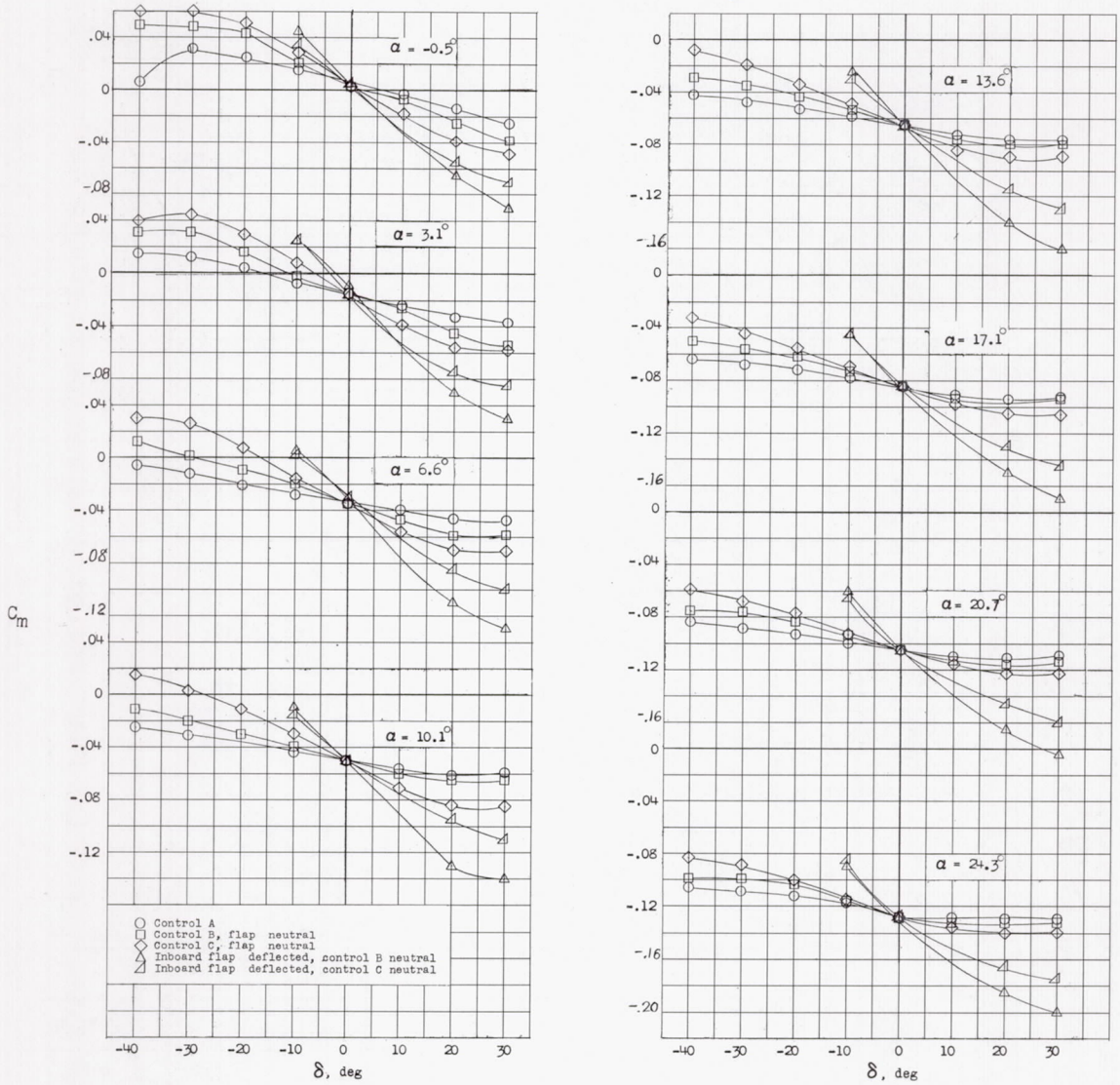


Figure 10.- Variation of pitching-moment coefficient with control deflection for controls A, B, and C with flap 0°.

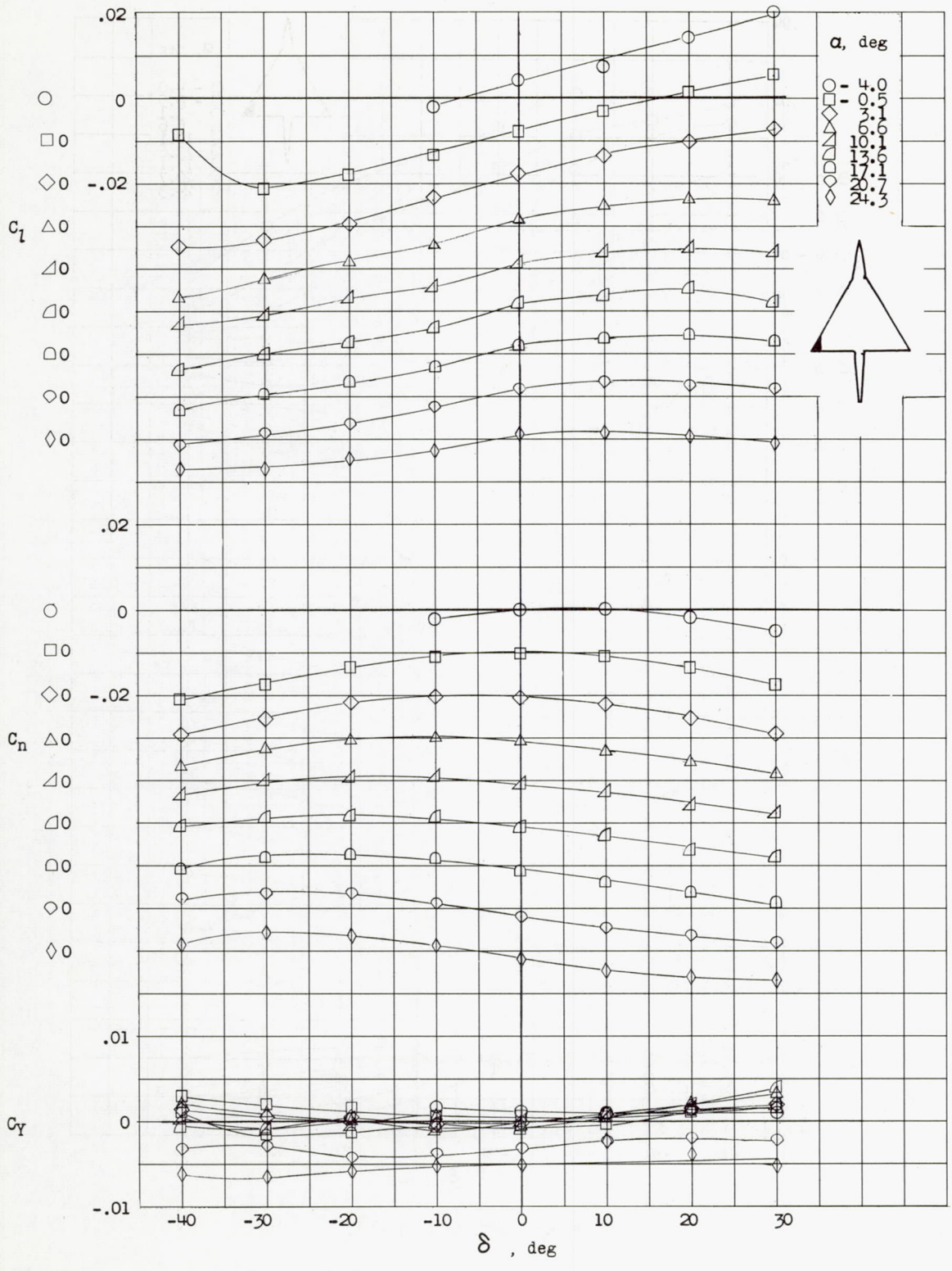
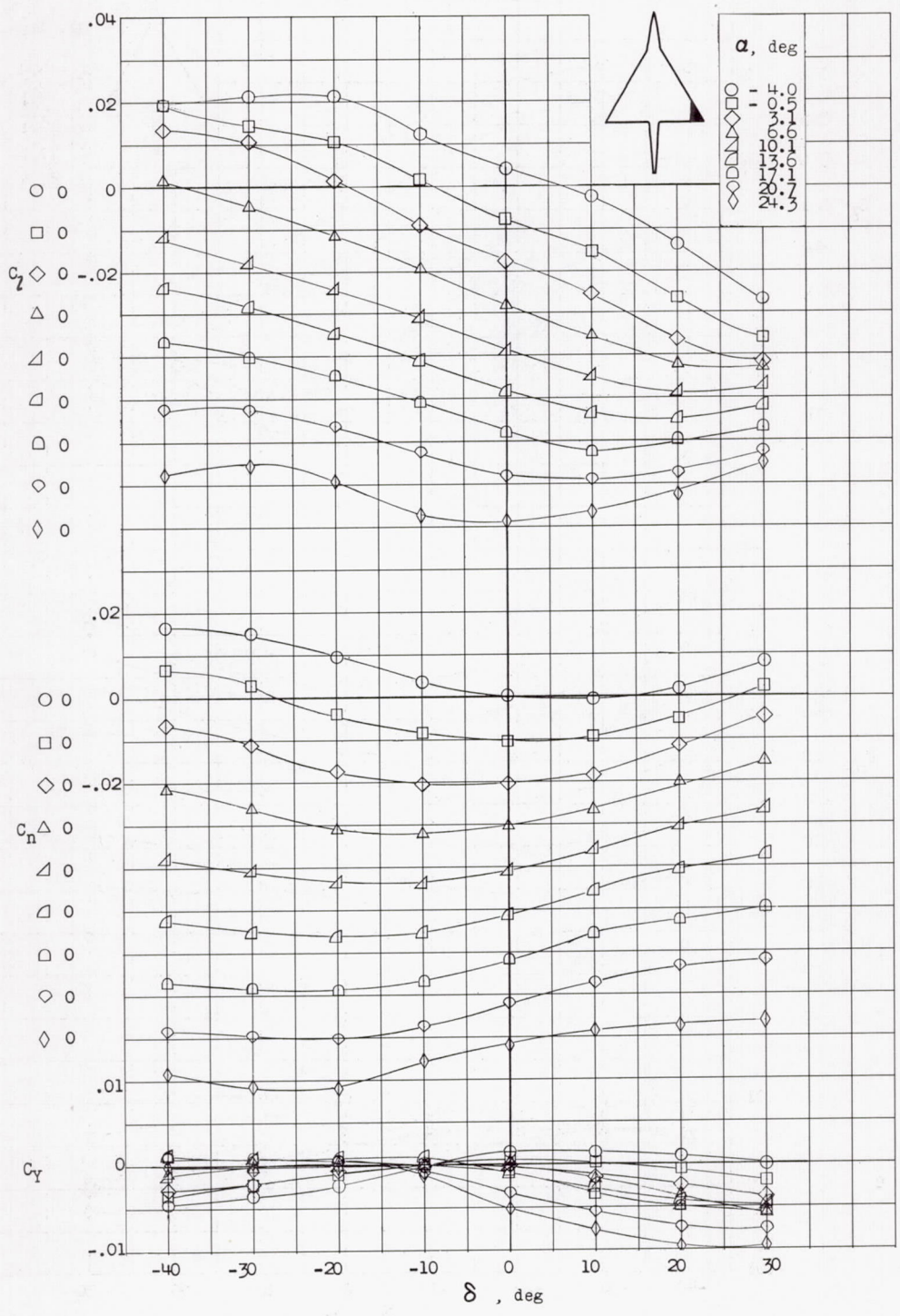
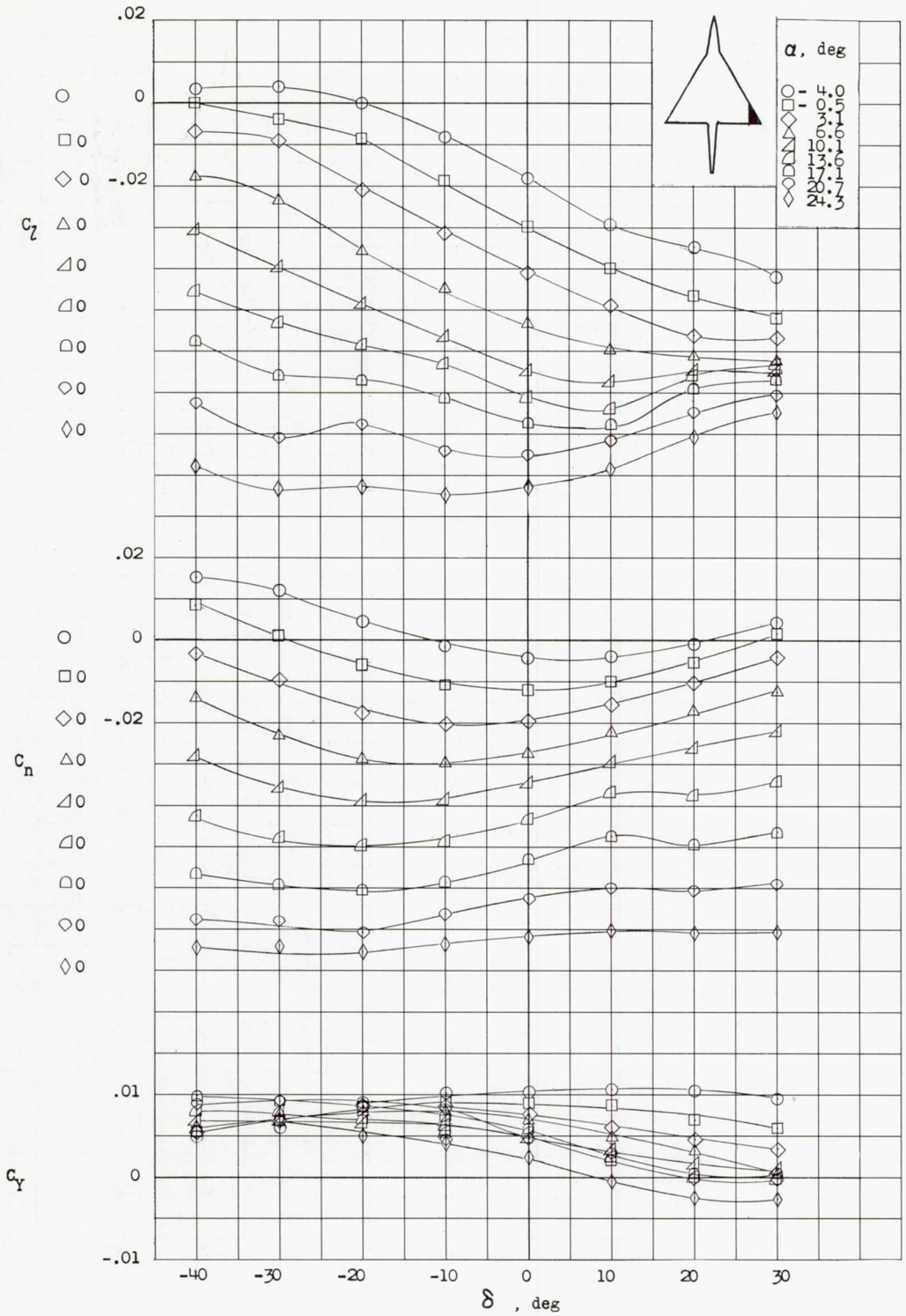


Figure 11.- Variation of C_l, C_n, and C_Y with control deflection. Flap deflection 0°. Control A.



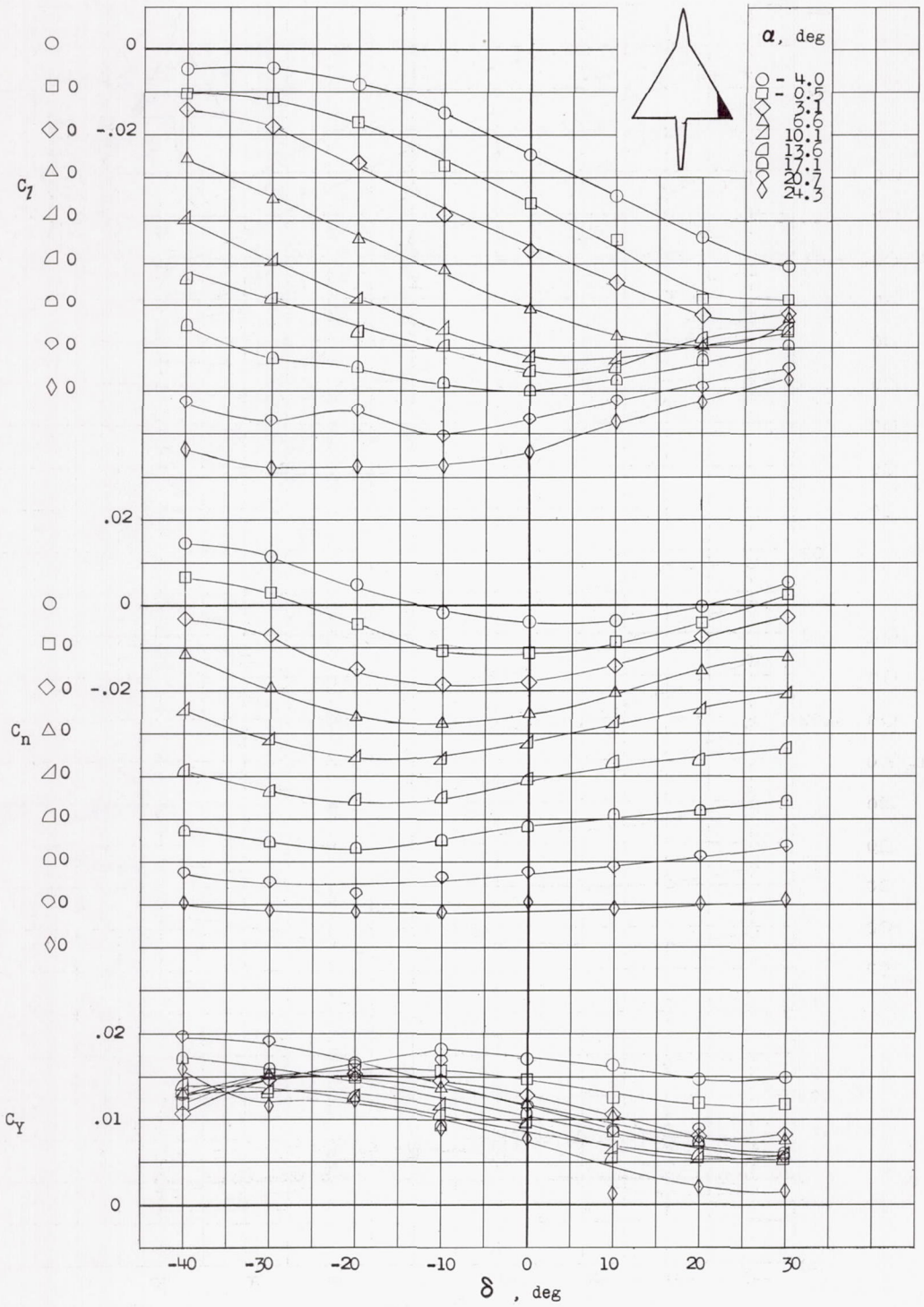
(a) Flap deflected 0°.

Figure 12.- Variation of C_l, C_n, and C_Y with control deflection with flaps deflected. Control B.



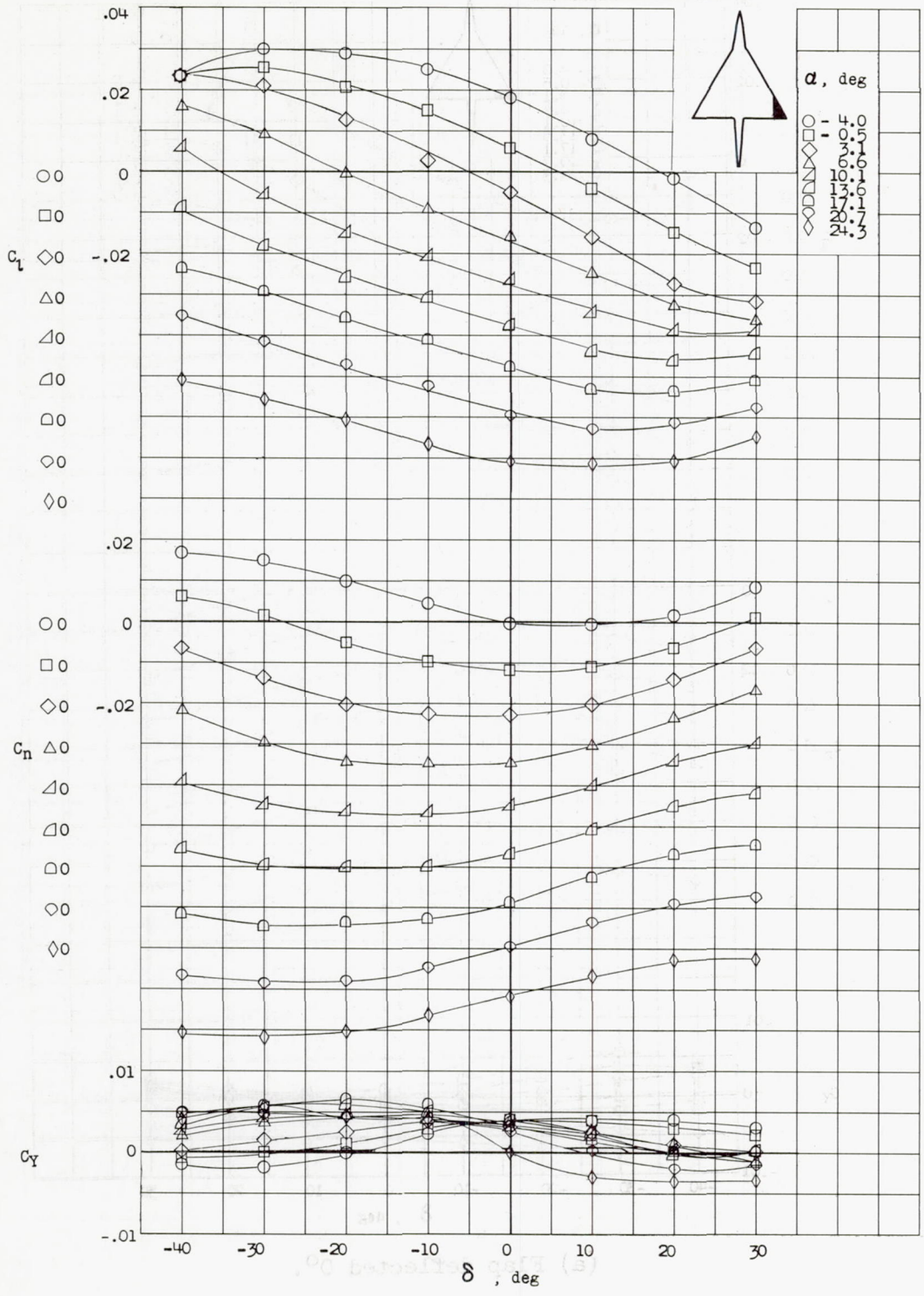
(b) Flap deflected 20°.

Figure 12.- Continued.



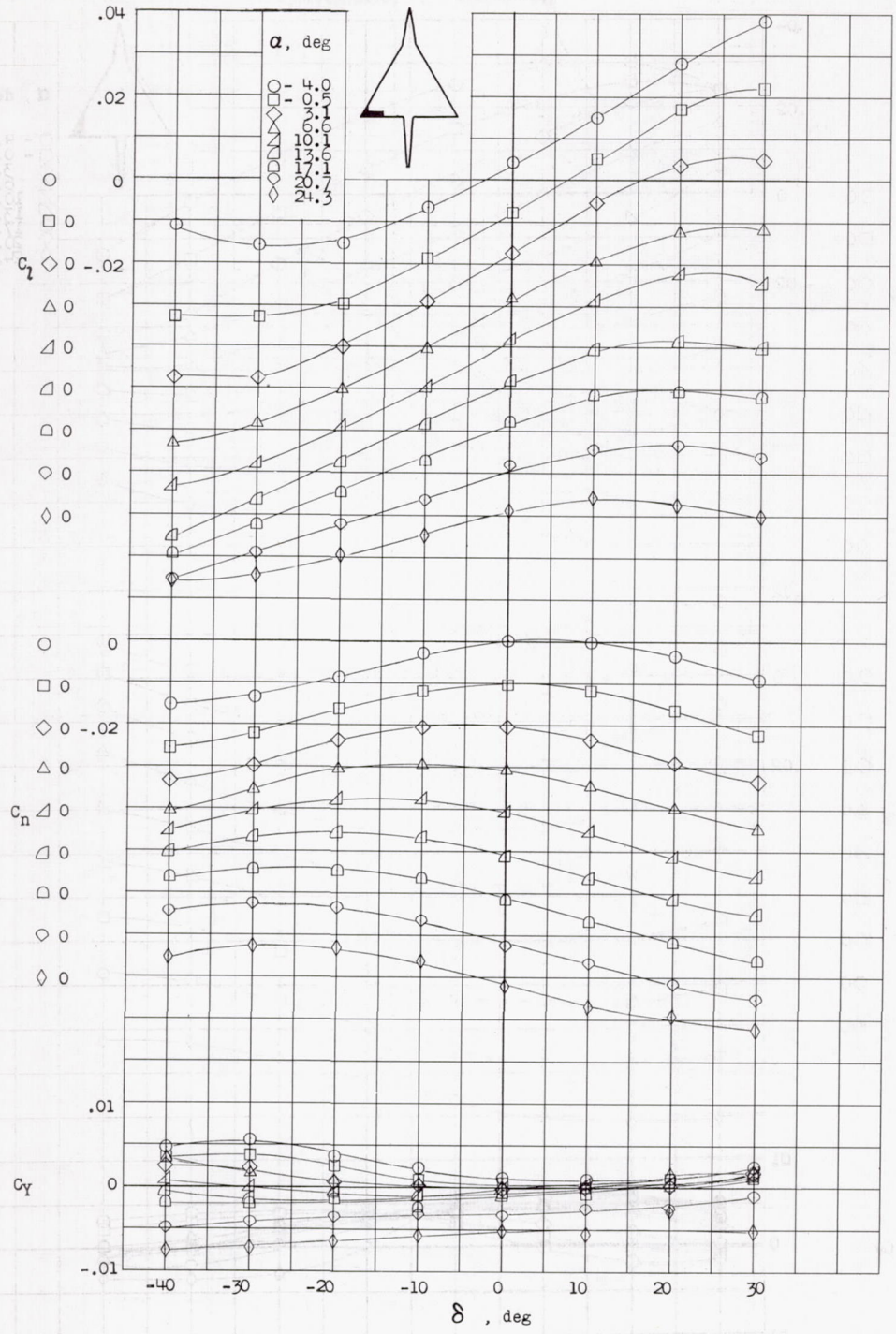
(c) Flap deflected 30°.

Figure 12.- Continued.



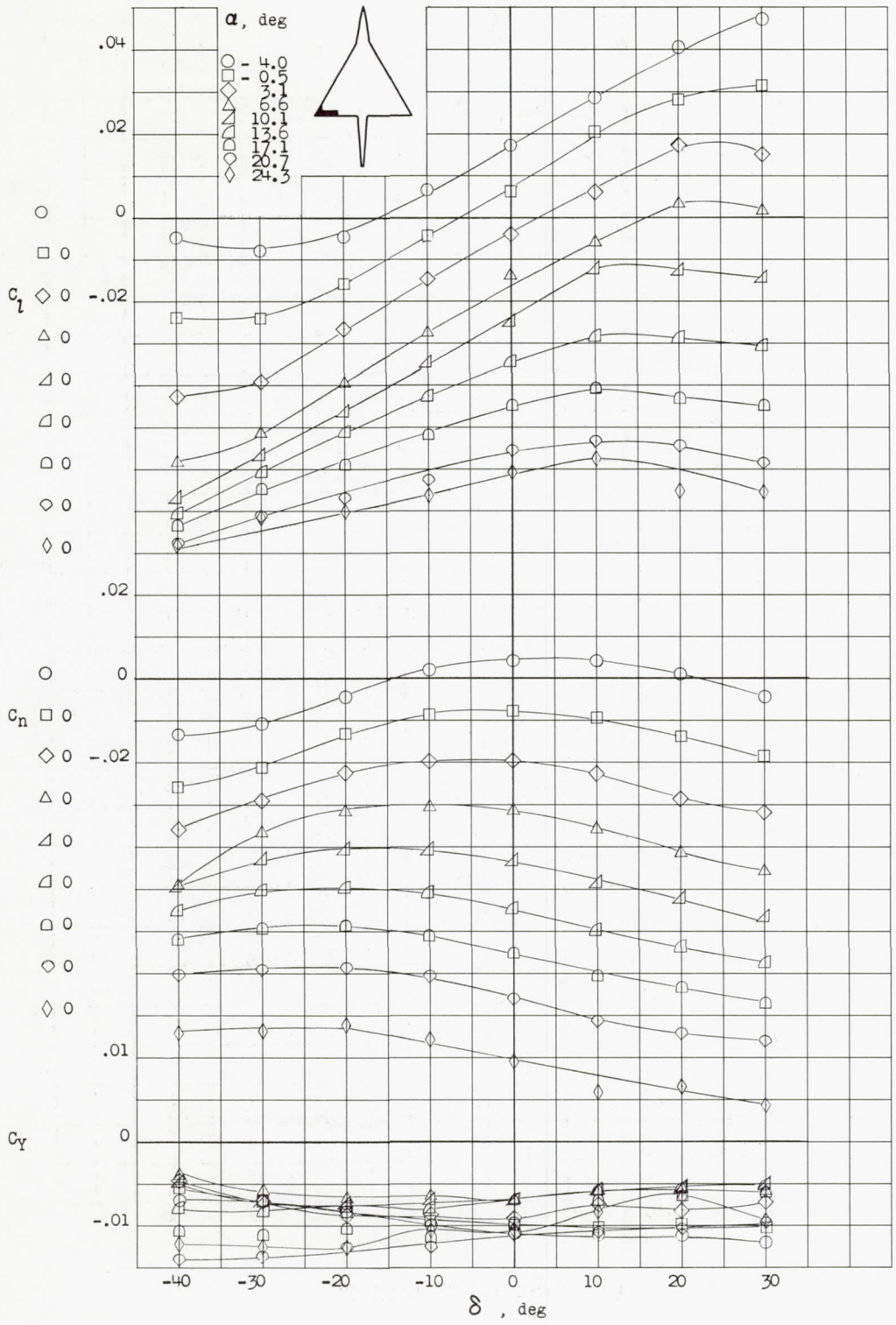
(d) Flap deflected -10°.

Figure 12.- Concluded.



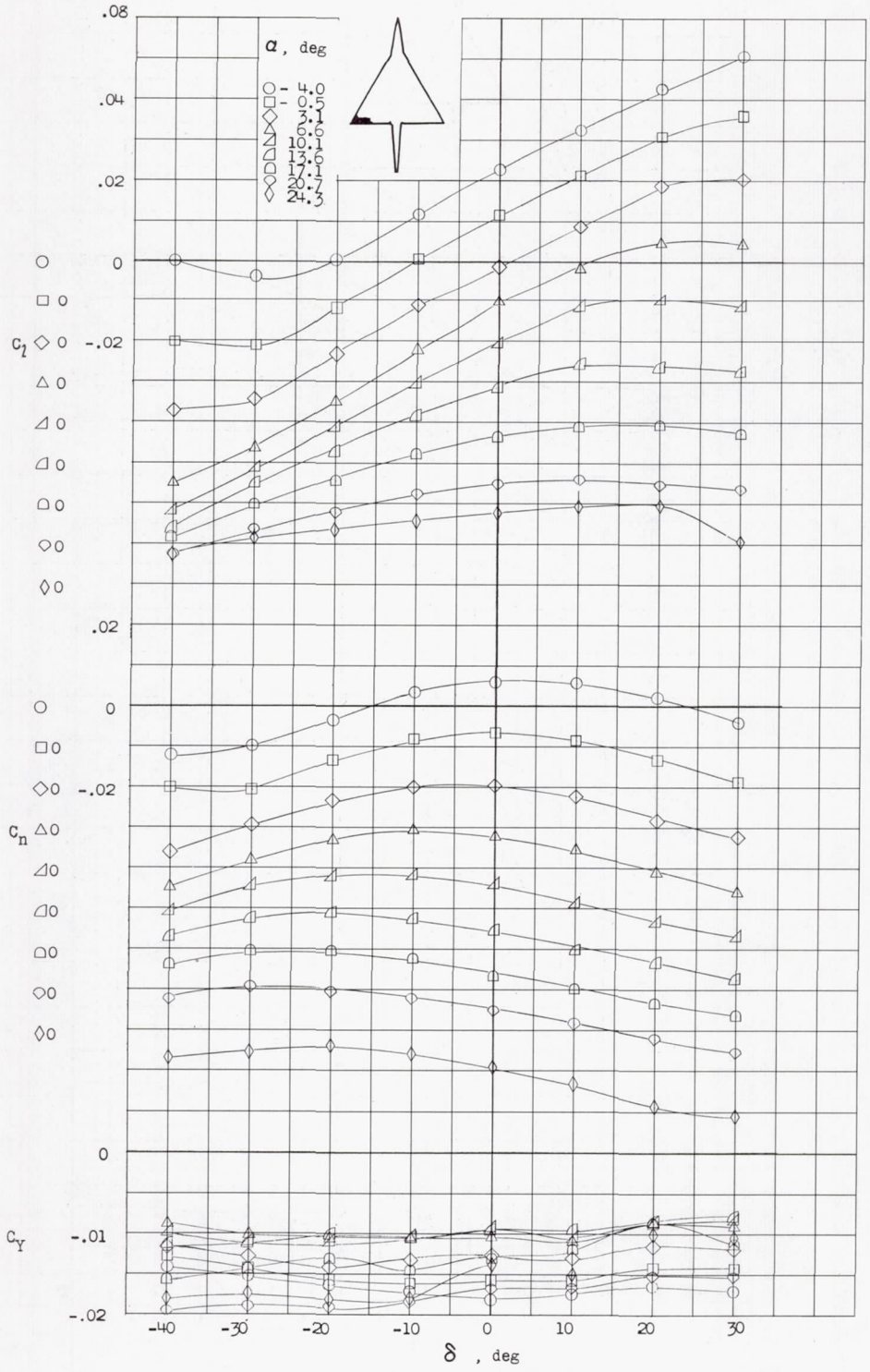
(a) Flap deflected 0°.

Figure 13.- Variation of C_l, C_n, and C_Y with control deflection with flaps deflected. Control C.



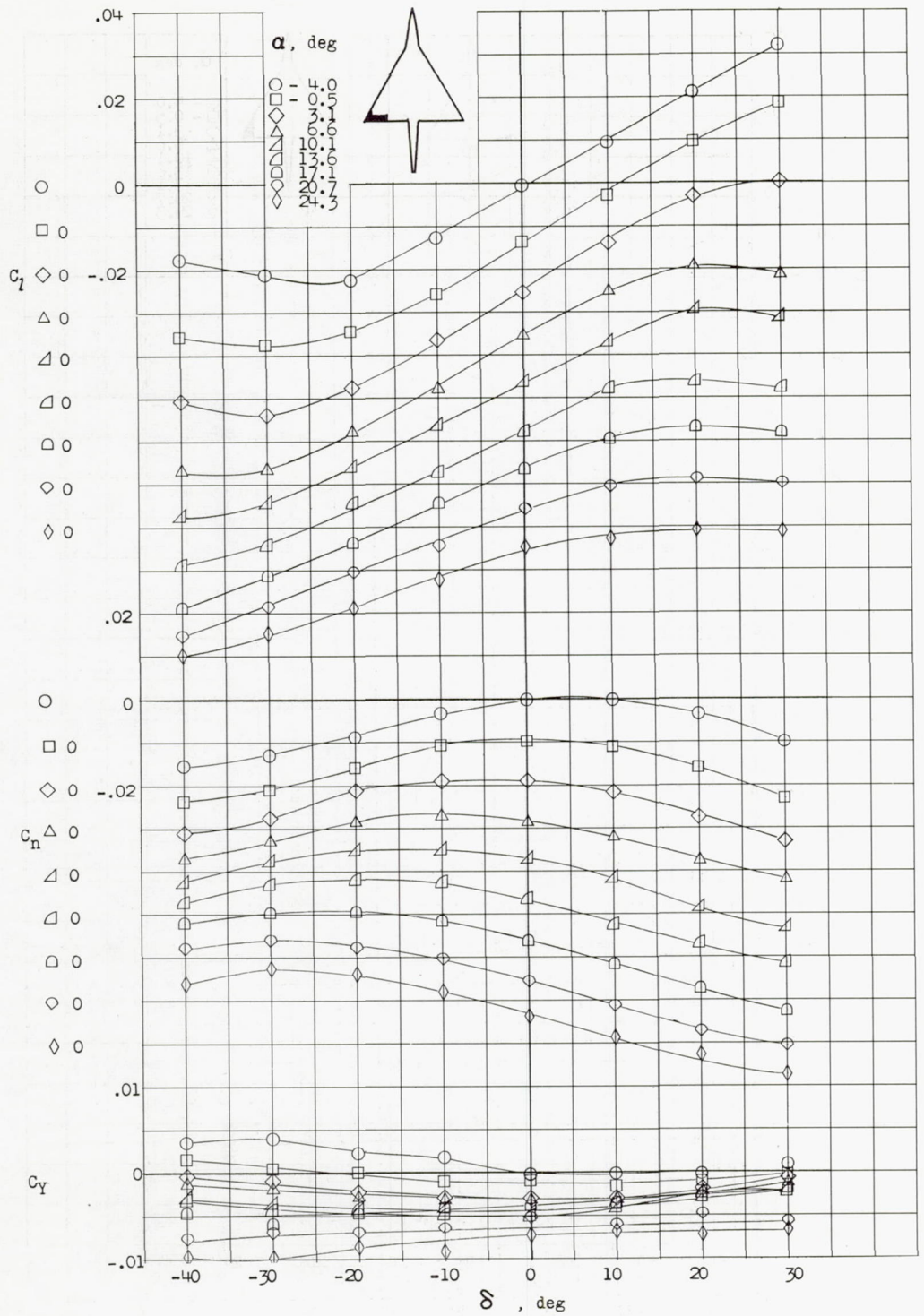
(b) Flap deflected 20°.

Figure 13.- Continued.



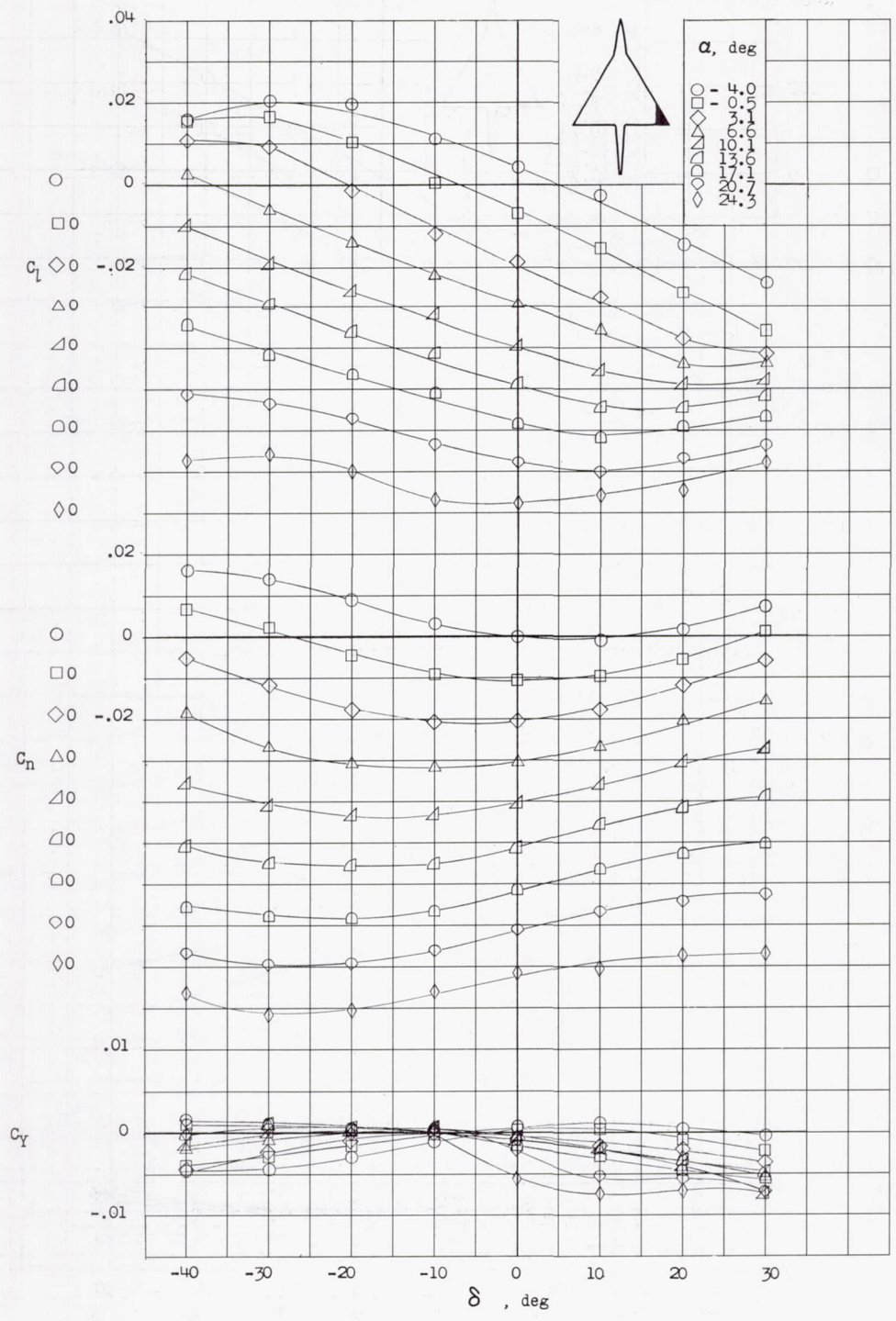
(c) Flap deflected 30°.

Figure 13.- Continued.



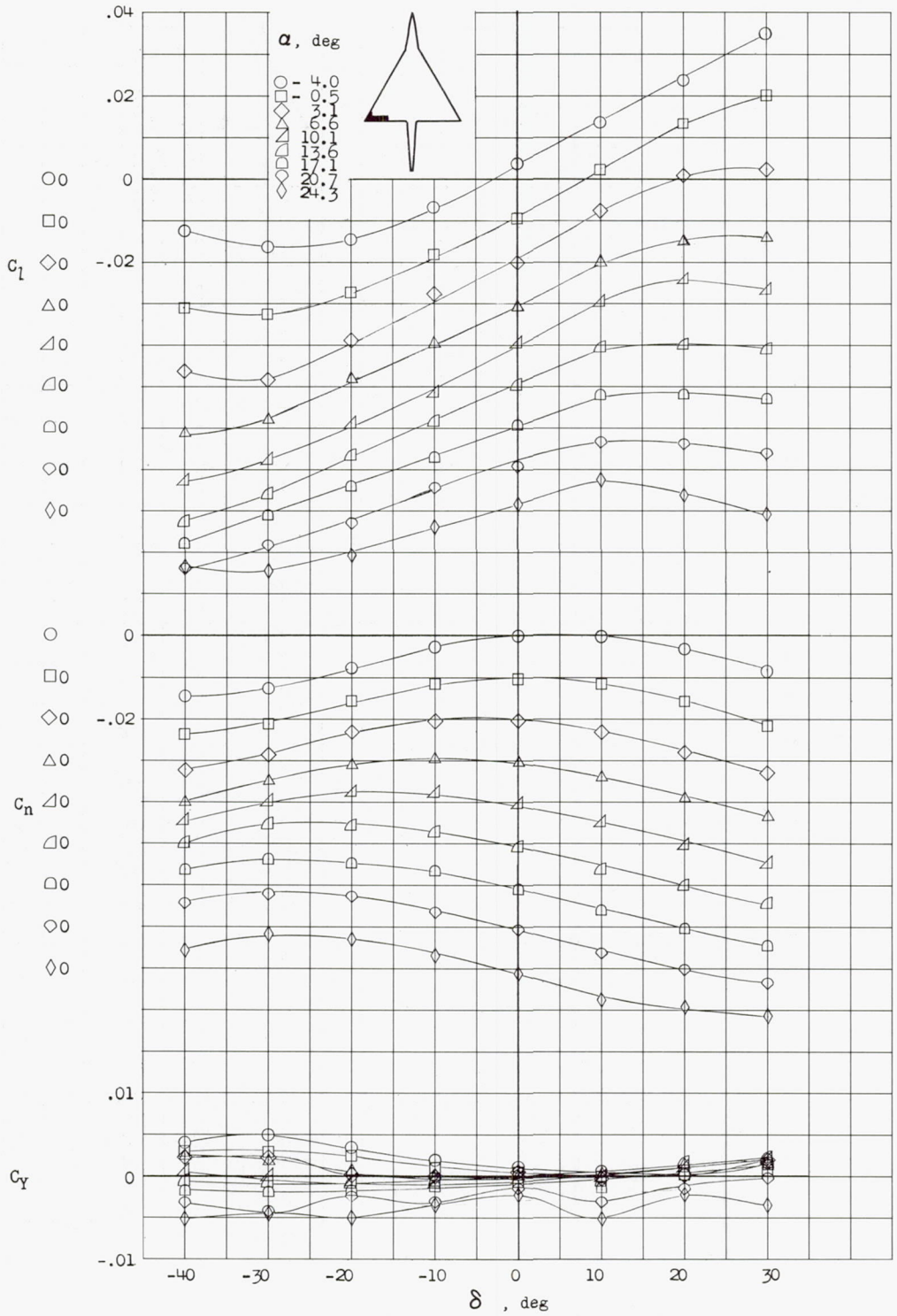
(d) Flap deflected -10°.

Figure 13.- Concluded.



(a) Control B with modified tip.

Figure 14.- Variation of C_l, C_n, and C_Y with control deflection. Flap deflected 0°.



(b) Control C with modified tip.

Figure 14.- Concluded.

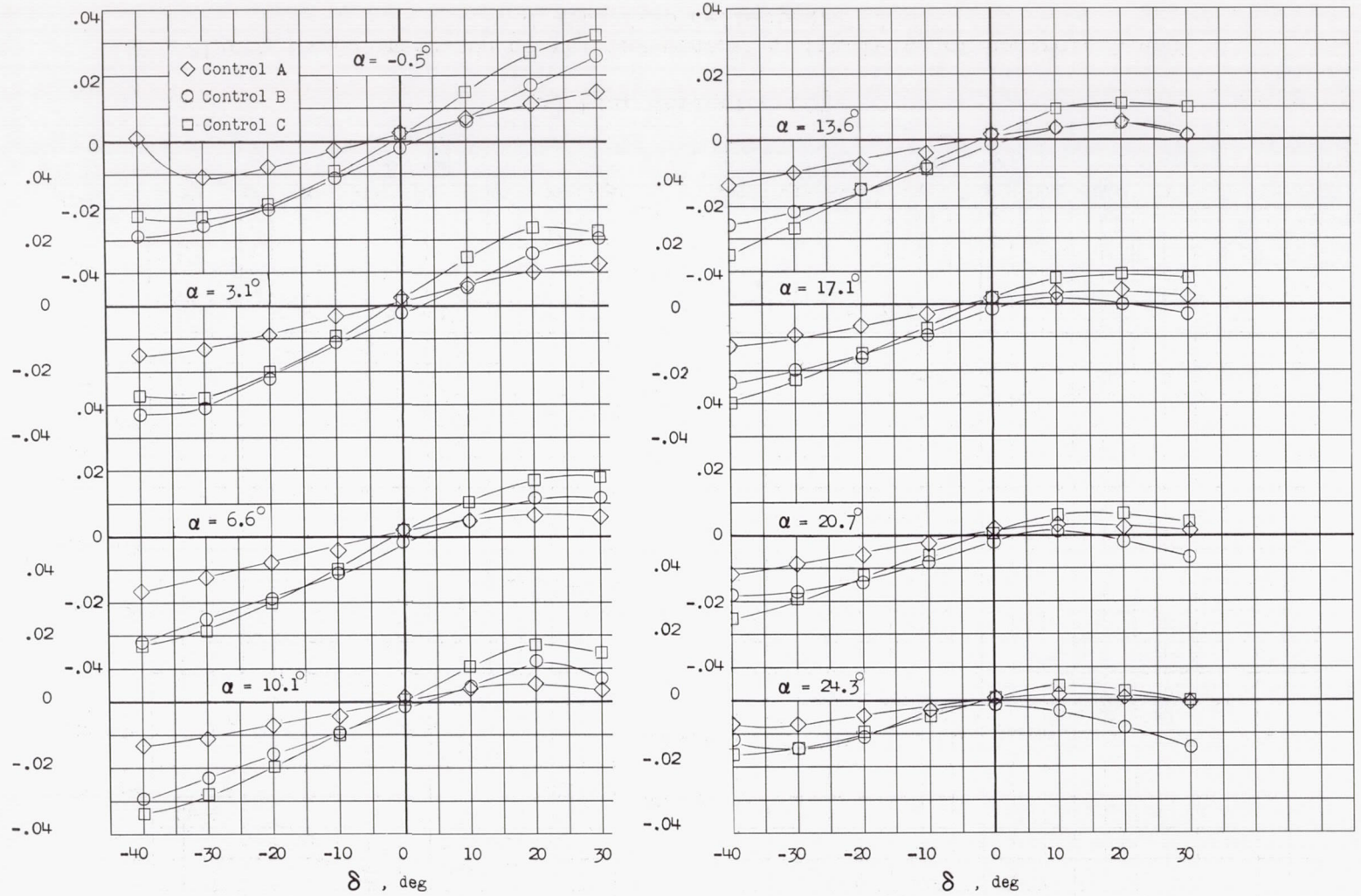
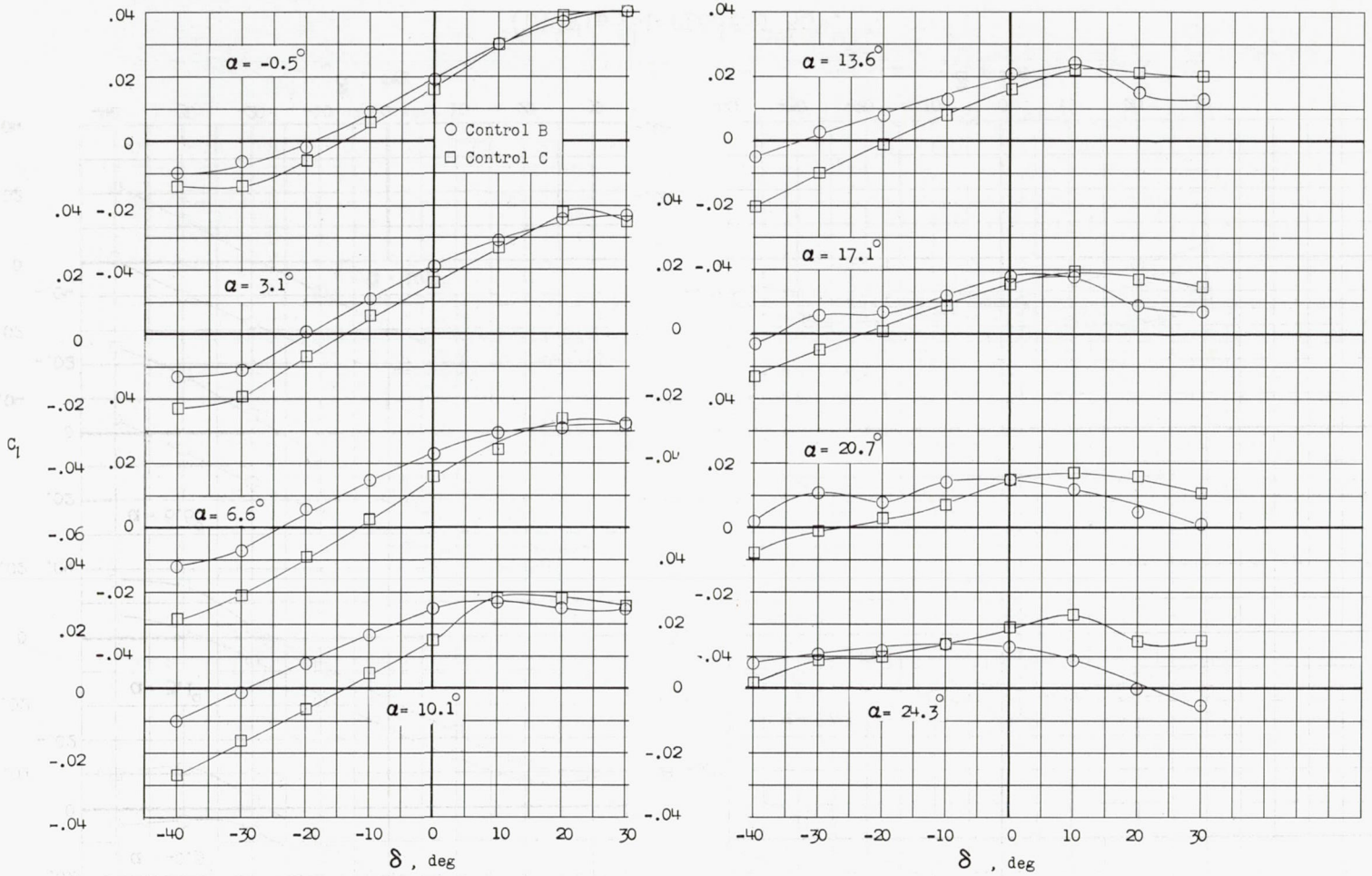


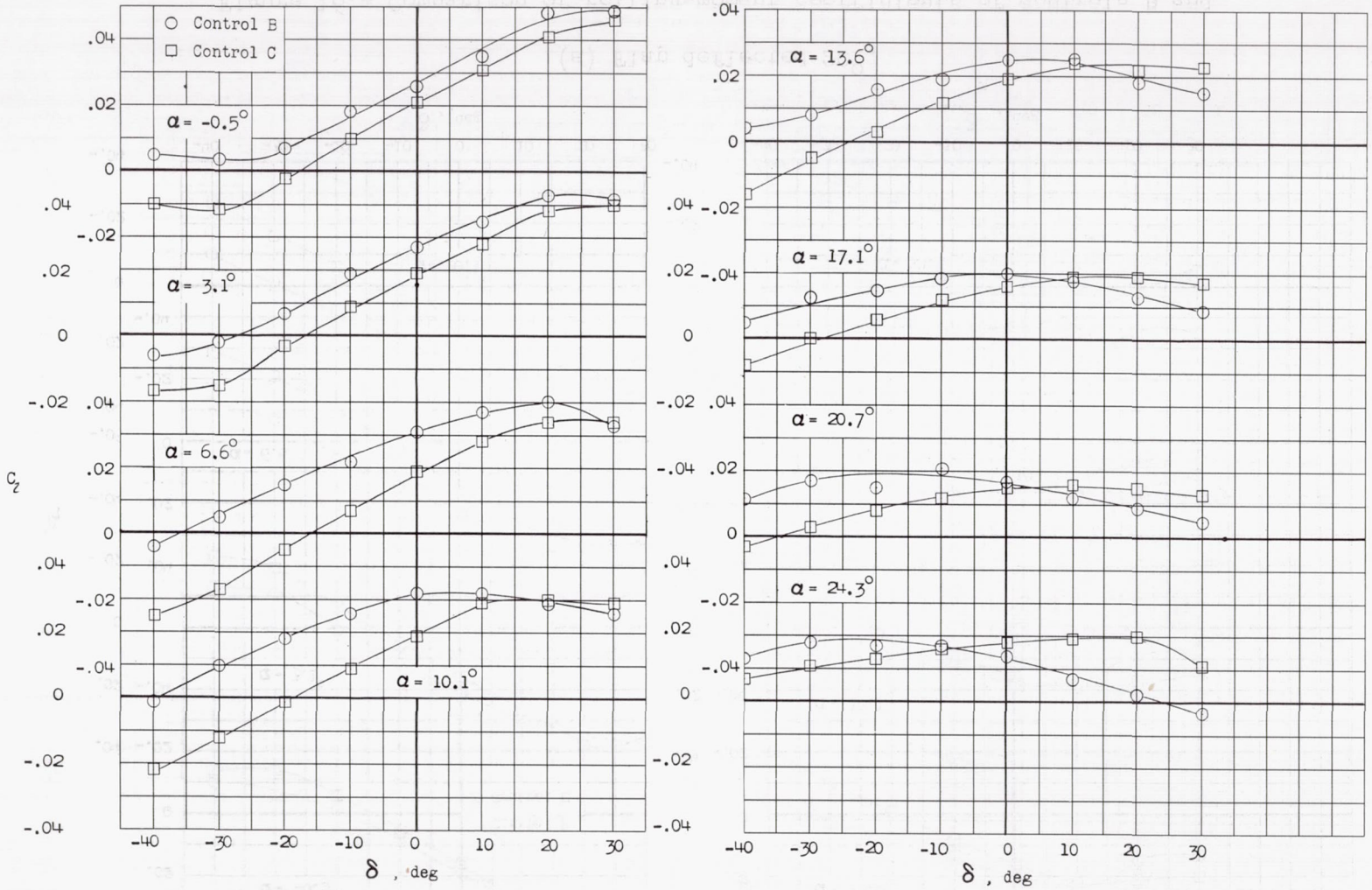
Figure 15.- Comparison of rolling-moment coefficients of controls A, B, and C. Flap deflected 0°.



(a) Flap deflected 20°.

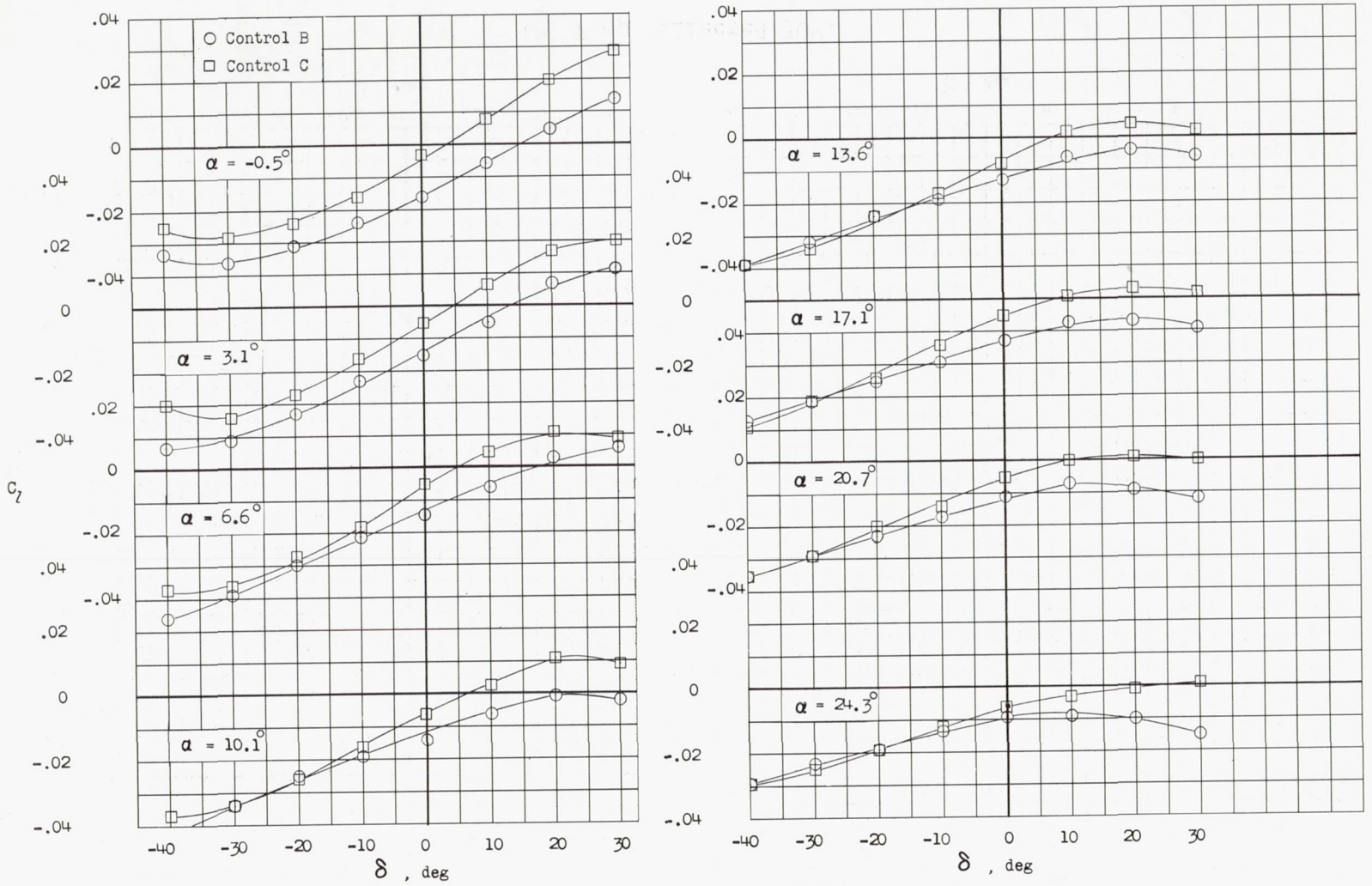
Figure 16.- Comparison of rolling-moment coefficients of controls B and C with flap deflected.

CONFIDENTIAL



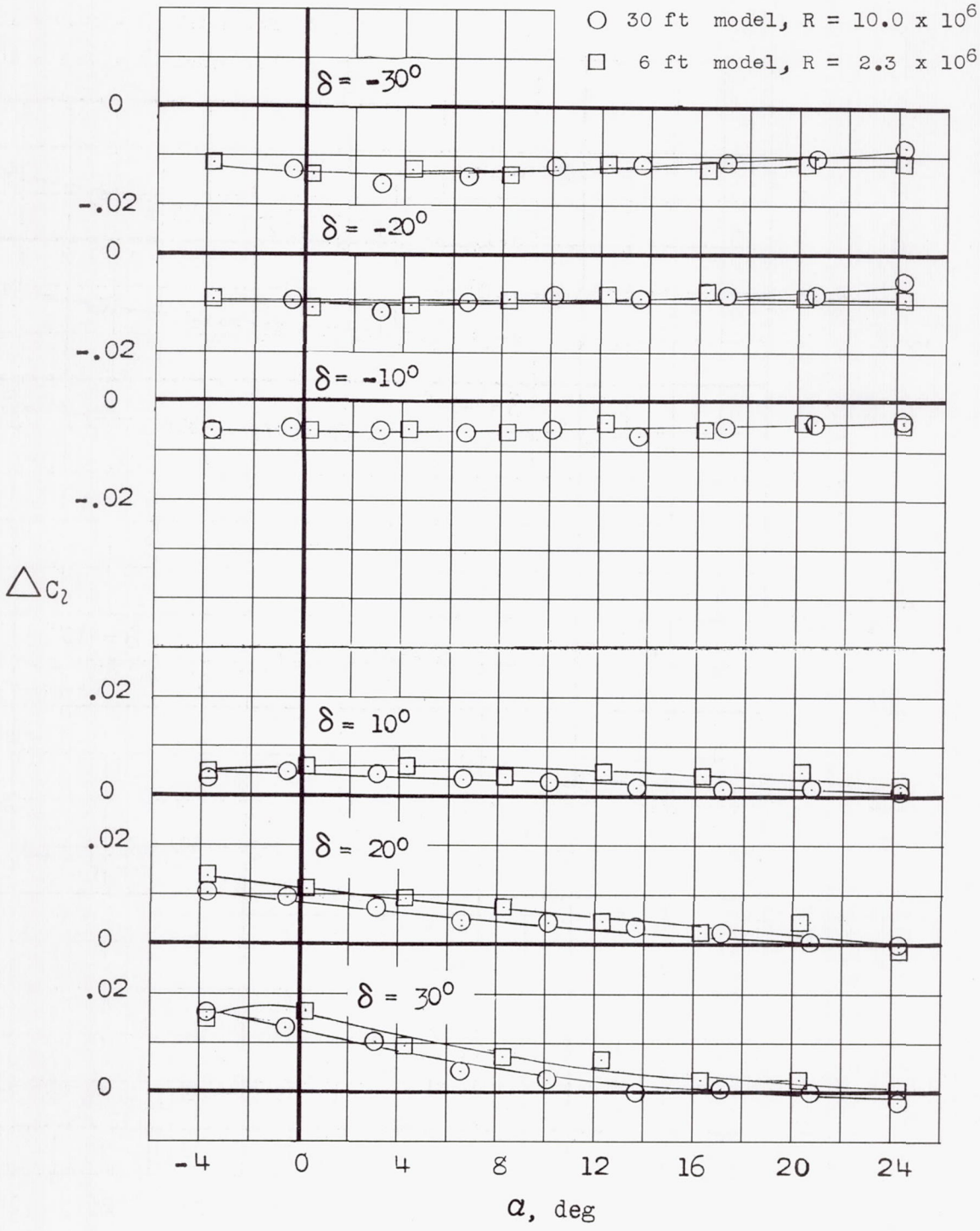
(b) Flap deflected 30°.

Figure 16.- Continued.



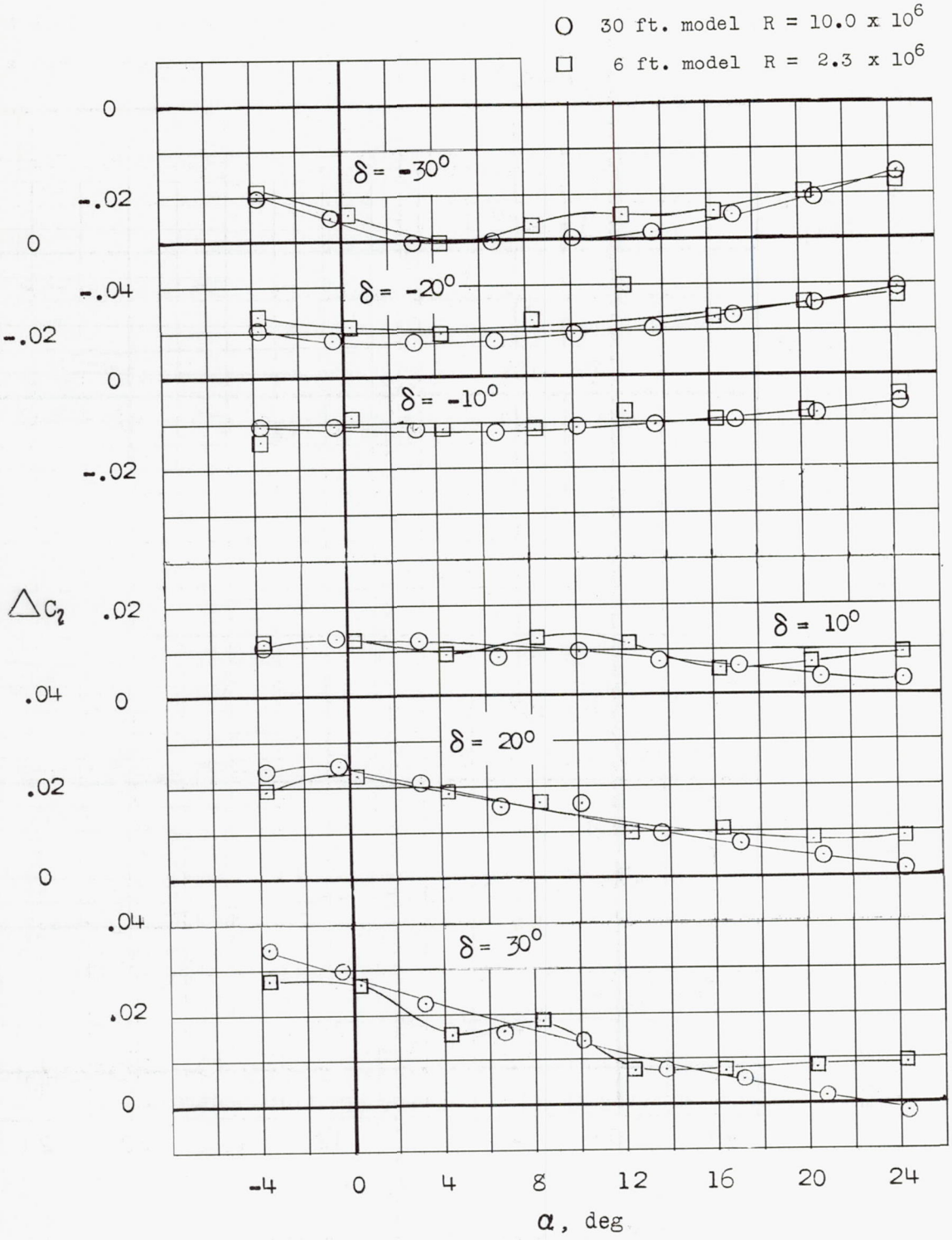
(c) Flap deflected -10°.

Figure 16.- Concluded.



(a) 5-percent half-delta control.

Figure 17.- Variation of rolling-moment coefficient with angle of attack for the 30-foot-span model and the 6-foot-span model of reference 1.



(b) 10-percent horn-balance-type control.

Figure 17.- Concluded.

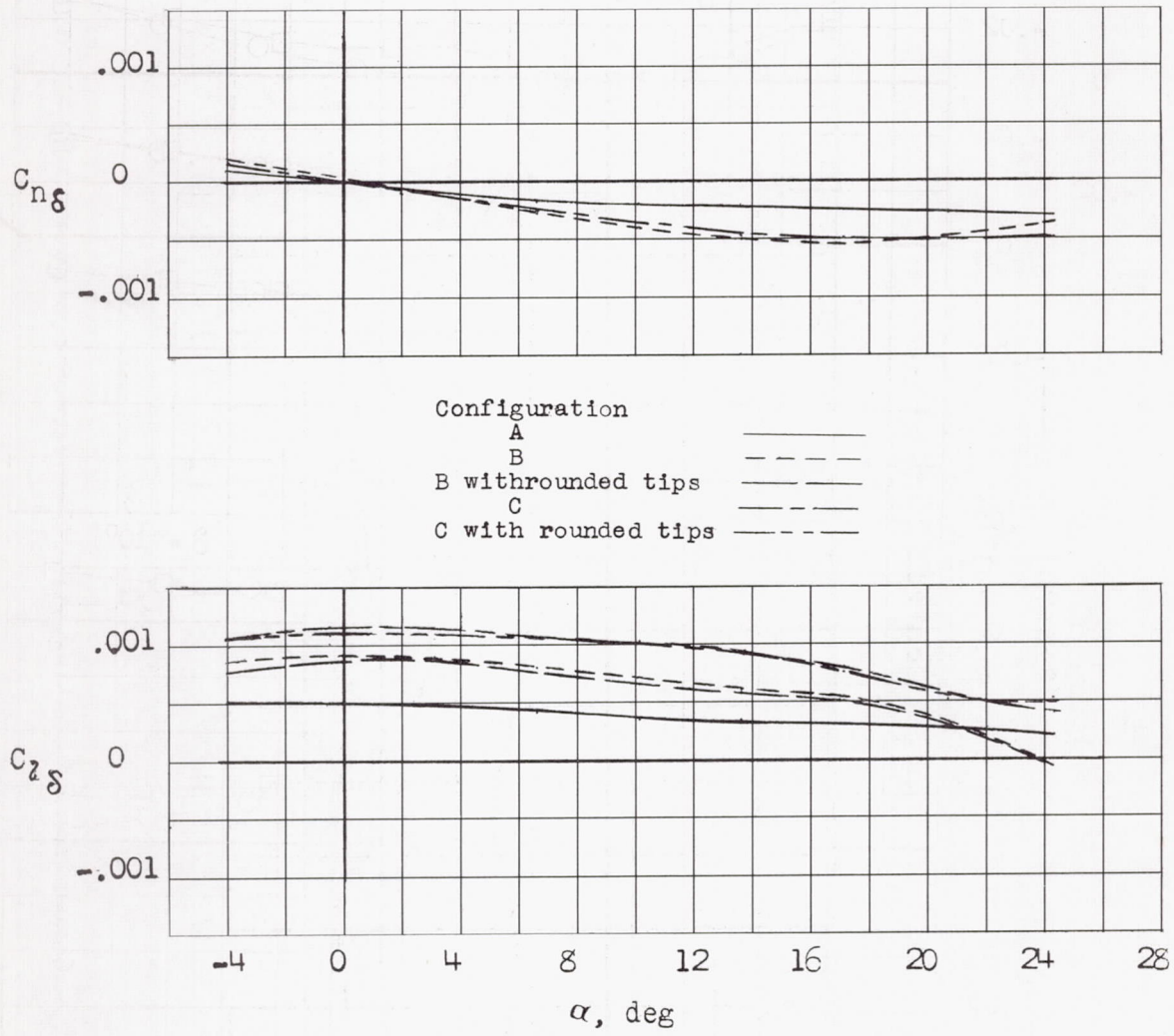


Figure 18.- Comparison of control parameters for the control configurations investigated. Trailing-edge flap neutral.

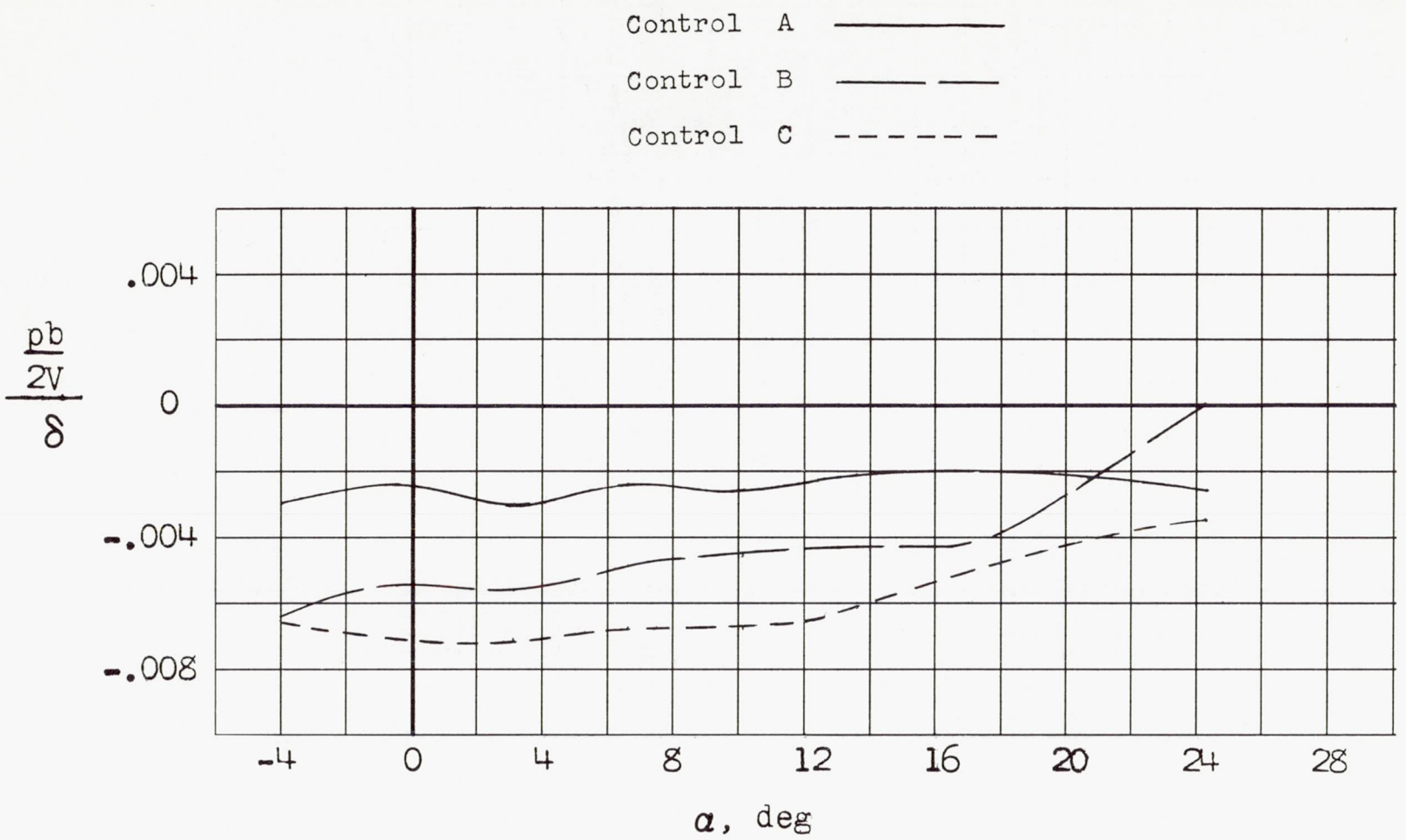


Figure 19.- Comparison of rolling effectiveness of controls A, B, and C.

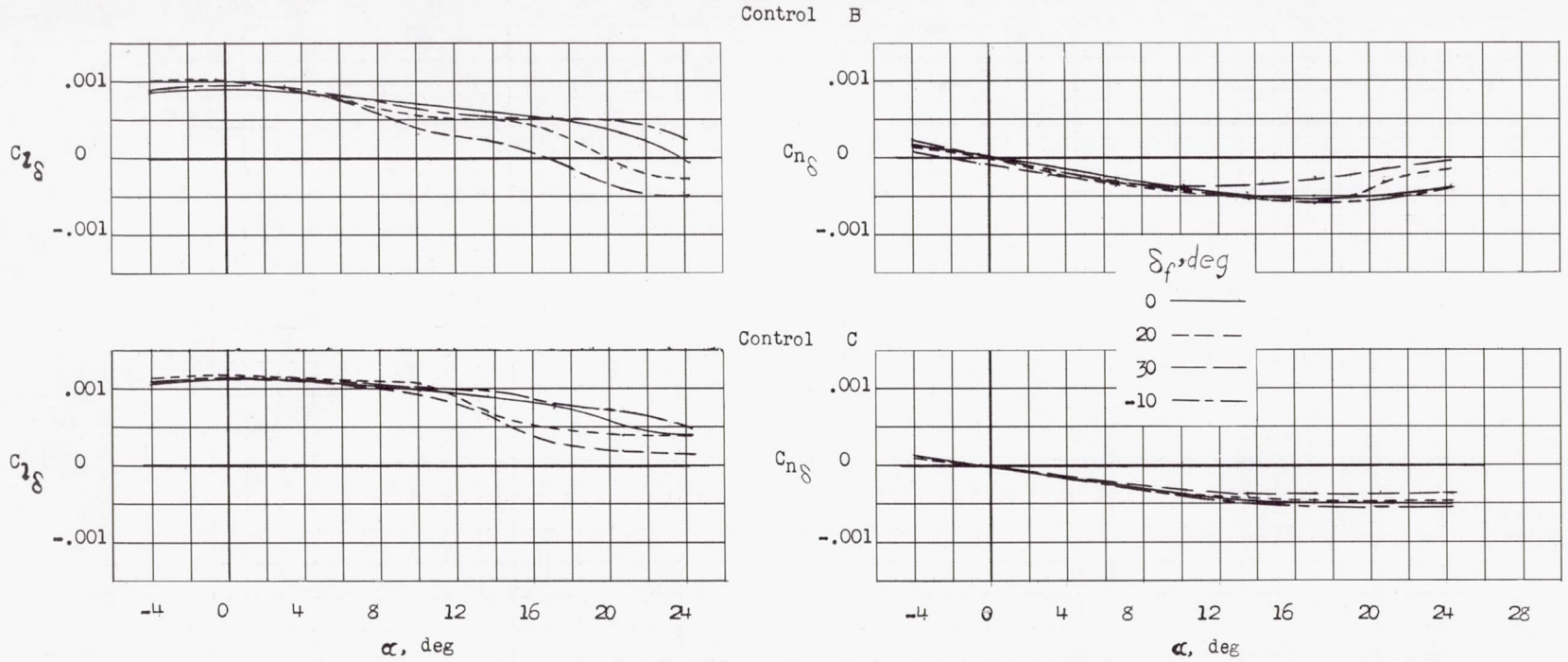
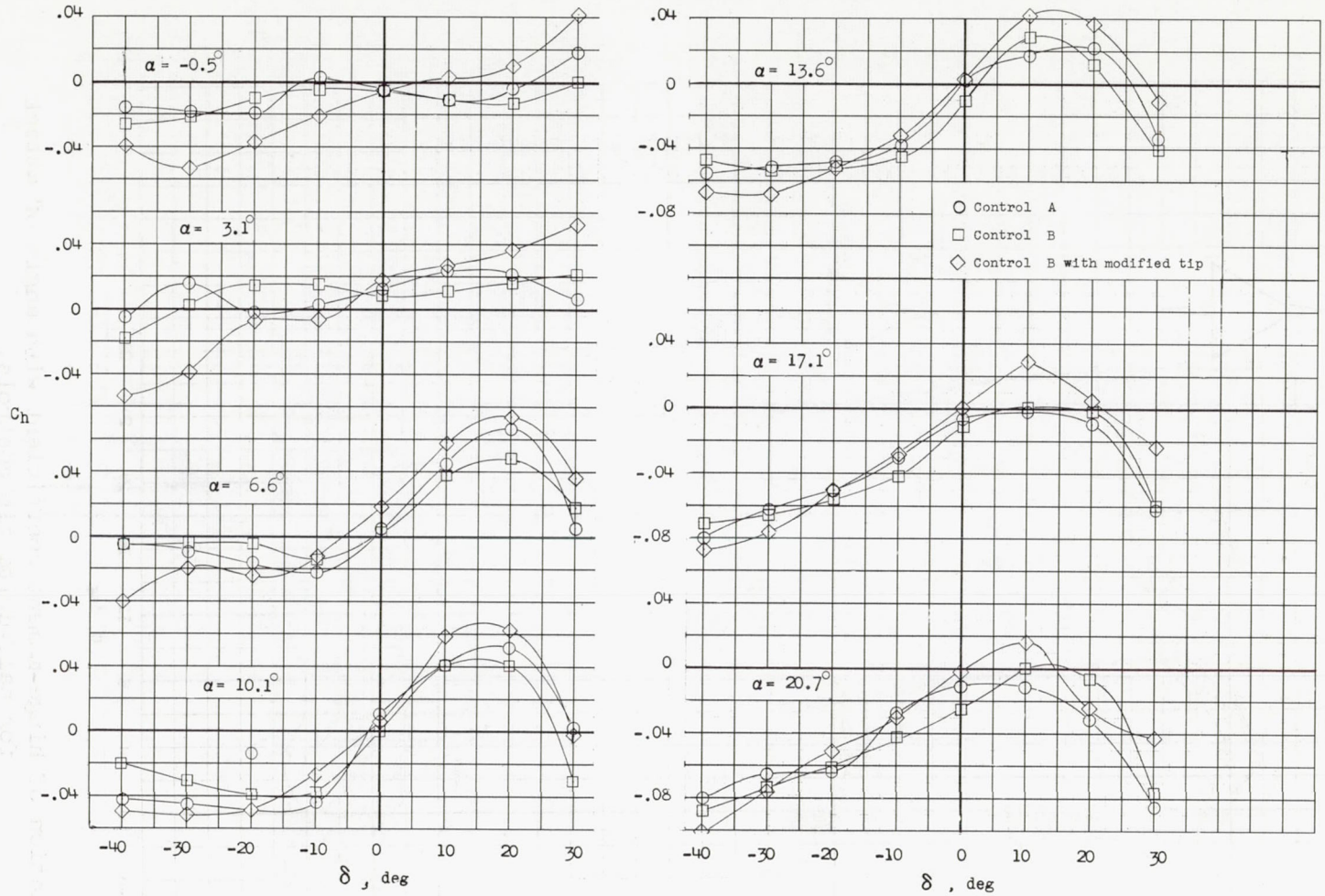
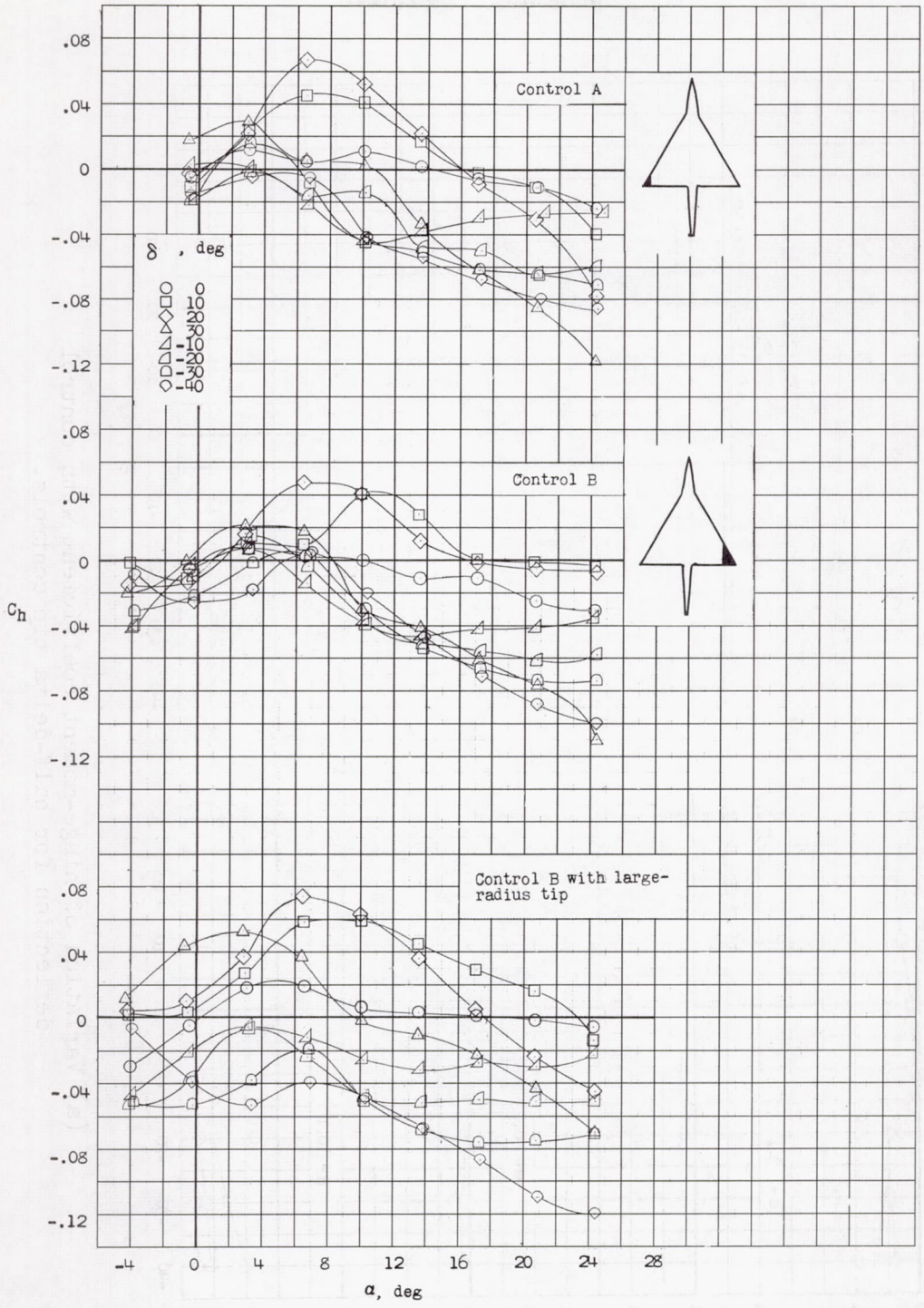


Figure 20.- Effect of trailing-edge flap deflection on the control parameters for controls B and C.



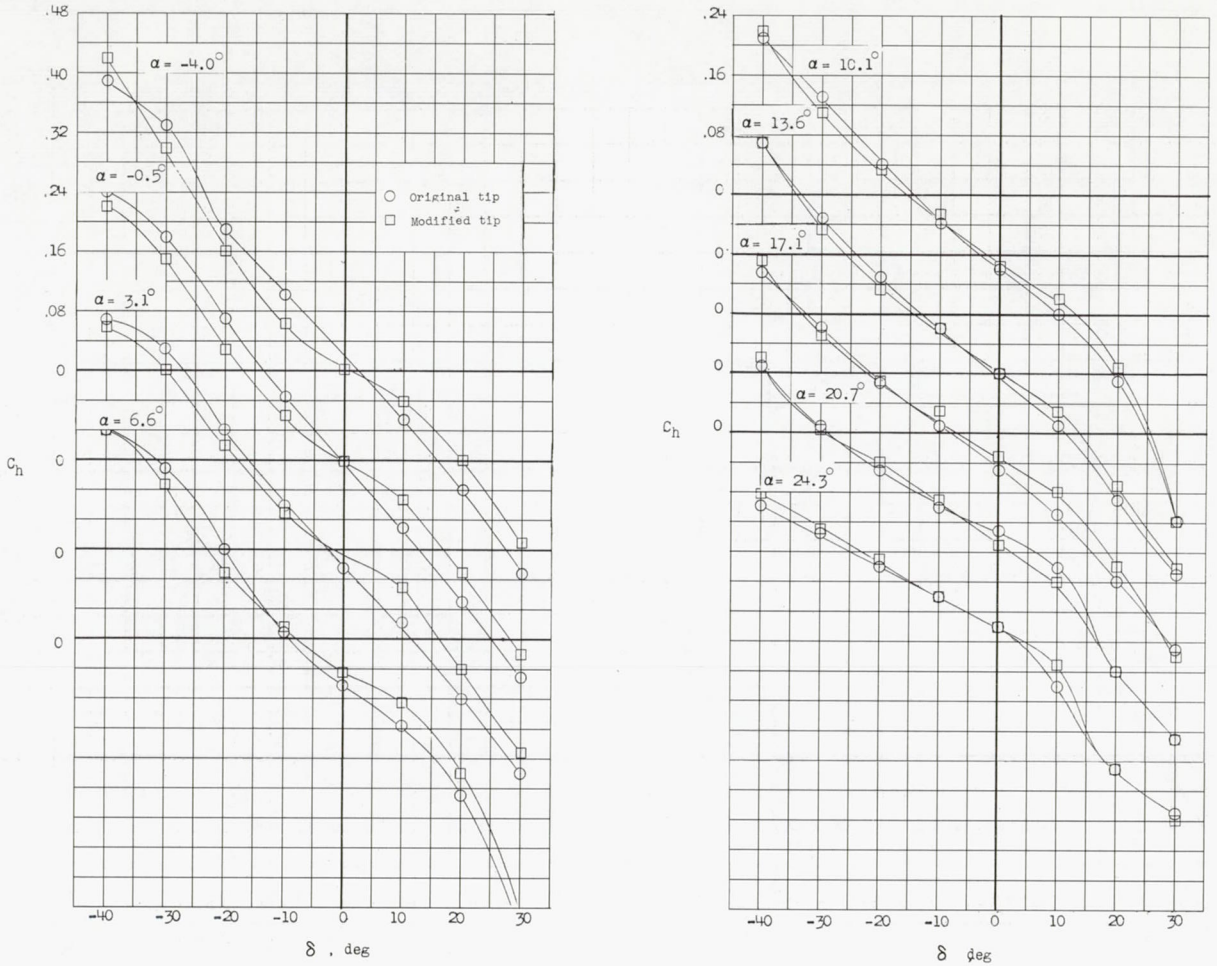
(a) Variation of hinge-moment coefficient with control deflection for half-delta tip controls.

Figure 21.- Hinge-moment characteristics for control configurations investigated.



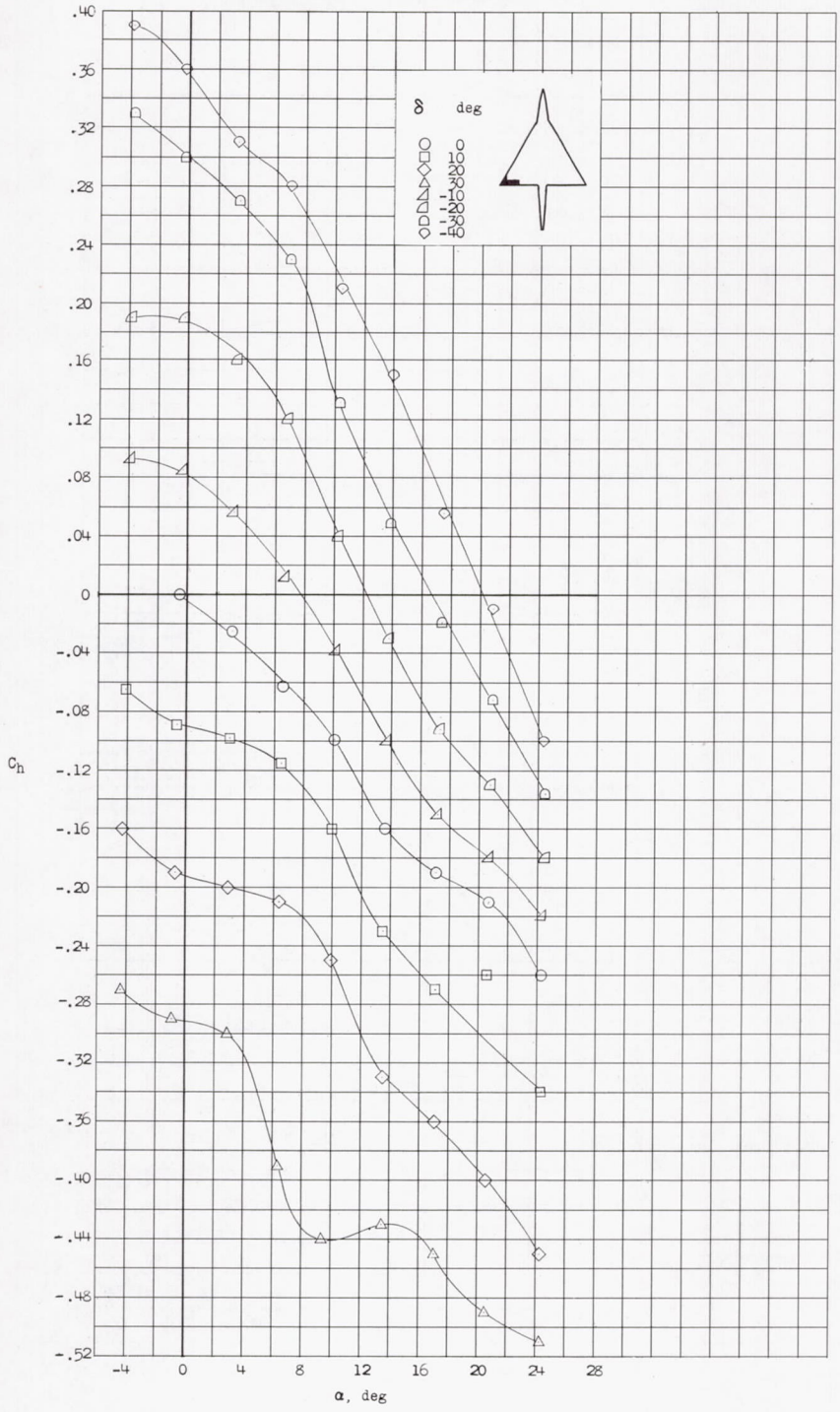
(b) Variation of hinge-moment coefficient with angle of attack for half-delta tip controls.

Figure 21.- Continued.



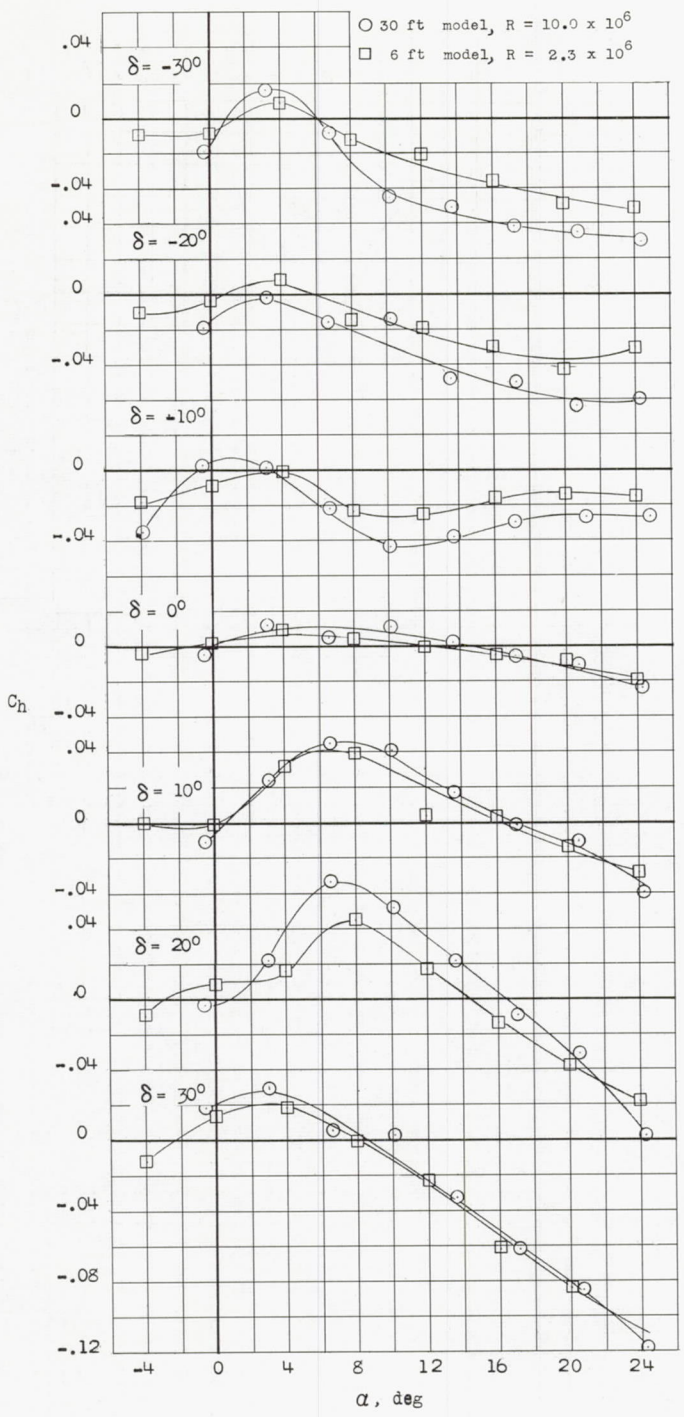
(c) Variation of hinge-moment coefficient with control deflection for horn-balance-type control (control C).

Figure 21.- Continued.



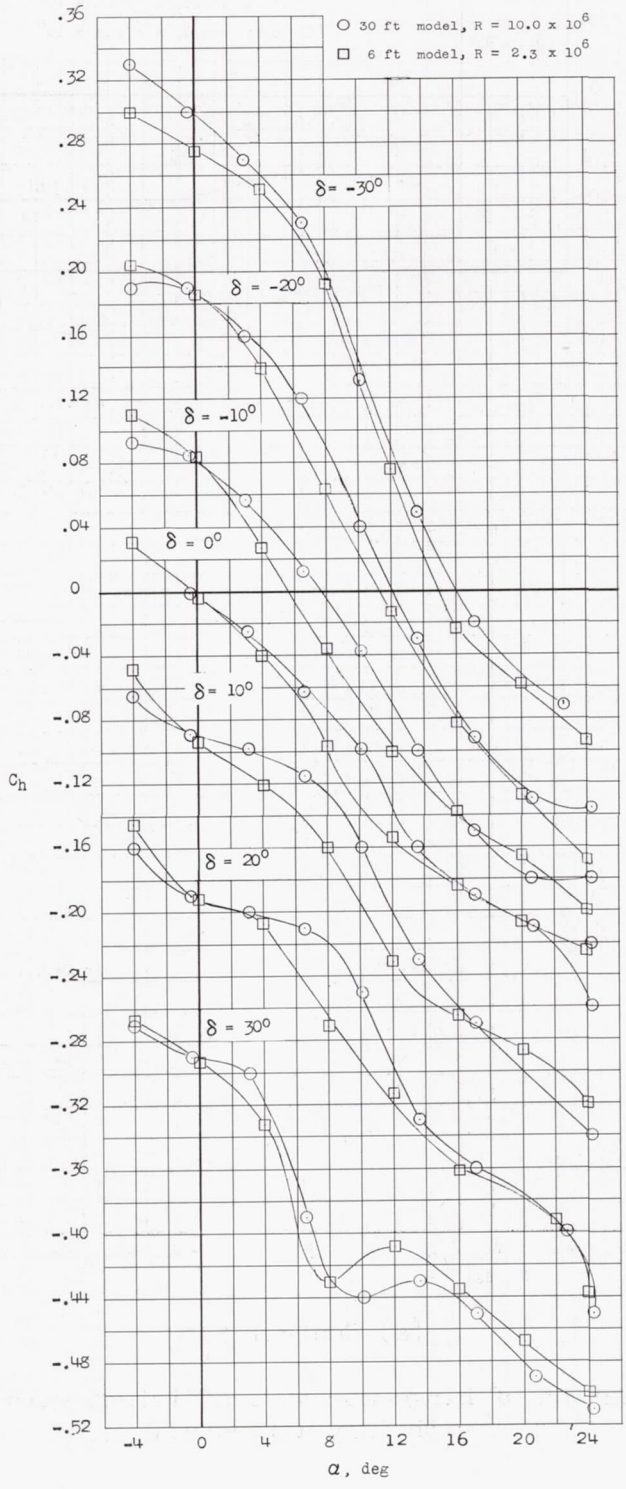
(d) Variation of hinge-moment coefficient with angle of attack for horn-balance-type control.

Figure 21.- Concluded.



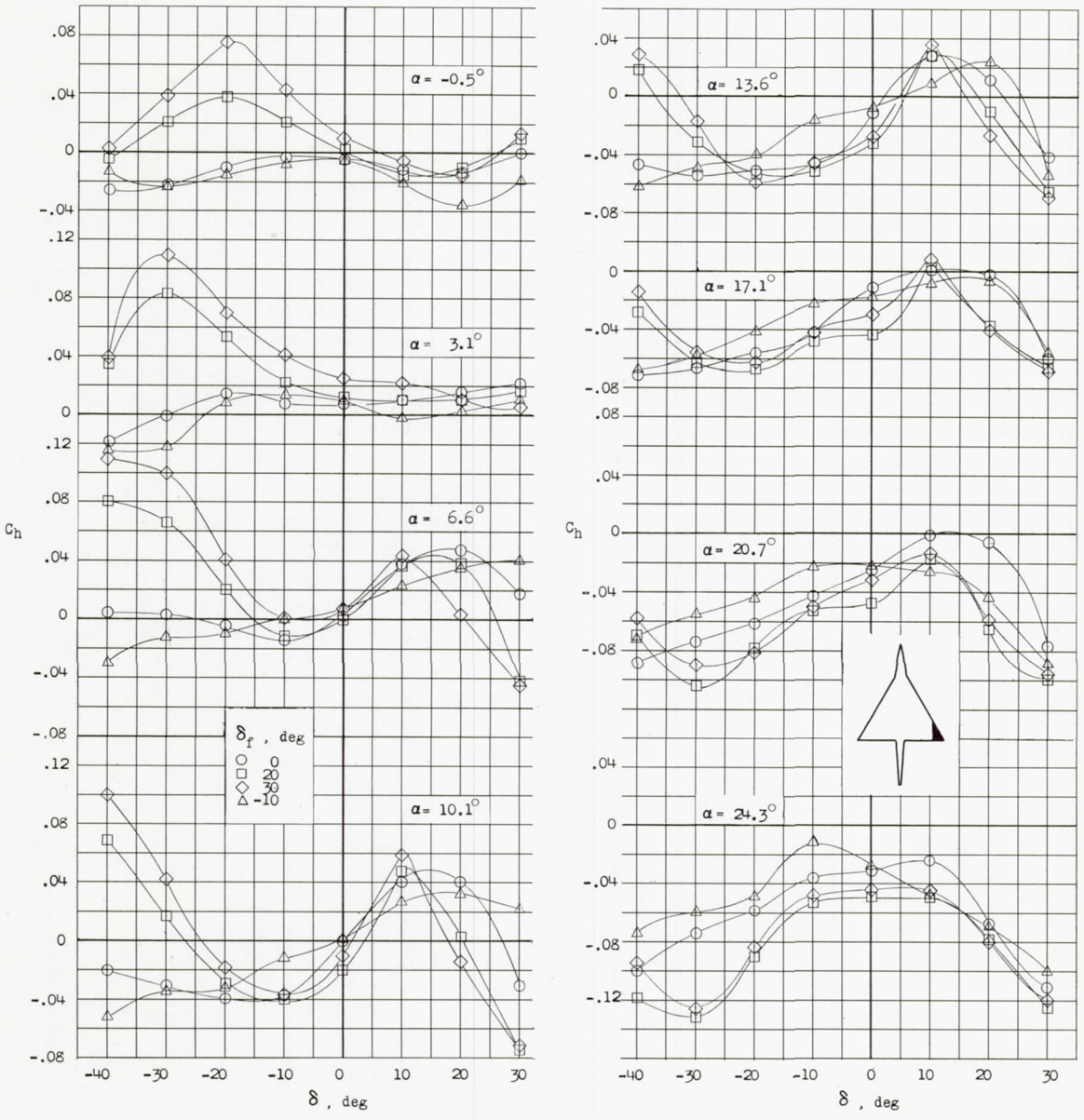
(a) 5-percent half-delta control.

Figure 22.- Variation of hinge-moment coefficient with angle of attack for the 30-foot-span model and the 6-foot-span model of reference 1 with the 5-percent half-delta tip control and the 10-percent horn-balance control deflected.



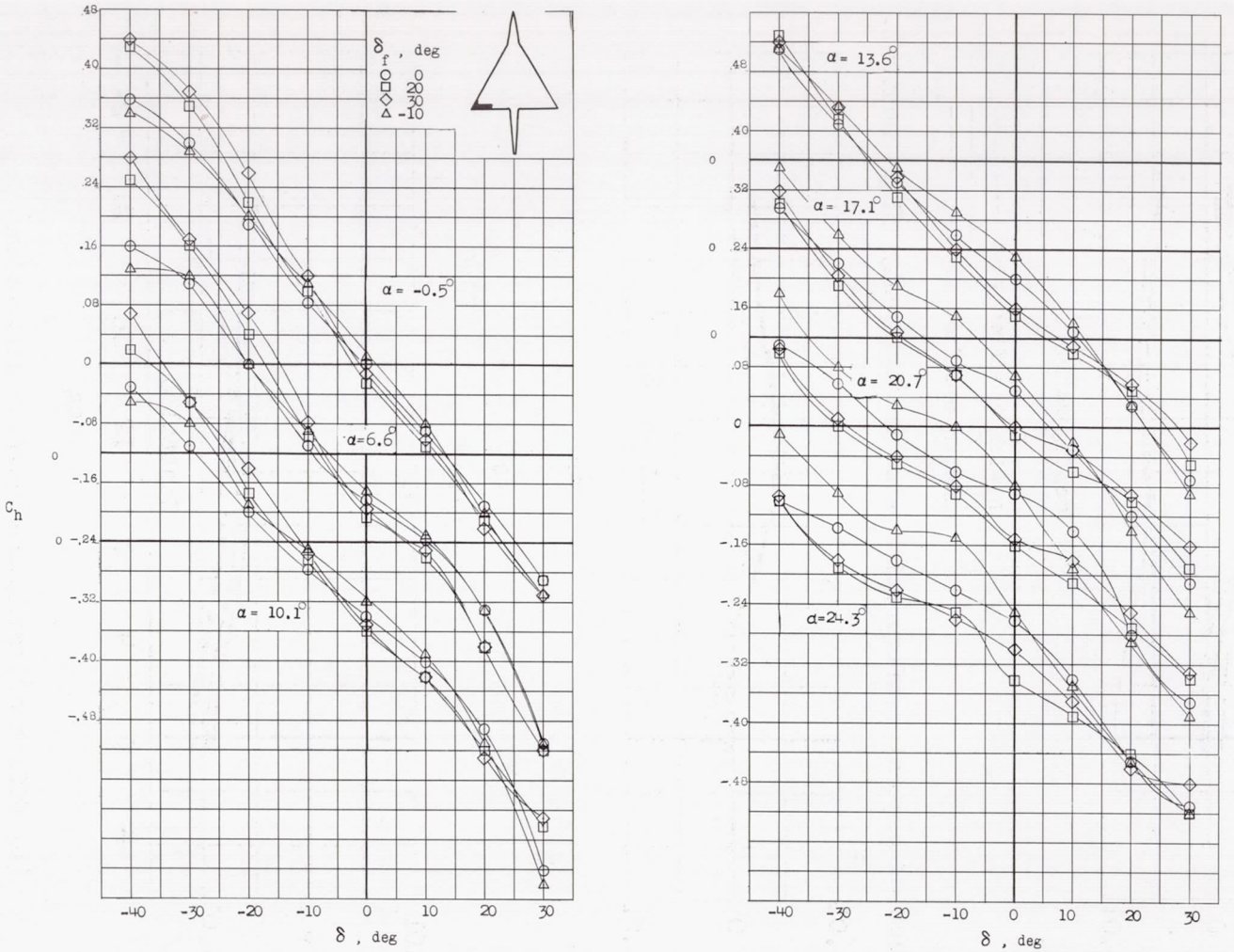
(b) 10-percent horn-balance control.

Figure 22.- Concluded.



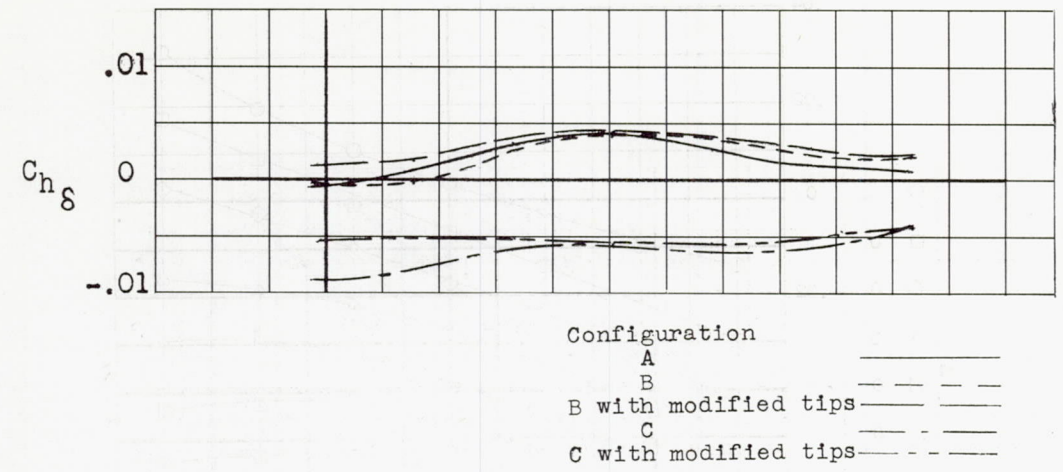
(a) Control B.

Figure 23.- Variation of hinge-moment coefficient with control deflection with flap deflected.

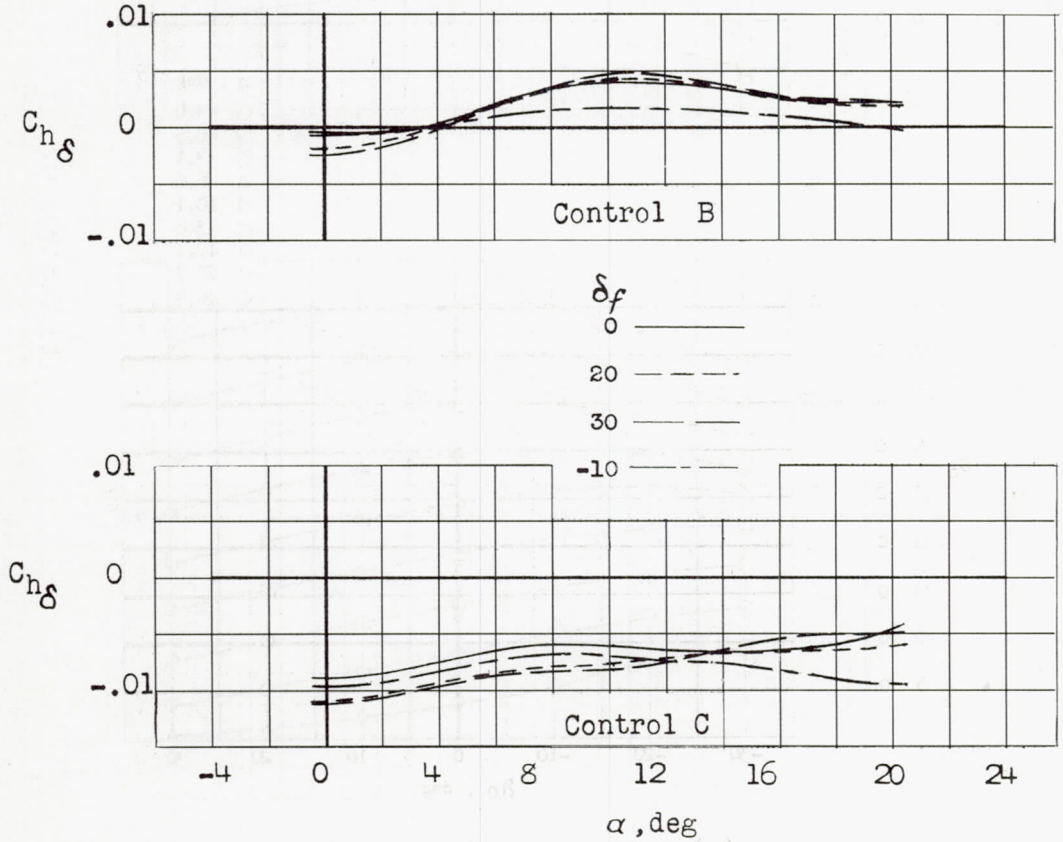


(b) Control C.

Figure 23.- Concluded.

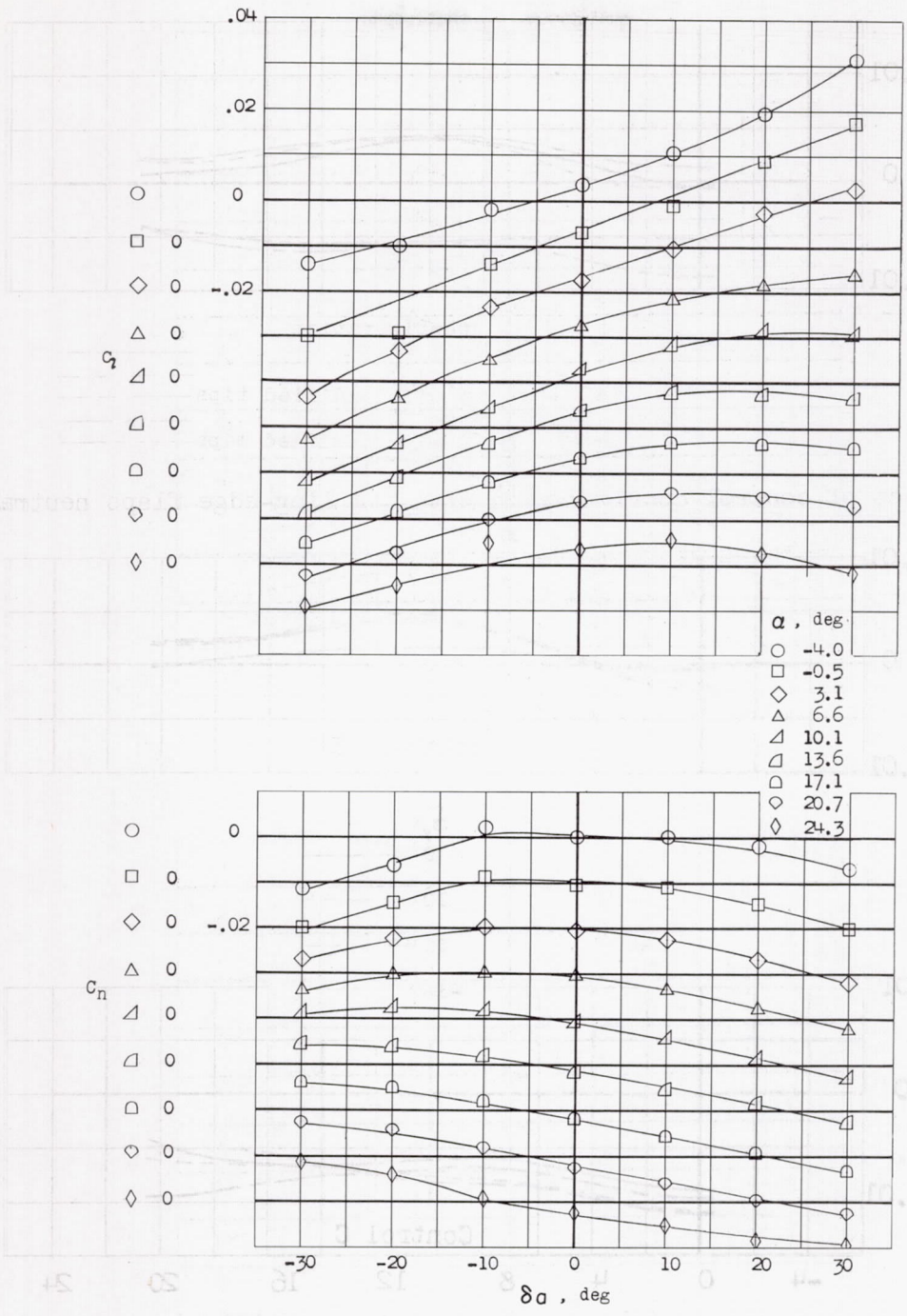


(a) Effect of control configuration with trailing-edge flaps neutral.



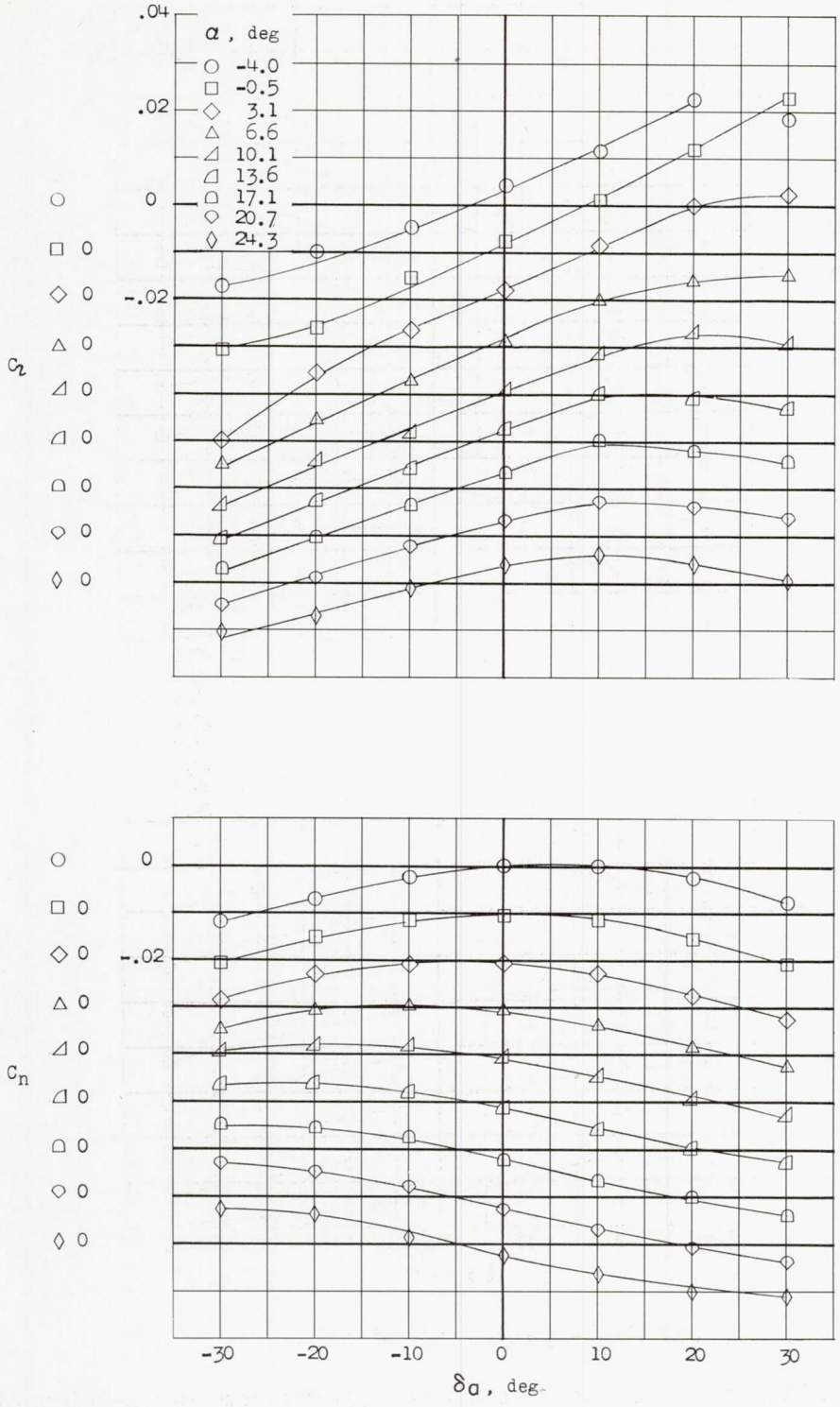
(b) Effect of trailing-edge-flap deflection for controls B and C.

Figure 24.- Effect of control configuration and trailing-edge-flap deflection on the hinge-moment parameter C_{h_δ}.



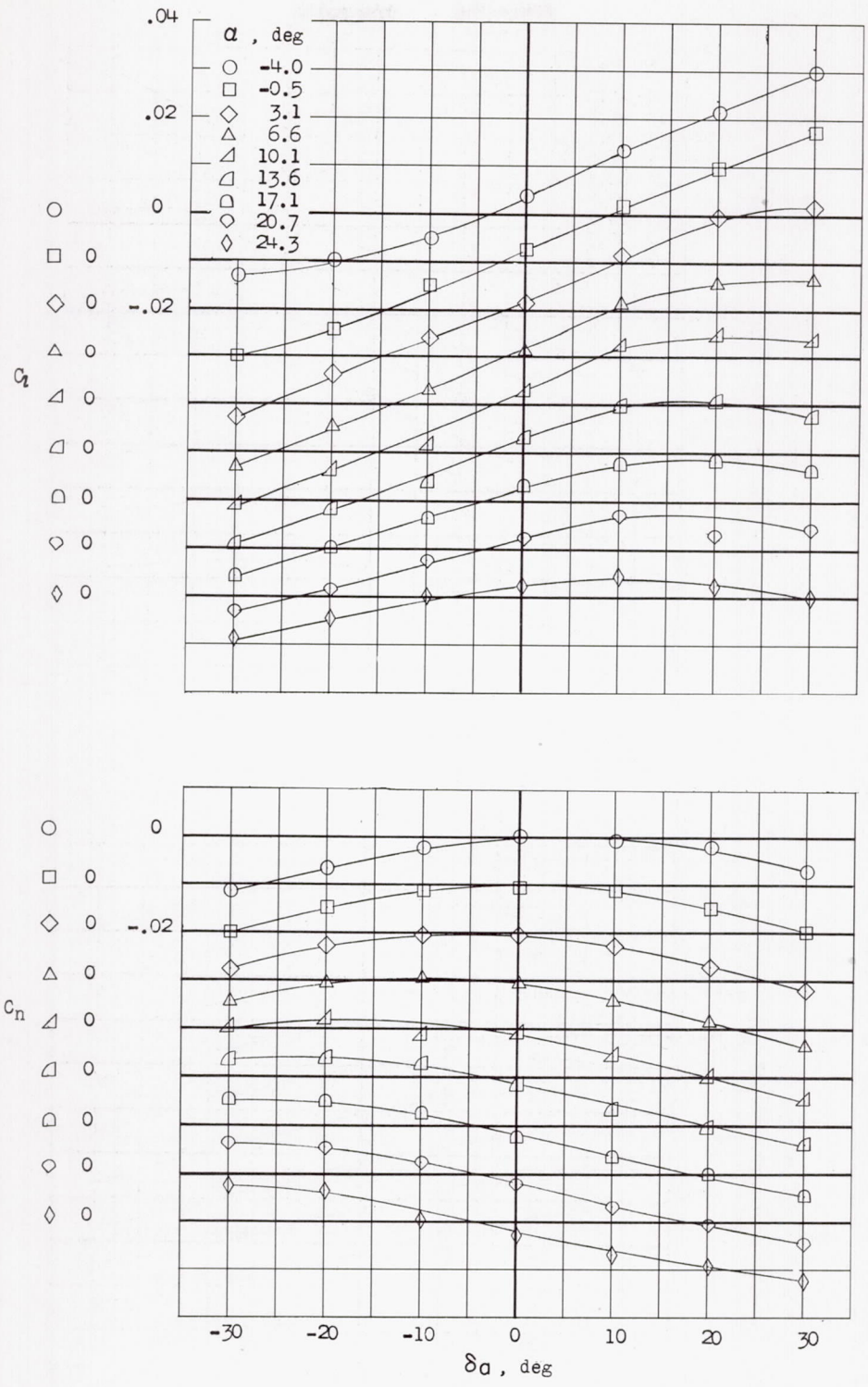
(a) Full-span attached tab.

Figure 25.- Variation of rolling-moment and yawing-moment coefficients with control deflection for a horn-balance control with five types of control balancing tabs installed. Left control deflected; right control neutral; $S_t/S_a = 0.10$; $\delta_t/\delta_a = -1.0$.



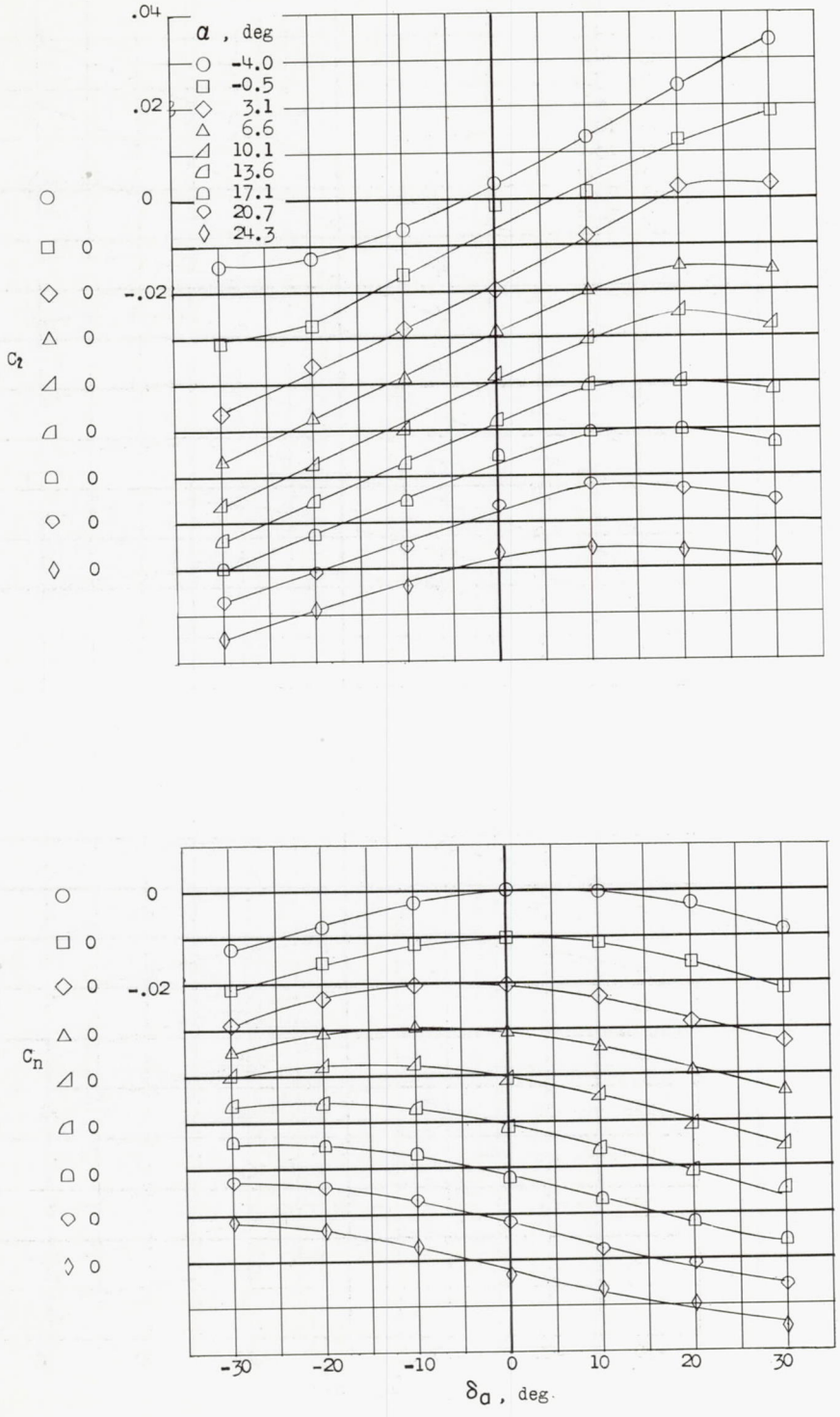
(b) Half-span inboard attached tab.

Figure 25.- Continued.



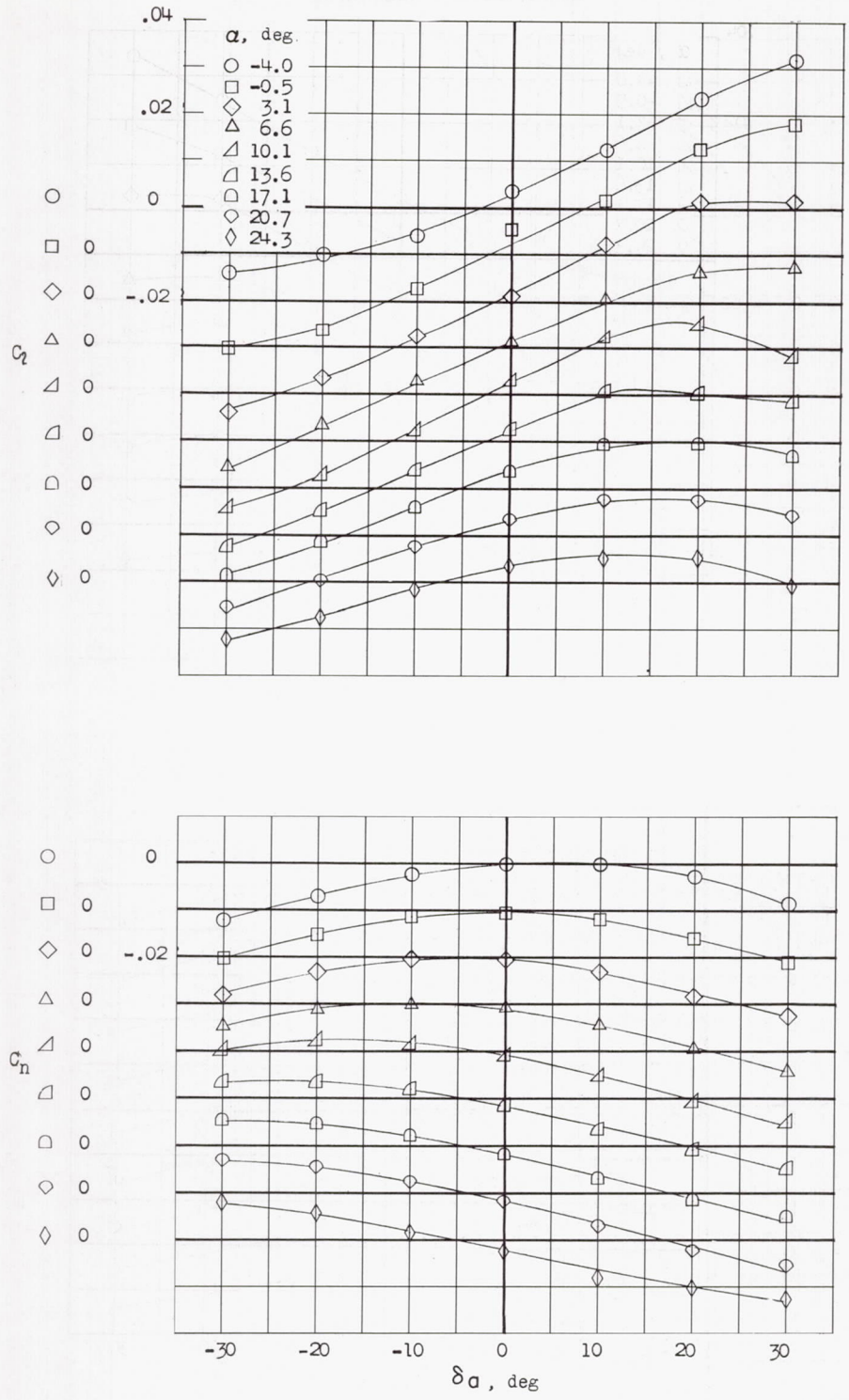
(c) Half-span outboard attached tab.

Figure 25.- Continued.



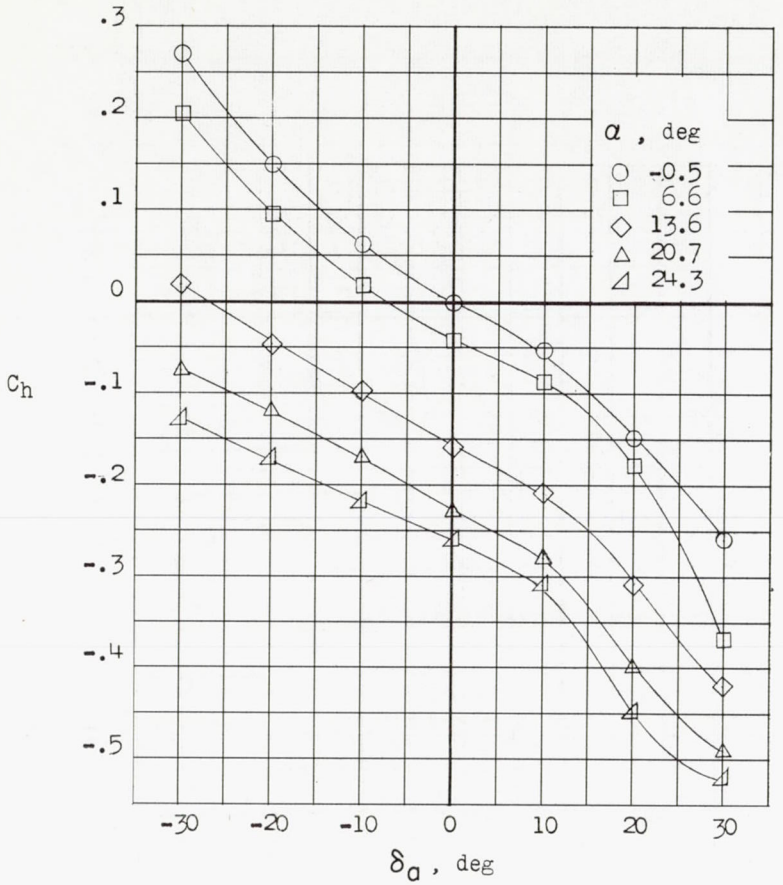
(d) Half-span inboard detached tab.

Figure 25.- Continued.

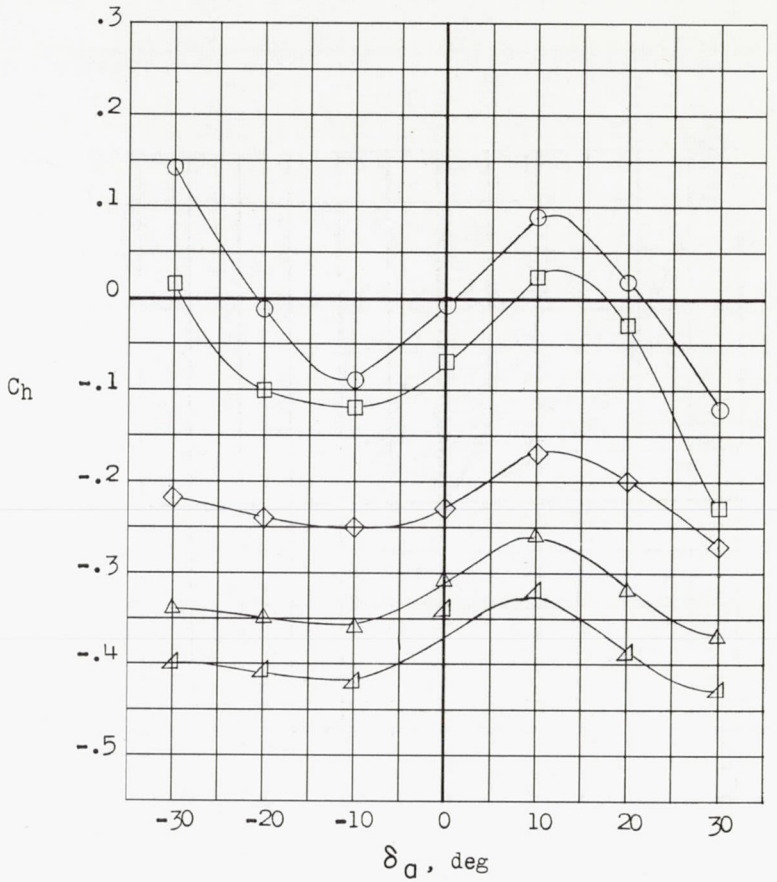


(e) Half-span outboard detached tab.

Figure 25.- Concluded.

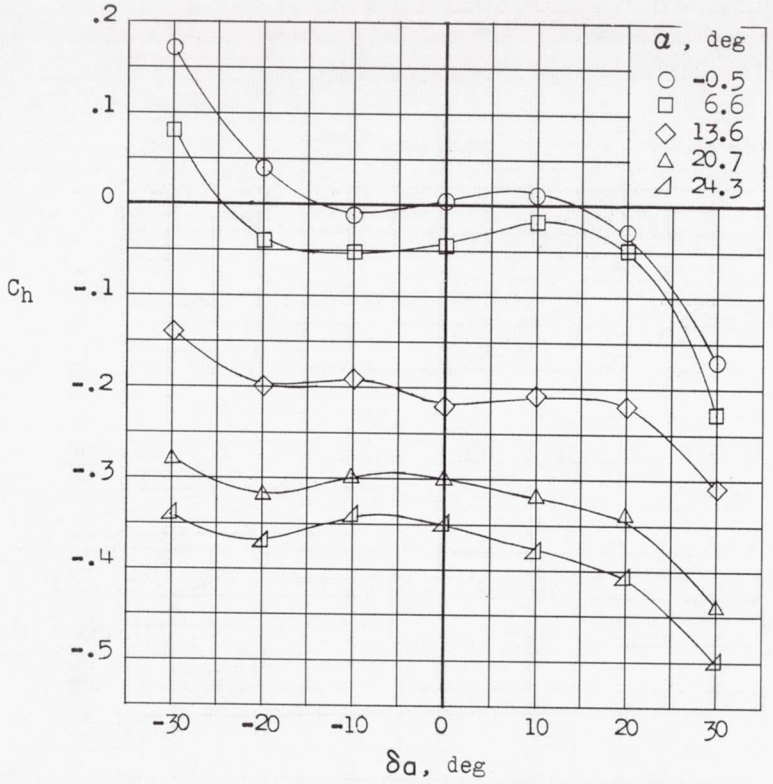


(a) Basic control without tab.

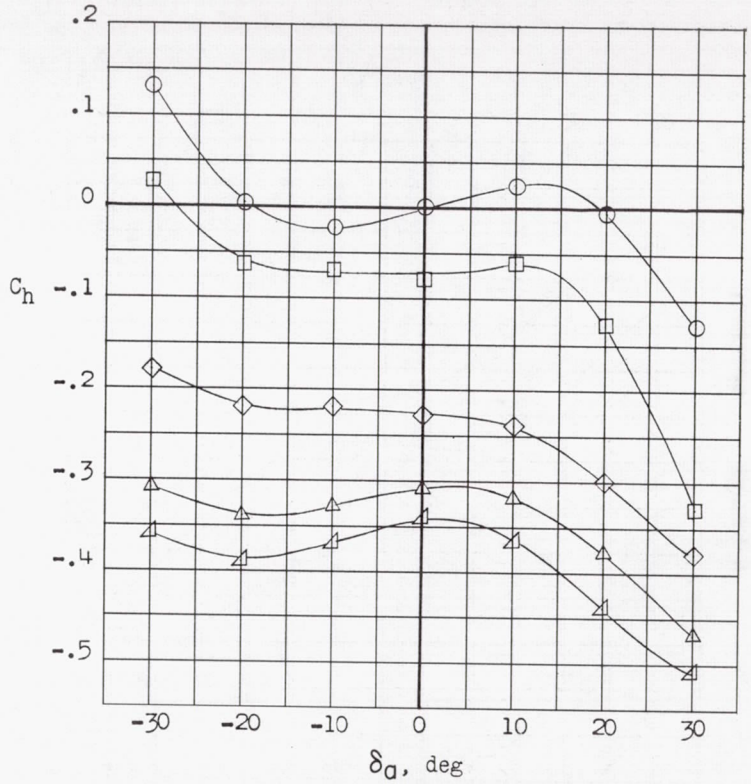


(b) Control with full-span attached tab.

Figure 26.- Variation of hinge-moment coefficient with control deflection for a horn-balance-type control with and without balancing tabs installed. $S_t/S_a = 0.10$; $\delta_t/\delta_a = -1.0$.

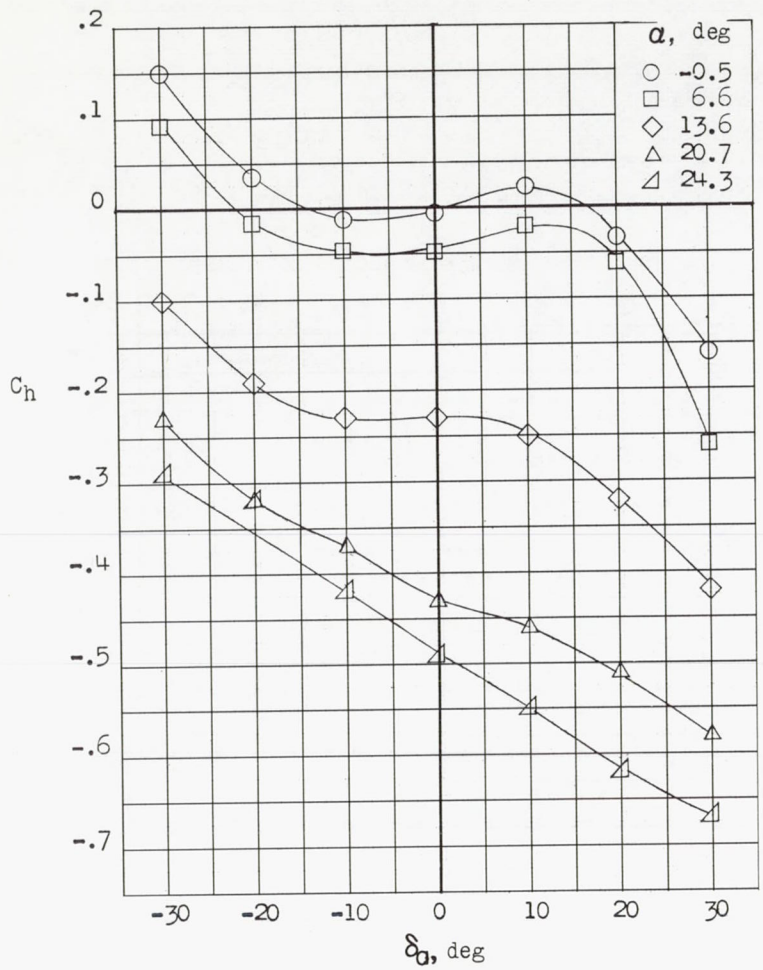


(c) Control with $0.5b_a/2$ inboard attached tab.

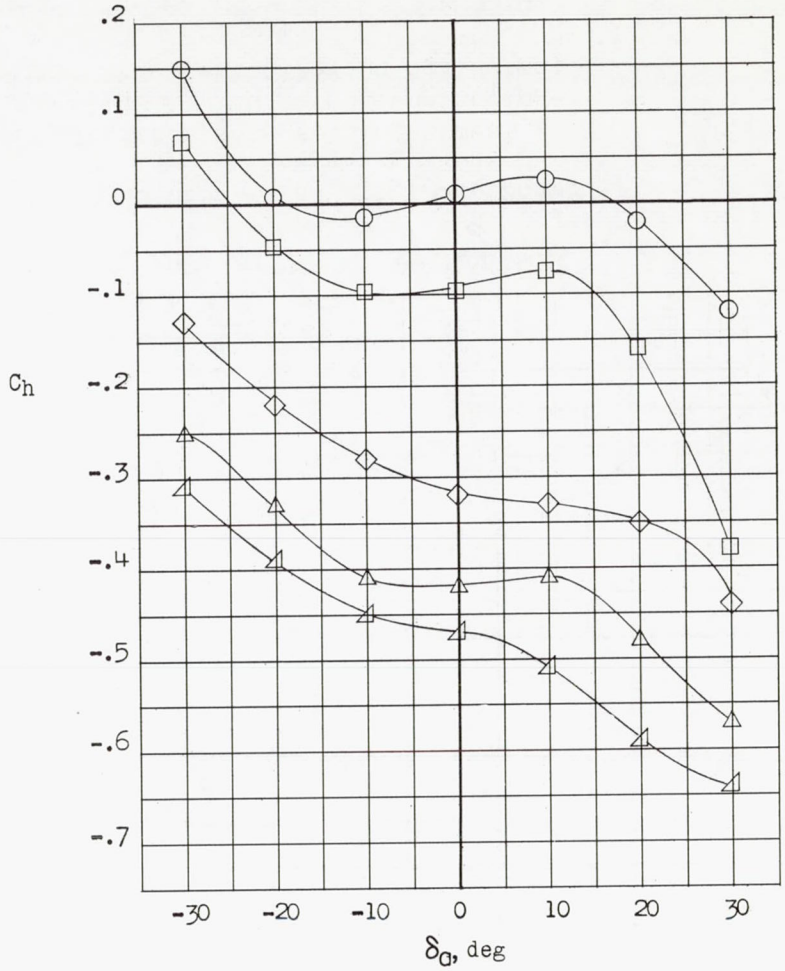


(d) Control with $0.5b_a/2$ outboard attached tab.

Figure 26.- Continued.



(e) Control with $0.5b_a/2$ inboard detached tab.



(f) Control with $0.5b_a/2$ outboard detached tab.

Figure 26.- Concluded.

CONFIDENTIAL

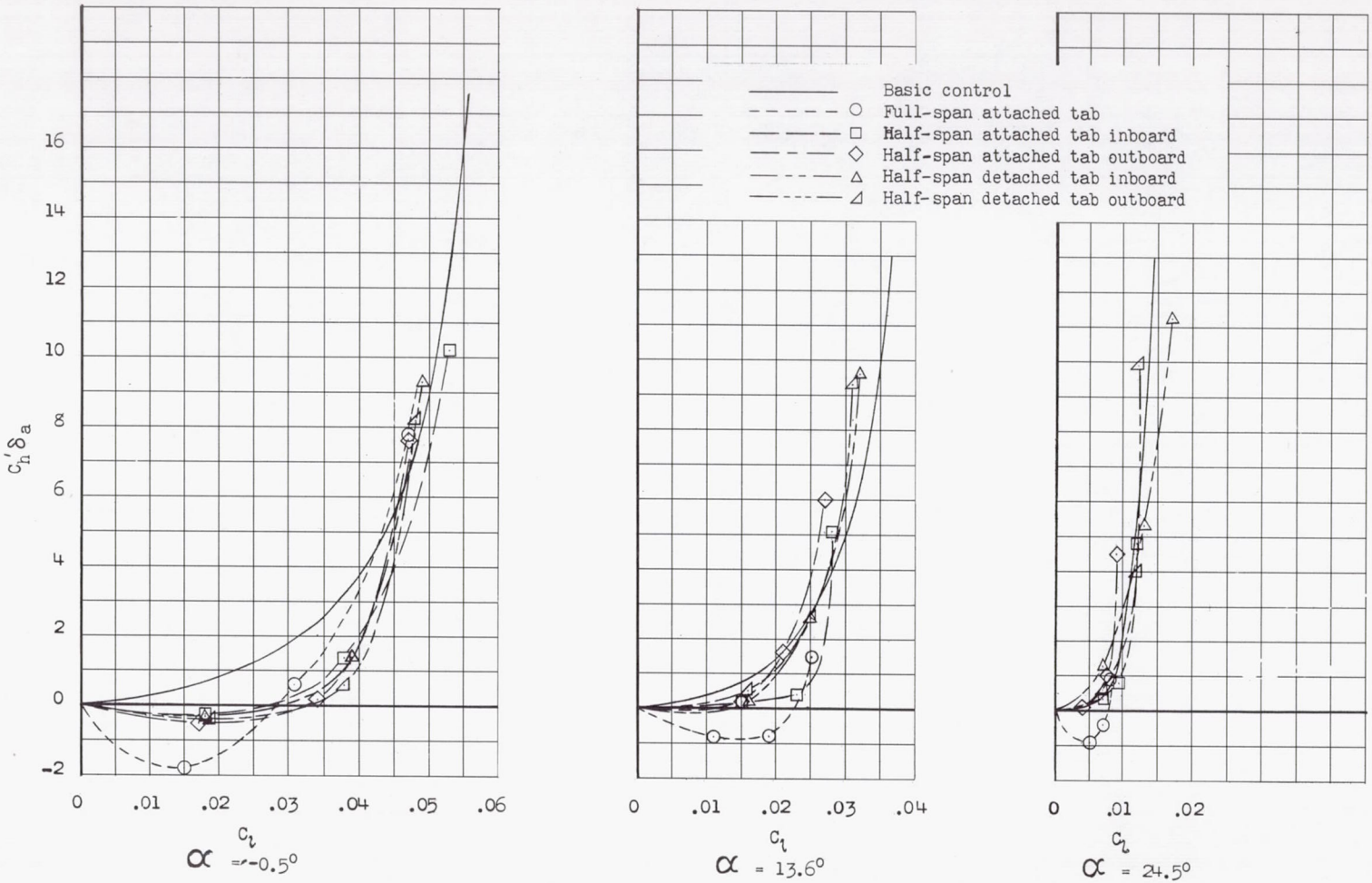


Figure 27.- Variation of hinge-moment parameter with rolling-moment coefficient for a horn-balance-type aileron with several balancing-tab arrangements. δ_t/δ_a = -1.0; left and right ailerons deflected; $(\delta_a)_L/(\delta_a)_R$ = -1.0.